Technical University of Munich
TUM School of Engineering and Design

ПJ∏

Design of hybrid nano-engineered bioprocesses
for wastewater treatment

Michele Ponzelli

Complete reprint of the dissertation approved by the TUM School of Engineering and Design of

the Technical University of Munich for the award of the

Doktor der Ingenieurwissenschaften (Dr.-Ing.)

Chair: Assoc. Prof. Dr. Sebastià Puig Broch

Examiners:

    1.   Prof. Dr.-Ing. Jörg E. Drewes

    2.   Dr. Maite Pijuan

    3.   Hon.-Prof. Dr. Sasha D. Hafner

The dissertation was submitted to the Technical University of Munich on 24 May 2023 and

accepted by the TUM School of Engineering and Design on 2 October 2023.

DOCTORAL THESIS

Design of hybrid nano-engineered bioprocesses for wastewater treatment

Michele Ponzelli

2023

DOCTORAL PROGRAMME IN WATER SCIENCE AND TECHNOLOGY

Supervisors: Prof. Jelena Radjenovic, Prof. Jörg E. Drewes, Dr. Konrad Koch

Tutor: Prof. Ignasi Rodríguez Roda-Layret

Thesis submitted to the University of Girona for obtaining the degree of Doctor

Acknowledgements

This part of my dissertation goes to those whom I am grateful for.

Words may not be enough to express my deepest gratitude to those people, but I would still make them count as much as possible.

I thank Giorgia, who has always been here. By my side. In every moment. When I wanted to vent out of frustration and when I was joyful about achievements. Giorgia, you are an everyday source of inspiration for me. You push me to be the best version of myself. Thank you, I feel blessed to have met you.

I thank my family. My sister, Allegra, for always believing in me and sending me all her love wherever I was, as if she were there cheering me up. My father, Sergio, for teaching me to listen and never give up. My mother, Viviana, for teaching me education, kindness, and independence.

I thank Tiziana, Daniele, Vittoria, and Fabio (and Sisi) for bringing lightness in some challenging moments and welcoming me from the first minute with their warmth.

I thank my supervisors. Jelena, for her tenaciousness, unwavering persistence, and for being an example for the scientific world in which talented women exist –all they need is just the right opportunities. Konrad, for always believing in me and my capabilities, giving me independence, and teaching me attention to details ("less is more"), and the art of careful planning. Jörg for transferring me the scientific research method and being a role model for many students.
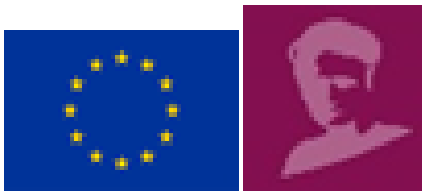
I thank my friends. Ghè and Gabri confirm the saying, "Who finds a friend, finds a treasure", and I am incredibly grateful to know them and have them by my side for almost 20 years. Nebojša and Nadja for all the evenings spent laughing together and their closeness in this journey. I thank Nick, Cana, Frenki, Edo, and Diego, my trusted friends since we were teens. I thank the friends I made during this path, like Matia and Bea, with whom I share the same passion for water, and from scratch, we built a community on it.

I thank the Nowelties Team for trusting me and supporting me in the role of blog manager. I thank all the ESRs for having shared these years despite the few meetings that strictly limited our interactions and the possibility of bonding. I hope this experience has been useful to everyone.

I also want to thank myself. Thank you, Michele, for not giving up. Thank you, Michele, for asking for help when you needed it. Thank you for trying to be true to yourself. Thank you for understanding that success and failure are two sides of the same coin and that you should never identify your value with none. Thank you for learning to feel vulnerable and closer to the inner you. You may not be perfect as you would like to appear, but you are unique, and that's where your worth comes from. Now make the most of this moment. And on your next journey, bring all the lessons you learned during this path.

Moreover, I also thank my therapist, Giulia, who guided me on an internal path of discovery, where I had the opportunity to face my unresolved issues. If I am more aware of my inner self, it's thanks to her. However, I am still a work in progress. I still have much more to discover and learn about myself.

Finally, I thank the European Commission for being a hub of international research excellence with the MSCA grants. Only with research is it possible to invest in the future and build a wealthier civilization. I feel grateful and proud to be part of Europe and to have had the chance to contribute firsthand.

Contents

Contents

Publications

Michele Ponzelli, Soraya Zahedi, Konrad Koch, Jörg E. Drewes, Jelena Radjenovic

Rapid biological reduction of graphene oxide: Impact on methane production and micropollutant transformation

Journal of Environmental Chemical Engineering

Volume 10, Issue 5, 2022, 108373, ISSN 2213-3437

https://doi.org/10.1016/j.jece.2022.108373

Michele Ponzelli, Jelena Radjenovic, Jörg E. Drewes, Konrad Koch

Enhanced methane production kinetics by graphene oxide in fed-batch tests

Bioresource Technology

Volume 360, 2022, 127642, ISSN 0960-8524,

https://doi.org/10.1016/j.biortech.2022.127642

Michele Ponzelli, Hiep H. Nguyen, Jörg E. Drewes, Konrad Koch

Improved recovery of overloaded anaerobic batch reactors by graphene oxide

Sustainability

Volume 15 (3), Number 2224, 2023

https://doi.org/10.3390/su15032224

Abbreviations

AC	Activated carbon
AD	Anaerobic digestion
AS	Activated sludge
AMPTS	Automatic methane potential test system
AnMBR	Anaerobic membrane bioreactor
bioRGO	Biologically reduced graphene oxide
BMP	Biochemical methane potential
CV	Cyclic voltammetry
DIET	Direct interspecies electron transfer
EPS	Extracellular polymeric substances
G	Graphene
GAC	Granular activated carbon
GO	Graphene oxide
HRT	Hydraulic retention time
IET	Interspecies electron transfer
MCC	Microcrystalline cellulose
OLR	Organic loading rate
OMPs	Organic micropollutants
PhACs	Pharmaceutically active compounds
PAC	Powdered activated carbon

RGO   Reduced graphene oxide

ROS   Reactive oxygen species

SMP   Specific methane production

SMX   Sulfamethoxazole

TMP   Trimethoprim

TP   Transformation product

TS   Total solids

UASB   Upflow anaerobic sludge blanket

VFAs   Volatile fatty acids

VS   Volatile solids

WAS   Waste activated sludge

WW   Wastewater

WWTP   Wastewater treatment plant

Figures

Tables

Summary

Day by day, drop by drop, freshwater is becoming scarce.

Reuse of water is therefore pursued. Several treatment options are available, from biological to advanced physical and chemical treatment. Due to the low energy requirement, the adoption of anaerobic wastewater treatment is gaining consensus and popularity. Anaerobic wastewater treatment entails the opportunity to recover resources like biogas and nutrients. Nonetheless, its applications in water reuse schemes are still scarce. One of the limitations of this technology is the slow interspecies electron transfer, which limits the organic material degradation.

Moreover, the presence of organic micropollutants (OMPs) in water constitutes a further constraint on the anaerobic treatment employment for water reuse purposes. OMPs such as pharmaceuticals and personal care products present at low concentrations (i.e., ng/L - µg/L), are of particular concern because of their possible long-term harmful effects. OMPs are difficult to remove in anaerobic treatments. Instead, advanced (and more energy-intense) treatment technologies are usually applied to remove OMPs from wastewater.

A possible solution to overcome this challenge is the introduction of low-cost, conductive nanomaterials, which stimulate organic material degradation through enhancing the electron transfer between anaerobic microorganisms. This dissertation aimed to explore the design of a hybrid nano-engineered system where anaerobic biological treatment is stimulated with graphene oxide (GO). The work focused on OMP removal and methane production, starting from batch configurations. To allow a better comprehension of the proposed hybrid system, the following research objectives were pursued:

- Collection, evaluation, and comparison of available studies on anaerobic biological systems amended with graphene-based materials.
- Assessment of the impact of GO addition on the removal efficiencies of selected OMPs, their biotransformation pathways, and on the specific methane production using biochemical methane potential (BMP) assays.

- Evaluation of the impact of GO addition in long-term BMP experiments on the degradation kinetics of two substrates at different rate-limiting conditions.

After thoroughly evaluating suitable experimental conditions, such as appropriate GO concentration levels, batch assays were performed. GO is a highly hydrophilic material and has insulating properties, yet by reducing its oxygen functionalities and partially restoring the conjugated structure of graphene, the resulting reduced graphene oxide (RGO) gains electrical conductivity. It was found that the biological reduction of GO from mixed anaerobic communities occurred within the first 24 hours. Remarkably, this was the first study proving that biologically reduced GO (bioRGO) formation occurred in a mixed anaerobic inoculum sampled from a full-scale digester facility instead of single or selected bacterial strains. Different characterization techniques were involved in proving the achievement of GO bioreduction, such as Raman spectroscopy, cyclic voltammetry, laser particle size analyzer, and optical microscopy. The measurements indicated an I_D/I_G ratio (intensity ratio of D and G bands measured with Raman spectroscopy) increase from 0.74 to 1.01 in one day, enhanced redox activities, and larger floc size, respectively. Thus, this evidence indicated the formation of bioRGO, which set the basis for an enhanced electron transfer due to the inherent electrical conductivity of RGO.

Regardless of the GO addition, the removal of the two selected indicator OMPs (i.e., sulfamethoxazole and trimethoprim) reached 90% in 48 hours. Thus, no notable improvement in their removal was observed after the GO addition. Nevertheless, the presence of ca. 50 mg of GO per g of volatile solids (VS) inhibited the formation of the identified transformation products (TPs) of sulfamethoxazole, showing a partial formation of the TPs compared with the control experiment, without added GO (i.e., 16%, and 40% TP257 formation of the initial amount of the parent compound, respectively). Thus, although there was no apparent impact of the GO on the parent compound removal kinetics, analysis of TPs demonstrated its impact on the biotransformation pathways of sulfamethoxazole, with a decreasing number of TPs with increase in GO concentration. Moreover, the presence of sulfamethoxazole TPs was detected in the experiments with sterilized (i.e., autoclaved) sludge (12% TP253 formation compared to the parent compound), suggesting a role of temperature-resistant enzymes in the biotransformation of this antibiotic, possibly released by the cell lyses after the autoclaving. On the other hand, GO addition caused biogas inhibition of up to 21% for concentrations higher than ca. 10 mg$_{GO}$/g$_{VS}$.

Based on these results, the investigation on batch assays was temporally expanded to simulate continuous systems. A fed-batch strategy consisting of five subsequent feeding cycles with two standard substrates (i.e., glucose and cellulose) was performed, focusing on methane production and model-obtained degradation kinetic values. It was hypothesized that different mechanisms could inhibit the expected and improved methane production performance of GO-amended systems. However, this inhibition is temporal and restricted to the early stage. The main identified factors behind were: (i) the consumption of electrons from the substrate used for biological reduction of GO; (ii) the initial bacterial inhibition caused by the nanomaterial addition; and (iii) the adsorption of the substrate to the graphene material, rather than its transformation to biogas.

Although no improvement and inhibition were noticed during the first two feeding cycles, from the third one, significant ($p < 0.05$) improvements in the degradation kinetics for both employed substrates were noticed when using concentrations greater than 10 mg$_{GO}$/g$_{VS}$. Therefore, the adoption of multiple feeds demonstrated that the inhibiting effect of GO is limited to the initial phase. On the other hand, the same refeeding strategy was adopted in anaerobic batch reactors under excessive organic loading conditions. The results confirmed the enhanced degradation kinetics and broadened the comprehension of GO amendment for the recovery of acidified anaerobic systems.

Overall, the thesis revealed that anaerobic biological treatment combined with GO is encouraged in continuously operating systems. However, a life cycle assessment of GO should be developed to prevent any possible environmental release. Similarly, the impacts of such nanomaterial in continuous systems at microbial levels are vastly unexplored, and long-term effects are unknown. Along with a comprehensive microbial characterization of changes of the microbial community, investigation of the fate of a wider set of OMPs and their TPs would throw more light on the effects of bioRGO in AD systems. Therefore, future hybrid nano-engineered bioprocesses should include all such aspects while aiming for continuously operated configurations capable of retaining GO.

Kurzzusammenfassung

Tag für Tag, Tropfen für Tropfen, wird das Süßwasser knapp.

Daher wird die Wiederverwendung von Wasser angestrebt. Es gibt verschiedene Behandlungsmöglichkeiten, von der biologischen bis zur fortgeschrittenen physikalischen und chemischen Behandlung. Aufgrund des geringen Energiebedarfs gewinnt die anaerobe Abwasserbehandlung immer mehr an Zustimmung und Beliebtheit. Die anaerobe Abwasserbehandlung bietet die Möglichkeit, Ressourcen wie Biogas und Nährstoffe zurückzugewinnen. Dennoch wird sie in der Wasserwiederverwendung nur selten eingesetzt. Eine der Einschränkungen dieser Technologie ist der langsame Elektronentransfer zwischen den Spezies, der den Abbau von organischem Material begrenzt.

Darüber hinaus stellt das Vorhandensein von organischen Mikroverunreinigungen (OMP) im Wasser eine weitere Einschränkung für die anaerobe Behandlung bei der Wasserwiederverwendung dar. Organische Mikroverunreinigungen wie Arzneimittel und Körperpflegeprodukte, die in niedrigen Konzentrationen (d. h. ng/L - µg/L) vorliegen, sind wegen ihrer möglichen langfristigen schädlichen Auswirkungen besonders besorgniserregend. OMPs lassen sich in anaeroben Verfahren nur schwer entfernen. Stattdessen werden in der Regel fortschrittliche (und energieintensivere) Behandlungstechnologien eingesetzt, um OMPs aus dem Abwasser zu entfernen.

Eine mögliche Lösung zur Überwindung dieser Herausforderung ist die Einführung kostengünstiger, leitfähiger Nanomaterialien, die den Abbau organischer Stoffe durch Verbesserung des Elektronentransfers zwischen anaeroben Mikroorganismen stimulieren. In dieser Dissertation wurde der Entwurf eines hybriden nanotechnologischen Systems untersucht, bei dem die anaerobe biologische Behandlung durch Graphenoxid (GO) stimuliert wird. Die Arbeit konzentrierte sich auf die Entfernung von OMP und die Methanproduktion, ausgehend von Batch-Konfigurationen. Um ein besseres Verständnis des vorgeschlagenen Hybridsystems zu ermöglichen, wurden die folgenden Forschungsziele verfolgt:

- Sammlung, Bewertung und Vergleich der verfügbaren Studien über anaerobe biologische Systeme, die mit Materialien auf Graphenbasis ergänzt wurden.

- Bewertung der Auswirkung des GO-Zusatzes auf die Entfernungseffizienz ausgewählter OMPs, ihre Biotransformationswege und auf die spezifische Methanproduktion unter Verwendung von biochemischen Methanpotential (BMP)-Tests.

- Bewertung der Auswirkungen des GO-Zusatzes in Langzeit-BMP-Experimenten auf die Abbaukinetik von zwei Substraten bei unterschiedlichen ratenbegrenzenden Bedingungen.

Nach gründlicher Evaluierung geeigneter Versuchsbedingungen, wie z. B. geeigneter GO-Konzentrationen, wurden Batch-Versuche durchgeführt. GO ist ein hochgradig hydrophiles Material mit isolierenden Eigenschaften. Durch die Verringerung seiner Sauerstofffunktionalitäten und die teilweise Wiederherstellung der konjugierten Struktur von Graphen gewinnt das resultierende reduzierte Graphenoxid (RGO) an elektrischer Leitfähigkeit. Es wurde festgestellt, dass die biologische Reduktion von GO aus gemischten anaeroben Gemeinschaften innerhalb der ersten 24 Stunden erfolgte. Bemerkenswerterweise war dies die erste Studie, die nachwies, dass die Bildung von biologisch reduziertem GO (bioRGO) in einem gemischten anaeroben Inokulum stattfand, das aus einer großtechnischen Fermenteranlage entnommen wurde, und nicht in einzelnen oder ausgewählten Bakterienstämmen. Zum Nachweis der biologischen GO-Reduktion wurden verschiedene Charakterisierungstechniken eingesetzt, darunter Raman-Spektroskopie, zyklische Voltammetrie, Laserpartikelgrößenanalyse und optische Mikroskopie. Die Messungen ergaben einen Anstieg des I_D/I_G-Verhältnisses (Intensitätsverhältnis von D- und G-Banden, gemessen mit Raman-Spektroskopie) von 0,74 auf 1,01 innerhalb eines Tages, erhöhte Redox-Aktivitäten bzw. eine größere Flockengröße. Dies deutet auf die Bildung von bioRGO hin, das die Grundlage für einen verbesserten Elektronentransfer aufgrund der inhärenten elektrischen Leitfähigkeit von RGO bildet.

Unabhängig von der Zugabe von GO erreichte die Entfernung der beiden ausgewählten Indikator-OMPs (d. h. Sulfamethoxazol und Trimethoprim) in 48 Stunden 90 %. Es wurde also keine nennenswerte Verbesserung ihrer Entfernung nach dem GO-Zusatz beobachtet. Dennoch hemmte das Vorhandensein von ca. 50 mg GO pro g flüchtiger Feststoffe (VS) die Bildung der identifizierten Transformationsprodukte (TP) von Sulfamethoxazol und zeigte eine teilweise Bildung der TP im Vergleich zum Kontrollexperiment ohne GO-Zusatz (d. h. 16 % bzw. 40 %

TP257-Bildung der ursprünglichen Menge der Ausgangsverbindung). Obwohl es also keinen offensichtlichen Einfluss des GO auf die Kinetik der Entfernung der Ausgangsverbindung gab, zeigte die Analyse der TPs seinen Einfluss auf die Biotransformationswege von Sulfamethoxazol, wobei die Anzahl der TPs mit steigender GO-Konzentration abnahm. Darüber hinaus wurde das Vorhandensein von Sulfamethoxazol-TPs in den Experimenten mit sterilisiertem (d. h. autoklaviertem) Schlamm nachgewiesen (12 % TP253-Bildung im Vergleich zur Ausgangsverbindung), was auf eine Rolle temperaturbeständiger Enzyme bei der Biotransformation dieses Antibiotikums hindeutet, die möglicherweise durch die Zelllyse nach dem Autoklavieren freigesetzt werden. Andererseits führte die Zugabe von GO zu einer Biogashemmung von bis zu 21 % bei Konzentrationen von mehr als ca. 10 mg_{GO}/g_{VS}.

Auf der Grundlage dieser Ergebnisse wurde die Untersuchung von Batch-Assays zeitlich erweitert, um kontinuierliche Systeme zu simulieren. Es wurde eine Fütterungsstrategie bestehend aus fünf aufeinanderfolgenden Fütterungszyklen mit zwei Standardsubstraten (d. h. Glukose und Zellulose) durchgeführt, wobei der Schwerpunkt auf der Methanproduktion und den mit dem Modell ermittelten kinetischen Werten für den Abbau lag. Es wurde die Hypothese aufgestellt, dass verschiedene Mechanismen die erwartete und verbesserte Methanproduktionsleistung von GO-angereicherten Systemen hemmen könnten. Diese Hemmung ist jedoch zeitlich begrenzt und auf das Anfangsstadium beschränkt. Die wichtigsten Faktoren, die dafür verantwortlich sind, sind: (i) der Verbrauch von Elektronen aus dem Substrat, das für die biologische Reduktion von GO verwendet wird; (ii) die anfängliche bakterielle Hemmung, die durch die Zugabe von Nanomaterialien verursacht wird; und (iii) die Adsorption des Substrats an das Graphenmaterial und nicht seine Umwandlung in Biogas.

Obwohl während der ersten beiden Fütterungszyklen keine Verbesserung und Hemmung festgestellt wurde, wurden ab dem dritten Zyklus signifikante ($p < 0,05$) Verbesserungen in der Abbaukinetik für beide verwendeten Substrate festgestellt, wenn Konzentrationen von mehr als 10 mg_{GO}/g_{VS} verwendet wurden. Die Verwendung mehrerer Fütterungen zeigte also, dass die hemmende Wirkung von GO auf die Anfangsphase beschränkt ist. Andererseits wurde die gleiche Strategie der Wiederbeschickung in anaeroben Batch-Reaktoren unter Bedingungen mit übermäßiger organischer Belastung angewandt. Die Ergebnisse bestätigten die verbesserte

Abbaukinetik und erweiterten das Verständnis der GO-Zusatzstoffe für die Wiederherstellung von angesäuerten anaeroben Systemen.

Insgesamt zeigte die Arbeit, dass die anaerobe biologische Behandlung in Kombination mit GO in kontinuierlich arbeitenden Systemen gefördert wird. Allerdings sollte eine Ökobilanz von GO entwickelt werden, um eine mögliche Freisetzung in die Umwelt zu verhindern. Ebenso sind die Auswirkungen solcher Nanomaterialien in kontinuierlichen Systemen auf mikrobieller Ebene noch weitgehend unerforscht, und die langfristigen Auswirkungen sind unbekannt. Neben einer umfassenden mikrobiellen Charakterisierung der Veränderungen in der mikrobiellen Gemeinschaft würde die Untersuchung des Verbleibs einer breiteren Palette von OMPs und ihrer TPs mehr Licht auf die Auswirkungen von bioRGO in AD-Systemen werfen. Daher sollten künftige hybride nano-technische Bioprozesse all diese Aspekte einbeziehen und gleichzeitig auf kontinuierlich betriebene Konfigurationen abzielen, die GO zurückhalten können.

Resumen

Día a día, gota a gota, el agua dulce empieza a escasear.

Por eso se persigue la reutilización del agua. Existen varias opciones de tratamiento, desde el biológico hasta el físico y químico avanzado. Debido al bajo consumo energético, la adopción del tratamiento anaeróbico de las aguas residuales está ganando consenso y popularidad. El tratamiento anaeróbico de las aguas residuales ofrece la oportunidad de recuperar recursos como el biogás y los nutrientes. Sin embargo, sus aplicaciones en esquemas de reutilización del agua son todavía escasas. Una de las limitaciones de esta tecnología es la lenta transferencia de electrones entre especies, que limita la degradación de la materia orgánica.

Además, la presencia de microcontaminantes orgánicos (OMPs) en el agua constituye otra limitación para el empleo del tratamiento anaerobio con fines de reutilización del agua. Los OMPs, como los productos farmacéuticos y de cuidado personal presentes en bajas concentraciones (es decir, ng/L - µg/L), son especialmente preocupantes debido a sus posibles efectos nocivos a largo plazo. Los OMPs son difíciles de eliminar en tratamientos anaerobios. En su lugar, se suelen aplicar tecnologías de tratamiento avanzadas (y más intensivas en energía) para eliminar los OMPs de las aguas residuales.

Una posible solución para superar este reto es la introducción de nanomateriales conductores de bajo coste, que estimulan la degradación de la materia orgánica mediante la mejora de la transferencia de electrones entre microorganismos anaerobios. El objetivo de esta tesis doctoral era explorar el diseño de un sistema híbrido de nanoingeniería en el que el tratamiento biológico anaerobio se estimula con óxido de grafeno (GO). El trabajo se centró en la eliminación de OMPs y la producción de metano, partiendo de configuraciones por lotes. Para permitir una mejor comprensión del sistema híbrido propuesto, se persiguieron los siguientes objetivos de investigación:

- Recopilación, evaluación y comparación de los estudios disponibles sobre sistemas biológicos anaerobios enmendados con materiales basados en grafeno.

- Evaluación del impacto de la adición de GO en las eficiencias de eliminación de los OMPs seleccionados, sus vías de biotransformación, y en la producción específica de metano utilizando ensayos de potencial bioquímico de metano (BMP).

- Evaluación del impacto de la adición de GO en experimentos BMP a largo plazo sobre la cinética de degradación de dos sustratos en diferentes condiciones de velocidad límite.

Tras evaluar minuciosamente las condiciones experimentales adecuadas, como los niveles apropiados de concentración de GO, se realizaron ensayos por lotes. El GO es un material altamente hidrófilo y tiene propiedades aislantes, pero al reducir sus funcionalidades de oxígeno y restaurar parcialmente la estructura conjugada del grafeno, el óxido de grafeno reducido (RGO) resultante gana conductividad eléctrica. Se comprobó que la reducción biológica del GO a partir de comunidades anaerobias mixtas se producía en las primeras 24 horas. Cabe destacar que este es el primer estudio que demuestra que la formación de GO reducido biológicamente (bioRGO) se produjo en un inóculo anaeróbico mixto muestreado de una instalación de digestión a gran escala en lugar de en cepas bacterianas individuales o seleccionadas. Para demostrar la biorreducción del GO se emplearon diferentes técnicas de caracterización, como la espectroscopia Raman, la voltamperometría cíclica, el analizador láser de tamaño de partícula y la microscopía óptica. Las mediciones indicaron un aumento de la relación I_D/I_G (relación de intensidad de las bandas D y G medida con espectroscopia Raman) de 0,74 a 1,01 en un día, un aumento de las actividades redox y un mayor tamaño de los flóculos, respectivamente. Así pues, estas pruebas indicaban la formación de bioRGO, que sentaba las bases para una mayor transferencia de electrones debido a la conductividad eléctrica inherente al RGO.

Independientemente de la adición de GO, la eliminación de los dos OMP indicadores seleccionados (es decir, sulfametoxazol y trimetoprima) alcanzó el 90% en 48 horas. Por tanto, no se observó ninguna mejora notable en su eliminación tras la adición de GO. No obstante, la presencia de unos 50 mg de GO por g de sólidos volátiles (VS) inhibió la formación de los productos de transformación (TPs) identificados del sulfametoxazol, mostrando una formación parcial de los TPs en comparación con el experimento de control, sin adición de GO (es decir, 16% y 40% de formación de TP257 de la cantidad inicial del compuesto original, respectivamente). Así, aunque no hubo un impacto aparente del GO en la cinética de eliminación del compuesto original, el análisis de los TPs demostró su impacto en las vías de biotransformación del

sulfametoxazol, con un número decreciente de TPs al aumentar la concentración de GO. Además, se detectó la presencia de TPs de sulfametoxazol en los experimentos con lodos esterilizados (es decir, tratados en autoclave) (12% de formación de TP253 en comparación con el compuesto original), lo que sugiere un papel de las enzimas resistentes a la temperatura en la biotransformación de este antibiótico, posiblemente liberadas por los lisados celulares tras el tratamiento en autoclave. Por otro lado, la adición de GO causó una inhibición del biogás de hasta el 21% para concentraciones superiores a unos 10 mg_{GO}/g_{VS}.

Basándose en estos resultados, la investigación sobre ensayos por lotes se amplió temporalmente para simular sistemas continuos. Se llevó a cabo una estrategia de alimentación fed-batch consistente en cinco ciclos de alimentación posteriores con dos sustratos estándar (es decir, glucosa y celulosa), centrándose en la producción de metano y en los valores cinéticos de degradación obtenidos mediante modelos. Se planteó la hipótesis de que diferentes mecanismos podrían inhibir el rendimiento esperado y mejorado de producción de metano de los sistemas modificados con GO. Sin embargo, esta inhibición es temporal y se limita a la fase inicial. Los principales factores identificados fueron (i) el consumo de electrones del sustrato utilizado para la reducción biológica del GO; (ii) la inhibición bacteriana inicial causada por la adición del nanomaterial; y (iii) la adsorción del sustrato al material de grafeno, en lugar de su transformación en biogás.

Aunque no se observaron mejoras ni inhibiciones durante los dos primeros ciclos de alimentación, a partir del tercero se observaron mejoras significativas ($p < 0,05$) en la cinética de degradación para ambos sustratos empleados cuando se utilizaron concentraciones superiores a 10 mg_{GO}/g_{VS}. Por tanto, la adopción de múltiples alimentaciones demostró que el efecto inhibidor del GO se limita a la fase inicial. Por otro lado, se adoptó la misma estrategia de realimentación en reactores anaerobios discontinuos en condiciones de carga orgánica excesiva. Los resultados confirmaron la mejora de la cinética de degradación y ampliaron la comprensión de la enmienda con GO para la recuperación de sistemas anaerobios acidificados.

En general, la tesis reveló que el tratamiento biológico anaeróbico combinado con GO es recomendable en sistemas de funcionamiento continuo. Sin embargo, debería realizarse una evaluación del ciclo de vida del GO para prevenir cualquier posible liberación al medio ambiente. Del mismo modo, los impactos de este nanomaterial en sistemas continuos a nivel microbiano

están ampliamente inexplorados y se desconocen los efectos a largo plazo. Junto con una caracterización microbiana exhaustiva de los cambios de la comunidad microbiana, la investigación del destino de un conjunto más amplio de OMP y sus TP arrojaría más luz sobre los efectos de los bioRGO en los sistemas AD. Por lo tanto, los futuros bioprocesos híbridos de nanoingeniería deberían incluir todos estos aspectos y, al mismo tiempo, aspirar a configuraciones de funcionamiento continuo capaces de retener el GO.

Resum

Dia a dia, gota a gota, l'aigua dolça esdevé escassa.

Per això es persegueix la reutilització de l'aigua. Hi ha diverses opcions de tractament disponibles, des de biològiques fins a tractaments físics i químics avançats. Degut a la baixa necessitat d'energia, l'adopció del tractament d'aigües residuals anaeròbies està guanyant consens i popularitat. El tractament d'aigües residuals anaeròbies implica l'oportunitat de recuperar recursos com el biogàs i els nutrients. No obstant, les seves aplicacions en esquemes de reutilització d'aigua encara són escasses. Una de les limitacions d'aquesta tecnologia és la lenta transferència d'electrons entre espècies, que limita la degradació del material orgànic.

A més, la presència de microcontaminants orgànics (OMPs) a l'aigua constitueix una restricció addicional a l'ús del tractament anaerobi per a la reutilització d'aigua. Els OMPs, com ara els productes farmacèutics i de cura personal presents a baixes concentracions (és a dir, ng/L - µg/L), són de particular preocupació per les seves possibles efectes perjudicials a llarg termini. Els MCO són difícils de treure en tractaments anaerobis. En lloc d'això, s'apliquen tecnologies de tractament més avançades (i més intensives en energia) per eliminar els OMPs de l'aigua residual.

Una possible solució per superar aquest desafiament és la introducció de nanomaterials conductors de baix cost, que estimulin la degradació del material orgànic mitjançant la millora de la transferència d'electrons entre microorganismes anaerobis. Aquesta dissertació tenia per objectiu explorar el disseny d'un sistema híbrid nanoenginyat en què el tractament biològic anaerobi es stimulés amb òxid de grafè (GO). El treball es va centrar en la eliminació de OMPs i la producció de metà, partint de configuracions de lot. Per permetre una millor comprensió del sistema híbrid proposat, es van perseguir els següents objectius de recerca:

- Recopilació, avaluació i comparació d'estudis disponibles sobre sistemes biològics anaerobis modificats amb materials basats en grafè.
- Avaluació de l'impacte de l'addició de GO en l'eficiència de remoció dels OMPs seleccionats, les seves vies de biotransformació i en la producció específica de metà mitjançant assajos de potencial de metà bioquímic (BMP).

- Avaluació de l'impacte de l'addició de GO en experiments de BMP a llarg termini sobre la cinètica de degradació de dos substrats en diferents condicions de limitació de velocitat.

Després d'avaluar a fons les condicions experimentals adequades, com ara els nivells adequats de concentració de GO, es van realitzar assajos per lots. El GO és un material altament hidrofílic i té propietats aïllants, però reduint les seves funcionalitats d'oxigen i restaurant parcialment l'estructura conjugada del grafè, el grafè oxidat reduït resultant (RGO) adquireix conductivitat elèctrica. Es va comprovar que la reducció biològica del GO a partir de comunitats anaeròbiques mixtes va ocórrer en les primeres 24 hores. Sorprenentment, aquest va ser el primer estudi que demostrava que la formació de GO biològicament reduït (bioRGO) va ocórrer en un inòcul mixt anaeròbic mostrejat d'una instal·lació de digestor a escala completa en lloc de sòls o soques bacterianes seleccionades. Diferents tècniques de caracterització van participar en la demostració de l'èxit de la bioreducció de GO, com ara l'espectroscòpia Raman, la voltametria cíclica, l'anàlisi de mida de partícules làser i la microscòpia òptica. Les mesures van indicar un augment de la relació I_D/I_G (relació d'intensitat de les bandes D i G mesurada amb espectroscòpia Raman) de 0,74 a 1,01 en un dia, una activitat redox millorada i una mida de flòc més gran, respectivament. Així, aquesta evidència va indicar la formació de bioRGO, la qual cosa va establir les bases per a una transferència d'electrons millorada a causa de la conductivitat elèctrica inherent del RGO.

Independentment de l'addició de GO, la remoció dels dos OMPs indicadors seleccionats (és a dir, sulfametoxazol i trimetoprim) va arribar al 90% en 48 hores. Així, no es va observar cap millora notable en la seva eliminació després de l'addició de GO. No obstant, la presència d'aproximadament 50 mg de GO per g de sòlids volàtils (VS) va inhibir la formació dels productes de transformació (TPs) identificats de sulfametoxazol, mostrant una formació parcial de TPs en comparació amb l'experiment de control sense GO afegit (és a dir, formació del 16% i el 40% del TP257 de la quantitat inicial del compost pare, respectivament). Així, tot i que no hi va haver cap impacte aparent del GO en la cinètica de la remoció del compost pare, l'anàlisi dels TPs va demostrar el seu impacte en les vies de biotransformació de sulfametoxazol, amb una disminució del nombre de TPs amb l'augment de la concentració de GO. A més, es van detectar TPs de sulfametoxazol en els experiments amb fangs esterilitzats (és a dir, autoclavats) (formació del 12% del TP253 en comparació amb el compost pare), suggerint un paper d'enzims resistents a la temperatura en la biotransformació d'aquest antibiòtic, possiblement alliberats per la lisi cel·lular

després de l'autoclavat. D'altra banda, l'addició de GO va provocar una inhibició del biogàs d'un 21% per concentracions superiors a aproximadament 10 mg$_{GO}$/g$_{VS}$.

Basant-se en aquests resultats, la investigació en assajos per lots es va ampliar temporalment per simular sistemes continus. Es va realitzar una estratègia d'alimentació en lots consistents en cinc cicles d'alimentació successius amb dos substrats estàndards (és a dir, glucosa i cel·lulosa), centrant-se en la producció de metà i en els valors cinètics de degradació obtinguts pel model. Es va hipotetitzar que diferents mecanismes podrien inhibir el rendiment esperat i millorat de la producció de metà dels sistemes amb GO afegit. No obstant, aquesta inhibició és temporal i es limita a la fase inicial. Els principals factors identificats van ser: (i) el consum d'electrons del substrat utilitzat per a la reducció biològica de GO; (ii) la inhibició bacteriana inicial causada per l'addició del nanomaterial; i (iii) l'adsorció del substrat al material de grafè, en lloc de la seva transformació en biogàs.

Tot i que durant els dos primers cicles d'alimentació no es van observar millores ni inhibicions, a partir del tercer cicle es van observar millores significatives (p <0,05) en les cinètiques de degradació per a ambdós substrats utilitzats quan es van utilitzar concentracions superiors a 10 mg$_{GO}$/g$_{VS}$. Per tant, l'adopció de múltiples alimentacions va demostrar que l'efecte inhibidor de GO està limitat a la fase inicial. D'altra banda, la mateixa estratègia de re-alimentació es va adoptar en reactors de lot anaerobis sota condicions d'excés de càrrega orgànica. Els resultats van confirmar les cinètiques de degradació millorades i van ampliar la comprensió de l'addició de GO per a la recuperació de sistemes anaerobis acidificats.

En general, la tesi va revelar que el tractament biològic anaerobi combinat amb GO es fomenta en sistemes d'operació contínua. No obstant això, s'hauria de desenvolupar una avaluació del cicle de vida de GO per prevenir qualsevol possible alliberament ambiental. De manera similar, els impactes d'aquest nanomaterial en sistemes contínus a nivell microbial són àmpliament inexplorats i els efectes a llarg termini són desconeguts. Juntament amb una caracterització microbiana exhaustiva dels canvis de la comunitat microbiana, la investigació del destí d'un conjunt més ampli d'OMPS i les seves TPs llançarien més llum sobre els efectes del bioRGO en els sistemes d'AD. Per tant, els futurs bioprocessos híbrids nano-enginyerats haurien d'incloure tots aquests aspectes mentre es busca la configuració d'operació contínua capaç de retenir GO.

1. Introduction

1.1. Motivation and background

Actual and future climate challenges will stress the water supply in many regions [1]. At the same time, potentially usable water for low water quality applications (such as irrigation) is discharged to water bodies rather than reused. The EU has recently stepped forward with new regulations and guidelines on minimum requirements for water reuse for agriculture irrigation [2,3]. Adopting a circular economy approach in the water field could help reduce the water demand and use reclaimed water in a cascade of applications according to its intended use and quality [4].

Anaerobic treatment is one of the most promising wastewater treatment technologies in recovering water and nutrients that can be energy neutral or even energy positive [5]. Anaerobic treatment indeed allows energy recovery in the form of energy-rich biogas and nutrients in the form of biosolids, which can be applied as a soil amendment.

On the other hand, the discharge of OMPs to water bodies is of increasing concern to society due to their persistence, ubiquitousness, and environmental and human health implications of their continuous exposure [6]. The most frequently investigated OMPs include pharmaceutically active compounds (PhACs), personal care products, and pesticides, and some of these (e.g., octocrylene, macrolide antibiotics) are included in the Water Framework Directive (WFD) Watch list as chemicals of potential concern [7,8].

Although anaerobic wastewater (WW) treatment is generally less effective in removing OMPs, it still has the potential to biotransform several classes of pollutants persistent to aerobic degradation to less persistent and less toxic forms, such as halogenated aromatics, e.g., polychlorinated biphenyls (PCBs), iodinated contrast media (ICM), nitroaromatics, dyes, sulfonamides, and many others [9]. However, these transformations usually proceed at slow rates because of electron transfer limitations [10]. Electron transfer involves the use of indirect interspecies electron transfer (IIET), such as hydrogen or formate. These molecules are capable of being oxidized and reduced reversibly; thus, they can carry electrons with them and let the anaerobic process proceed. The carried electrons perform the main chemical and biological reactions of the two dominant communities in an anaerobic treatment, i.e., the bacteria (hydrogen

and acetate producing) and the archaea (including hydrogen and acetate consuming methanogens). Due to the low thermodynamic yield and slow electron transfer process, anaerobic systems are subject to various drawbacks, which may ultimately lead to failure. For example, different growth kinetics between acidogenic bacteria and acetoclastic methanogens may favor the accumulation of volatile fatty acids (VFAs), resulting in an acidic environment ($pH < 6.0$), inhibiting to methanogens [11].

1.2 Direct interspecies electron transfer

A new electron transfer process has been identified, which does not involve any indirect interspecies such as hydrogen or formate. Direct interspecies electron transfer (DIET) can enhance anaerobic treatment performance by directly connecting the microorganisms present in the medium [12]. DIET can be achieved through biological nanowires, e-pili, or conductive abiotic materials (Figure 1-1). The main advantage of DIET over IIET is the possibility of relying on cell-to-cell connection rather than depending on the availability of redox mediators. The benefits include avoiding the development of an acidified environment due to VFAs accumulation or high hydrogen partial pressure.

Since biological DIET can occur only for some bacteria such as *Geobacter*, and certain energy would be needed for such bacteria to produce these filamentous protein extensions, scientists started to investigate the use of conductive material to enhance DIET [14]. Conductive materials employed for electron transfer purposes are usually carbon-based materials, such as granular activated carbon (GAC), powdered activated carbon (PAC), biochar (BC), reduced graphene oxide (RGO), carbon nanotubes (CNTs), or iron oxides, such as magnetite (Fe_3O_4) and hematite (Fe_2O_3) [15]. These materials are characterized by the high electrical conductivity and often high specific surface area. Syntrophic bacteria can attach to the surface of these conductive materials and use them for electron exchange, resulting in an enhanced DIET [16]. Using an artificial conductive material avoids the synthesis of conductive pili, an energy- and time-consuming process for microbes.
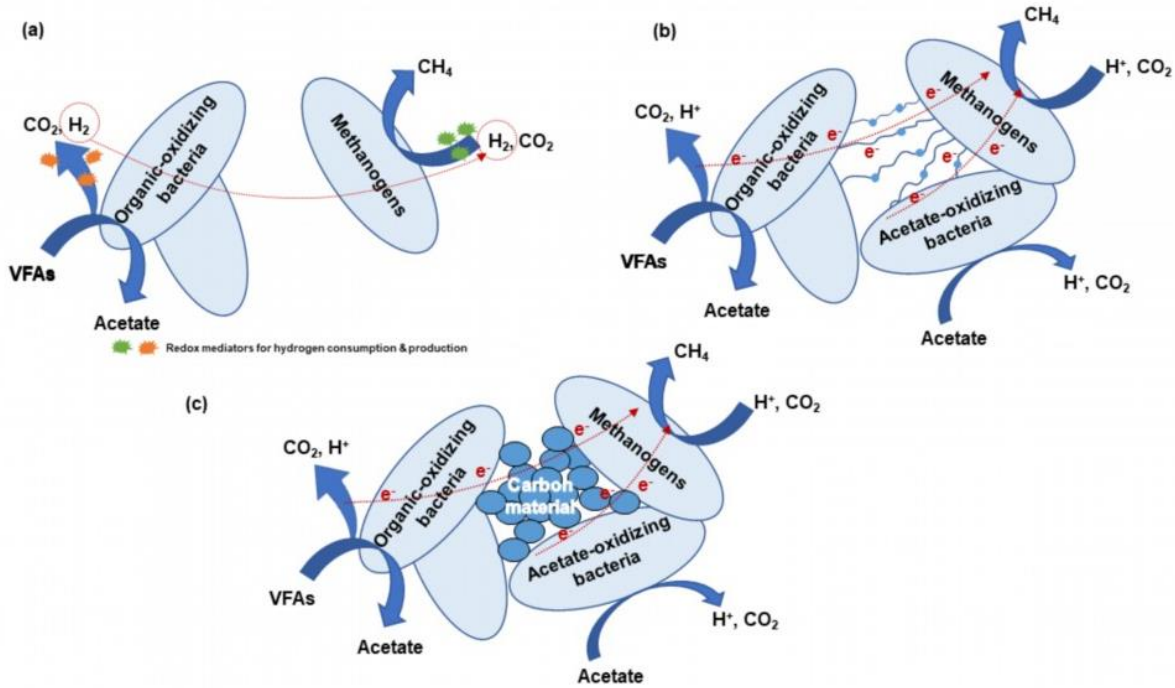
Figure 1-1: Illustrations of (a) indirect interspecies electron transfer (IIET), (b) direct interspecies electron transfer (DIET) via biological nano-wires, and (c) DIET via carbon-based material (figure adapted from Baek et al., 2018 [13]).

The addition of conductive materials can increase methane production and enhance the tolerance of the microbial community to higher organic loading rates [17,18]. Among the carbon-based materials listed above, graphene may perform better than other carbon materials like GAC but with lower dosages. For example, GAC concentrations adopted for DIET purposes range from 0.5 to 5 g/L, while graphene dosages are only around 0.1 g/L, achieving similar stimulation of the methanogenesis [19].

1.3. Biologically reduced graphene oxide (bioRGO)

Low-cost graphene oxide (GO), which has a similar structure to graphene, but presents some defects due to oxygen functional groups, can be reduced to RGO through its biological reduction when these defects are partially restored (Figure 1-2).
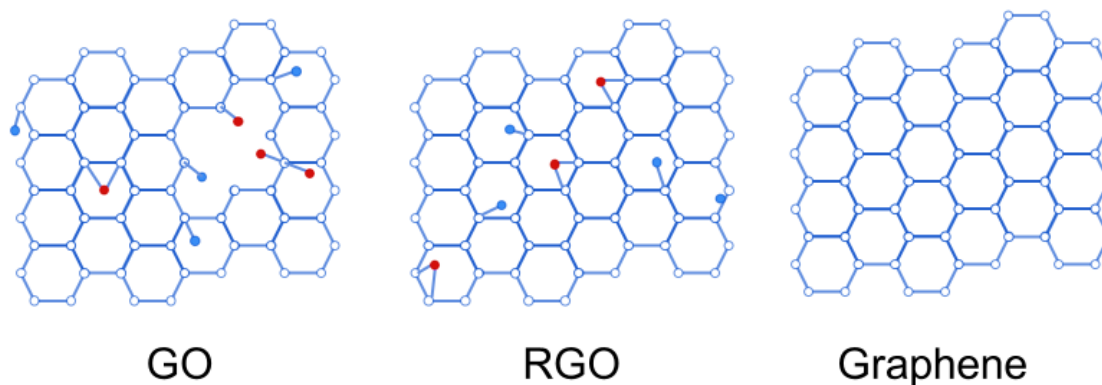
Figure 1-2: Illustrations of the structure of graphene oxide (GO), reduced graphene oxide (RGO), and graphene.

Water-soluble GO added to an anaerobic consortium is reduced to bioRGO through bacterial respiration using single and mixed bacterial strains [20–22]. Previous studies demonstrated that GO can serve as an external electron acceptor, thus reducing it in a matter of hours [23] or a few days (2.5 days) [20]. Hence, it can acquire relatively high conductivity and enhance the electron transfer within the anaerobic microbial community. Table 1-1 provides an overview of the studies available in literature where GO and RGO were used in biological systems along with the employed operational conditions. As can be seen, most of the studies achieved bioRGO formation using different type of microbial communities in diverse reactor configurations.

Table 1-1: GO reduction and RGO uses in biological systems.

Material	Dose	Inoculum	Substrate	Reactor						Remarks	Reference
				Type	Working Volume (L)	pH	HRT (h)	Temp. (°C)	Mixing (rpm)		
GO	500 mg/L	*E. Coli* biomass	Luria-Bertani broth	Batch	0.5		72	37	120	Reduction of GO using *E. Coli* in aqueous medium. Confirmed by UV–visible spectroscopy, SEM and Raman spectroscopy.	[21]
GO		*E. Coli*	Luria-Bertani broth. Glucose at 0.2 g/L	Batch Anaerobic		7	0-48	37		GO reduction mainly due to metabolic activity of bacteria, partly to glucose. Without glucose addition GO reduction is not significant. While GO seems biocompatible, bioRGO inhibits proliferation and reduces metabolic activity of bacteria.	[24]
GO	200 mg/L	*Ca. Brocadia* and *Ca. Scalindua*	Inorganic synthetic medium	Batch Anoxic	0.1	7.5-8.0	24	35 (*Brocadia*) and 20-25 (*Scalindua*)	150	Ammonium oxidation can be carried out via GO as external electron acceptor, rather than via nitrites and nitrates. Raman spectroscopy confirmed GO reduction by anammox bacteria.	[25]
GO	170 mg/L	*Shewanella* spp., *E. Coli*, *Bacillus subtilis*, *Acetobacter tropicalis*, *Weissela Cibaria*	Sodium acetate medium	Batch Anaerobic	0.011	6-6.5, 5.5-6.0, and 7		28		Not all the anaerobic communities can form bioRGO-hydrogel. Dead cells were still able to reduce GO, suggesting an enzymes role in GO bioreduction. The secreted EPS seems to work as a "glue" for cell attachment.	[26]
GO	500 mg/L	*Shewanella oneidensis*	Tryptic Soy Broth	96 well plates Aerobic &			48	Room temp.	250	Higher surface-area-to-thickness ratio and better storability of microbially-RGO compared to chemically-RGO with	[27]

				Anaerobic						hydrazine. Conductance increased of 2.1 to 2.7 orders of magnitude. No harmful effects on bacteria cells by GO.	
GO	1, 5, 10, 20, 50, 100, and 150 mg/L	*Shewanella putrefaciens CN-32*	Sodium lactate	Luria-Bertani (LB) medium			48-60	30	150	In 48 h bioRGO was formed, and at 60 h precipitated. Biological GO reduction was confirmed by increased I_D/I_G ratio.	[28]
GO	60 mg/L	AOB, NOB	Glucose and NO_3-N	Aerobic Erlenmeyer Flask	1.5	7.0	4	25	140	GO promoted bioactivity of ammonium nitrifying bacteria and EPS production.	[29]
GO	88.6 mg/L	Mixed community of EA microbes	Sodium acetate	Bio-Electrochemical System (BES) Anoxic				22		Operated for 110 days. GO reduced in 2.5 days to RGO forming thick biofilms	[22]
GO	200 mg/L	5 *Shewanella* strains	Lactate	Serum bottle Anaerobic	0.01					72 h total incubation time. Visually evident reduction after 24 h. XPS analysis confirmed loss of oxygen, and increase of C—C bonds from 28% (GO) to 95% (bioRGO).	[20]
GO	150 and 5 to 50 mg/L	Light AND Freshwater algae: *Chlorella pyrenoidesa*		Quartz-tube	0.1	6.95-7.05		25		GO at 150 mg L^{-1} was photoreduced in 8 days, confirmed from Raman and XPS spectra. Photo-reduced GO inhibits growth inhibition up to 66%, more than GO (55%). Physical membrane damage was significant due to produced low molecular weight species from GO reduction.	[30]
GO	0 to 150 mg/L	Anammox bacteria from lab scale upflow column reactor	$(NH_4)_2SO_4$ and $NaNO_2$	Batch Anaerobic	0.1		42	35	150	At 100 mg/L of GO, the anammox activity increased of 10.26% compared to the control.	[31]

				Serum bottle					EPS production is also increased. However, at 150 mg/L of GO both the anammox activity and EPS production are inhibited.	
GO	500 mg/L	Three microalgal strains *Leptolyngbya* JSC-1, *Scenedesmus vacuolatus* (211-11n), *Chlorella saccarhophilum* (211-9a)		Thermostatic bath	0.2	24 h	95		Efficient reduction of GO. RGO used then to adsorb heavy metals at 100 mg/L. RGO adsorbed up to 93% of Cu in 30 mins. Almost complete adsorption was seen after 6 hours.	[32]
GO		*Shewanella oneidensis* MR-1	Quinone						GO reduction by microbially reduced anthraquinone-2-sulfonate.	[33]
GO	5, 25, 50, 152.5, and 300 mg/L	Full scale UASB	Starch or glucose	Glass serum bottles	0.05		25		GO sheets wrap the starch granule, this limits the hydrolysis and thus only the soluble starch will be available for methanogenesis	[34]
GO	10, 50 and 300 mg/L	Full scale granular UASB	Basal medium + acetate or methanol at 2 g COD/L (or H2)	Serological bottles	0.01		30	120	Microbial reduction of GO had adverse effect on methanogenesis because electrons from oxidized substrates were used to reduce GO.	[35]
GO	100, 200, 400, 600, 800, 1000 mg/L	*Geobacter Sulfurreducens*	DMSZ medium + 20 mM acetate + 50 mM fumarate	Sealed serum vial	0.02	216	30	0 (static)	Biologically GO reduction proved by electrochemical test, TEM, SEM, FTIR, XPS, XRD, Raman, and UV-vis. A mechanism for extracellular electron transfer at cell/GO interface was proposed.	[23]
GO	20 mg/L	*E. coli*	Luria-Bertani (LB) medium	Aerobic and anaerobic saline			37	Contin.	30 minutes aerobic GO reduction that led to cell death due to the formation of superoxide anions. XPS,	[36]

				cell suspension						XRD, Raman and FTIR spectroscopy results confirmed the aerobic GO reduction by *E. coli*.	
G and GO	5 and 100 mg/L	granular sludge	Synthetic wastewater	SBR	0.5	7.0	24			60 days. I_D/I_G ratios increased for all the four different conditions. Biological transformation of graphene material occurred. Shift in microbial species.	[37]
G and GO	1 and 5 mg/L	Aerobic activated sludge	Synthetic WW	SBR	3.5		24			Operated for 10 days. Significant reduction, especially for GO rather than G, in COD and nutrients removal performance, but steady state after 8 days. Some microorganisms are not sensitive to G and GO presence.	[38]
GO and RGO	0, 0.5, 5, 10, 50, 100, 250, 500 mg/L	*E. Coli Staphylococcus aureus*	Luria-Bertani medium	96 well plates			2 d	37	0 and 250	Cell growth inhibition for RGO at 50 to 250 mg L^{-1}. GO enhanced biofilm formation and cell growth at 50 to 500 mg L^{-1}. XPS analysis showed decreased intensities of C—O peaks, indicating GO reduction due to bacteria activity. RGO was oxidized by LB medium and bacteria, producing ROS.	[29]
RGO	15 mg/L	Suspended anammox sludge	Synthetic mineral medium	SBR < 0.1 DO	5.0	7.6	24	10-30		17% increase in anammox activity. After 109 days, Raman analysis confirmed RGO oxidation.	[39]
RGO	100 mg/L	Activated sludge	Synthetic	Upflow column reactor Anoxic (<0.5 DO)	0.3	7.0	6	35		Anammox start-up time reduced by 27%. Removal rate of total nitrogen increased of 27%.	[40]

Some studies show the capability of certain microorganisms to reduce GO at room temperature through their cytochromes [27,41], while others demonstrated the reduction of GO in hydrogel matrices [26]. Surprisingly, Shen et al. [26] found evidence of anaerobic reduction of GO in assays containing dead cells, suggesting possible participation of the enzyme in the GO reduction process. However, other studies reported that enzymatic reactions were involved in the oxidation of GO or its degradation, rather than its reduction [42,43]. Therefore, enzymes involvement concerning GO reduction should require a specific investigation.

Besides, it is also interesting to understand the process behind such biological reduction of GO and the role played by GO. Jiao et al. [44] investigated the GO reduction pathway using *Shewanella oneidensis* MR1 bacteria in an anaerobic environment. They revealed that several proteins were involved in the Mtr respiratory pathway and used GO as an electron acceptor. Also, they found a faster reduction when external electron shuttles such as riboflavin and 9,10-anthraquinone-2,6-disulfonicacid (AQDS) were added to the system. Lu et al. [23] proposed an analogous mechanism for GO reduction occurring at the outer cell of *Geobacter sulfurreducens* and the GO interface.

However, the role of GO does not seem to be merely of an electron sink; it also plays a role in the microorganisms' metabolism. Yoshida et al. [45] demonstrated that the growth of selected electrochemically active bacteria (or exoelectrogenic bacteria) depends on the GO presence. Exoelectrogenic bacteria, such as *Geobacters* (capable of DIET [46]), were found within the GO structure. The produced bioRGO and the microbes tend to aggregate and form a complex, probably due to π-π stacking [47]. For example, Virdis et al. [22] have proven that a mixed anaerobic community could reduce GO and make a porous network of bioRGO and bacteria that supports the biomass growth and enhances electron exchange.

1.4. Impact of bioRGO on the removal and biotransformation of OMPs

The biological reduction of GO could also lead to a faster OMPs transformation (Table 1-2). Enhanced biological reduction of OMPs to non-halogenated metabolites (e.g., by the cleavage of halide substituents), amino-substituted products (e.g., by the reduction of nitro to the amino group), and other products less persistent to aerobic degradation would facilitate their downstream degradation by aerobic biological treatment or simply lower their environmental persistence. For

example, anaerobic environments and the presence of graphene promoted the conversion of persistent pollutants, such as nitrobenzene and iopromide, to their more biodegradable and oxidizable equivalents, aniline and deiodinated iopromide, respectively [48,49]. Colunga et al. [50] observed a 3.6-fold increase in the reduction rates of azo dyes under anaerobic conditions within 150 hours by adding 5 mg/L of GO. Similarly, GO at 2 mg/L improved the anaerobic reduction of nitrobenzene to aniline [51]. Iopromide underwent complete dehalogenation, for which up to 70% removal was observed within ten days by adding 5 mg/L of magnetic nanoparticle-containing RGO [52]. A similar study on iopromide by Toral-Sanchez et al. [53] reported a 5.2-fold increase in the removal rate of iopromide when RGO was added. Moreover, Wang et al. [49] demonstrated the enhanced biotransformation of nitrobenzene when GO is amended to anaerobic sludge.

There are two main mechanisms that seem responsible for removing OMPs such as azo dyes, nitro compounds, and iodinated compounds, and for the enhanced degradation noticed in anaerobic culture amended with GO. The first is adsorption through the porous GO/RGO structure, and the second is biodegradation by the bacterial consortia. Studies show that π bonds can promote the adsorption of aromatic organic contaminants [54]. All organic pollutants that are electron acceptors can undergo a transformation process if placed in a reductive environment, like the anaerobic one [55].

However, it is unclear which mechanisms leads to enhanced removal for processes the contain the bioRGO complex. For example, researchers have proposed that once bioRGO is formed, the graphene material within it acts as a core network platform for enhancing the electron activity of the bacterial consortium and fostering the microbial connection. To confirm such a supposition, Wang et al. [56] indirectly measured the electron transport activity through the dehydrogenase activity (DHA), showing that the catalytic activity increased significantly. Also, a critical role in bridging and creating connections between bacterial cells and the graphene sheets is provided by the excretion of extracellular polymeric substances (EPS). In fact, a positive correlation was found between excreted EPS and enhanced biotransformation of nitrobenzene [49,56] and 2-chloroaniline [57]. At the core of such enhanced catalytic processes seems to be the presence of zigzag edges and GO defects [58,59]. In fact, Gao et al. [58] found that for both RGO and GO, the conversion yield of nitrobenzene into aniline was 94.2% and 91.1%, respectively, for repeated

cycles. On the contrary, the conversion yield for graphene (produced by the arc-discharge method) reached only 13.1%.

BioRGO might also be responsible for accentuating or suppressing specific enzyme and catalytic activities, leading to the biological transformation of organic contaminants. Gonzalez-Gil et al. [60] showed that the addition of oxidizing or reducing cofactors (e.g., GO) triggered oxidoreductase activities, which led to the biotransformation of some OMPs, i.e., acesulfame, acyclovir, and iopamidol.

Another critical role seems to be played by donors of electrons such as glucose for the reduction of nitrobenzene. Although an AD system involves the production of VFAs, which is an easily carbonaceous substrate to be assimilated by the microorganisms, VFAs do not seem to be used for nitrobenzene reduction [61]. Only in the presence of glucose and RGO, Li et al. [61] observed a complete transformation of nitrobenzene into aniline in 20 hours, while two days were needed in the absence of RGO. Meanwhile, when only anaerobic sludge was present (i.e., without RGO and glucose added), the removal proceeded much more slowly (i.e., in 60 hours) and only about 20% nitrobenzene was transformed. Similarly, Tawfik et al. [62] reported an 18% increase in the bioreduction of 4-nitrophenol to 4-aminophenol in a multistage anaerobic system.

Overall, bioRGO systems have shown potential for enhancing the biodegradation OMPs. Nevertheless, to date, no studies have yet investigated the potential impact of bioRGO on the biotransformation pathways of OMPs, which can have significant implications for their environmental fate and toxicity. Their TPs may have different physicochemical properties, toxicity, and environmental fate compared to the parent compounds. Therefore, besides the OMPs removal, assessing their biotransformation pathways can help predict their fate in the environment and evaluate their potential risks to human health and the ecosystem.

Table 1-2: Organic micropollutants (OMPs) removal and degradation for different studies involving graphene oxide (GO).

OMP and dose	Graphene material and dose	Inoculum	Substrate	Reactor						Remarks	Reference
				Type	Working Volume	pH	HRT	Temp. (°C)	Mixing		
Nitrobenzene at 0.8 mM	GO	*Shewanella putrafaciens*	Lactate	Serum bottles	100 mL			30	150	RGO presence increased the reduction efficiency of nitrobenzene	[28]
Methyl orange at 50 mg/L	GO	*Shewanella oneidensis MR-1*	MM medium	Serum bottles	160 mL	7.0-7.2		30	90	In 30 min, GO-containing condition achieved 89.7% MO removal compared to 84.2% in the control condition	[63]
Reactive red 2 and 3-chloronitrobenzene at 0.05 mM	GO at 2.5-50 mg/L	Anaerobic granular sludge	Basal medium and sulfide	Batch	60 mL			25	120	Simultaneous presence of sulfide and GO allowed a 99% reduction of reactive red in 170 h.	[50]
4-nitrophenol	Chemically RGO at 30 mg/gVS	Anaerobic digester	Industrial wastewater	Multistage anaerobic reactor	27.6 L		8.3 h	17-33		Continuously operated system over 300 days achieved $65.6 \pm 4.8\%$, while with GO $83.7 \pm 4.9\%$.	[62]
Congo red at 0.05-0.4 g/L, methylene blue at 0.01-2.0 g/L	GO prepared from graphite through modified Hummer´s method	*Shewanella xiamenensis BCO1*	Synthetic dye wastewater	Batch	24 mL	6, 7, 8, 9		22, 28, 37		99% and 97% decolorization efficiency in 55 h for Congo red and methylene blue.	[64]
2-chloroaniline at 20 mg/L	0-80 mg/L 2-aminoanthraquinone-graphene oxide (AQ-GO)	Anaerobic sludge	Deoxiginated basal medium (pH 7)	Batch serum bottles	135 mL		30 d	30		Bacterial consortium was cultivated to enrich degrading-chloroanilines bacteria.	[57]
Iopromide at 400 µg/L	GO at 5 mg/L RGO at 5 mg/L (chemically, using L-ascorbic acid)	Anaerobic granular sludge (UASB)	1. Ethanol / lactate (1 g COD L^{-1}) 2. Na$_2$SO$_4$ (1 g sulfate L^{-1})	Batch	50 mL		48 h	30	125	Sludge acclimated for 30 days in lab-scale UASB reactors.	[48]

Iopromide	Magnetite containing RGO nanosacks	Methanogenic granular sludge from UASB	Basal medium (sulfide as electron donor)	Batch	50 mL	7.3	10 d			Up to 77% iopromide removal efficiency in 10 days. Some TPs are identified	[52]
Nitrobenzene at 0.4 mM	300 mg/L RGO	Anaerobic sludge	Glucose at 1 g L^{-1}	Serum bottles	180 mL	7.2		35	200	Electron donors like glucose are fundamental for nitrobenzene reduction. VFAs are not the utilized source to reduce nitrobenzene.	[61]

1.5. Impact of bioRGO on biogas production

BioRGO also impacts the biogas yield and a loss of BMP is an unavoidable side effect of its bioreduction. Electrons available in the system are allocated to reduce GO instead of being consumed for biogas production. Table 1-3 illustrates the performance comparison of different experimental set-ups where graphene materials were employed. Existing studies report contradictory findings, with both improvement in the biogas formation with the addition of GO (e.g., of up to 19.5%) [65] and negative impact and decrease in the formed biogas quantity (e.g., 17.1% less) [66].

For example, Bueno-Lopez et al. [67] evaluated the methanogenic activity of anaerobic sludge using two simple substrates, i.e., glucose and starch. They observed a 14% and 114% increase in the maximum methanogenic activity for the two substrates compared to the control after adding 300 mg/L of RGO. This finding is contrary to Zhang et al. [68], who found a decrease in the biogas formation by 13.1%, 10.6%, 2.7%, and 17.1% at GO concentrations of 5, 50, 100, and 500 mg/L, respectively. Other authors found a bell-shaped methane production inhibition related to the GO concentration. Therefore, a clear consensus on the impact of GO addition and concentration range for improvement or inhibition seems to be currently missing.

Table 1-3: Impact of graphene materials on biogas production.

Material	Dose	Inoculum	Substrate	Reactor						Remarks	Reference
				Type	Working Volume	pH	HRT	Temp. (°C)	Mixing		
98% graphene with 80% single layer ratio	30 and 120 mg/L	Anaerobic digestor	Synthetic WW + glucose (2000 mg COD / L)	Batch	150 mL			35	100 rpm	Increased methane production rates of 17.0% and 51.4%. Limited period. No blank, no positive control.	[69]
99% graphene nanoplatelets (<30 layers)	0, 0.5, 1.0, and 2.0 g/L	Lab-scale digester treating cellulose	Ethanol	Batch	300 mL	7.5		35		Improved methane yield for each concentration. 1.0 g/L achieved both the highest yield improvement of 25.0% and production rate of 19.5%.	[65]
Graphite, Graphene, GO	1.1mg/gvs (6.25 mg/L)	Municipal anaerobic digestor	Sewage sludge, Food waste	Batch	225 mL	7		55	120 rpm	All the three materials reached higher cumulative methane production (graphene > graphite > GO). Highest SMP reached by graphene was 36.09% higher than control.	[70]
GO	54 and 108 mg$_{NGO}$/gvs (720 and 1440 mg/L)	10 L anaerobic reactor	WAS	Batch	78 mL			35	100 rpm	Inhibition of cumulative methane production of 7% and 12.6%.	[71]
GO	5, 25, 50, 152.5, and 300 mg/L (8.3, 41.7, 83.3, 254, and 500 mg$_{GO}$/gvs)	1.5 L UASB reactor	Starch and glucose (100 mg COD / L)	Batch	50 mL			25		Only lowest GO concentration with glucose showed 10% increase. Limited to 40 h period. No blanks, no positive control.	[34]
GO	5, 50, 100, 500 mg/L (0.155, 1.55, 3.10, and 15.5 mg$_{GO}$/gvs)	Anaerobic digestate	Swine manure	AMPTS II	400 mL			37	150 rpm (1 min ON, 1 min OFF)	Bell-shaped methane production inhibition related to GO concentration. Lower CH$_4$ inhibition for 100 mg/L.	[66]
RGO	300 mg/L	Full-scale up flow anaerobic digester for	Glucose and starch	Batch				30	120 rpm	Maximum methanogenic activity improved up to 14% for glucose, and 114% for starch.	[35]

1.5. Impact of bioRGO on biogas production

		brewery WW								
RGO	10, 20, 30 mg/L (0.025, 0.05, 0.074 mg$_{GO}$/g$_{VS}$)	Municipal anaerobic digestor	Cow manure	Batch	300 mL	7.2	35	Not specified	Increase of 65% with 20 mgrGO/L is far higher than what tyipically reported. No blanks, no positive ctrl, plateau phase not reached, low ISR (0.60), no replicates, no data validation. Although the promising results, reproducibility is compromised.	[72]
RGO	0, 10, 20, 30 mg/L	Municipal anaerobic digestor	Municipal organic solid waste	Batch	300 mL		37		50% more biogas at 20 mg/L and ISR of 1 compared to control.	[73]

1.6. Toxicity of bioRGO

When understanding the role of GO in biological systems, an important aspect to be considered are mechanisms of its interaction with the microorganisms. Different mechanisms have been reported to inhibit the microbial growth for graphene-based materials, such as membrane and oxidative stress and wrapping isolation [74]. In particular, the wrapping effect was suggested to be related to the differences between the inner part of the GO layer compared with its borders. The GO edges may indeed represent the first region to get reduced and turn from hydrophilic (due to the oxygen functional groups) to hydrophobic, while the inner region would remain hydrophilic. These differences in properties within the same GO layer make it bend itself at the corners and wrap around the bacteria [26], thus inhibiting or limiting their proper growth and functioning.

In addition, the antimicrobial effect seems to be directly dependent on the concentration of graphene [75]. While GO concentration below 10 mg/L did not show any significant toxicity effects [50], 5,000 mg/L of GO led to a complete inhibition of the bacterial activity [76]. However, the bacteria were still alive. In fact, their inactivity was due to the wrapping effect of the graphene sheets. When the graphene was removed from the medium by using sonication, the bacteria regained their normal activity.

However, it is also important to distinguish between GO and RGO regarding the inhibitive impact of such nanomaterials on the microbial growth. Guo et al. [77] selectively examined the impact of both graphene materials on the biofilm formation. Interestingly, for the two microorganisms investigated (i.e., *E. coli* and *S. aureus*), GO enhanced the biofilm formation while RGO inhibited it when concentrations above 50 mg/L were applied. The antimicrobial effect of RGO became more significant when shaking was applied. On the other hand, Liu et al. [75] reported a higher antibacterial activity of GO compared to RGO at 40 mg/L for *E. coli* culture. Another study dealing with activated sludge (AS) systems pointed to GO's higher toxicity than graphene, possibly due to its oxygen functional groups and release of reactive oxygen species (ROS) due to the reduction of GO to RGO [38]. Although a significant performance reduction in the nutrient removal activities was noticed, the remaining cultures, tolerant to the nanomaterial, could still perform the nutrient removal. Therefore, a clear indication on the inhibitive concentration of GO seems to be lacking.

Another factor to examine when considering the interaction among the graphene material and the microorganisms is the contact or retention time (i.e., for how long the microbes are in contact with the nanomaterial). The aforementioned studies were conducted in batch set-up, i.e., a one-time GO application was performed, and GO impact assessment was limited to some days. Only one study expanded the timeframe to multiple cycles or feeds. Pan and Chen [28] observed a significant improvement in the survival rate of *Shewanella putrefaciens CN-32* from the second dose of substrate. This temporal inhibition was supposed to depend on the degree of GO reduction. Indeed, the presence of oxygen functional groups decreased for a reduced GO, and the toxicity impact on the culture was limited [78]. Therefore, it is suggested that longer retention times could be beneficial in terms of microbial livelihood.

Moreover, the interaction of microorganisms and the GO size should be also considered when defining the state-of-the-art of such biological system amended with GO. Xu et al. [78] found that the GO sheet area assumed a central aspect for *Shewanella* inhibition and formation of an agglomerated GO-microorganisms complex (i.e. hydrogel). In particular, GO sheet area greater than 0.30 µm^2, and a relatively high degree of GO reduction (i.e., C/O ratio greater than 1.75, or I_D/I_G ratio > 1.01) were found crucial for rapid development of such hydrogel structure. Furthermore, the lower presence of oxygen functional groups resulted in a more hydrophobic surface that in turn attracted further microbes leading to faster hydrogel formation. Thus, indicating that certain GO sheet size might also play a role in the toxicity or livelihood of microbial communities.

2. Research objectives and hypothesis

The hitherto published studies on the role of bioRGO in the anaerobic digestion process are generally promising, but conflicting or limited findings are reported. Therefore, the following research objectives have been formulated to better understand the impact of bioRGO.

The **first research objective** of this thesis is to determine the impact of GO addition at different concentrations on the anaerobic biotransformation of model persistent contaminants in a mixed microbial community. The biogas production will also be evaluated. Biochemical methane potential (BMP) assays will be employed due to their ease of control.

The **second research objective** is to investigate the impact of prolonged adaptation of the mixed anaerobic sludge to the presence of GO using a fed-batch strategy and evaluate the impact of added GO on the hydrolysis rate, VFA rate, and maximum methane production rate, and determine whether the anaerobic digestion process can be directly stimulated by GO amendment.

The **third research objective** is to evaluate if GO can help overloaded anaerobic reactors to recover faster by conducting batch tests with different levels of GO and different inoculum substrate ratios (ISRs) to simulate overloading conditions.

2.1. Research objective 1

Evaluation of selected organic micropollutants (OMPs) removal in biochemical methane potential (BMP) assays amended with graphene oxide.

Bench-scale experiments were initially conducted to determine the capacity of a mixture of digestate and GO (at different concentrations) to remove model persistent contaminants. Studies in the literature reported an improved biotransformation of several OMPs, like dyes [79], halogenated aromatics [48], and nitroaromatics [50,61]. In this study, the following two contaminants were selected as model OMPs: sulfamethoxazole (SMX) and trimethoprim (TMP). Both are antibiotics typically prescribed together and are selected due to their inclusion in the "EU Watch List Under the Water Framework Directive" [7]. Moreover, despite their extensive use in

human and veterinary medicine, the fate of these antibiotics in anaerobic WW treatment is not reported yet. Thus, the following hypothesis was conceived:

> **Hypothesis 1**: *The presence of bioRGO significantly improves the biotransformation of selected OMPs and the specific methane yield when compared with a control, i.e., without GO addition.*

Different GO dosages have been set to statistically analyze the data in view of a factorial 2k design. The dosage levels were selected according to the previous literature studies, which indicate a range of concentration between 0 mg/L and 500 mg/L ($\sim$ 50 mg_{GO}/g_{VS}) as most suitable [31,71,80]. As a first experimental step and to obtain preliminary results, biochemical methane potential (BMP) assays were employed due to their simplicity and the possibility of testing multiple reaction conditions at once [81]. Also, control experiments without the added GO, antibiotics, and with sterilized sludge were used to investigate the possible OMPs removal mechanisms (i.e., biotransformation and/or adsorption). In contrast to most other studies, the established guidelines for BMP tests were followed, allowing a better comparison with future investigations. Moreover, advanced analytical techniques such as ultra-performance liquid chromatography (UPLC) coupled to quadrupole linear ion trap mass spectrometer (QqLIT-MS), were used to monitor the degradation of target contaminants spiked at low μg/L concentrations.

Preliminary tasks to prove hypothesis 1

Obtaining biological reduction of graphene oxide is the pre-requisite of **hypothesis 1**. Only if bioRGO is formed **hypothesis 1** can be tested. Even if a considerable amount of literature reported the biological reduction of GO through bacterial respiration [20,21,24], this was achieved with pure cultures, and proof of bioRGO formation with a mixed anaerobic culture was firstly pursued in this study.

As described by Pei S. and Cheng H. [82], two measurable criteria exist to determine the degree of GO reduction. Namely, a change in the carbon to oxygen ratio (C/O) of the formed bioRGO compared with the initial GO (**a**) and a change in the electrical properties (**b**). Furthermore, anaerobic sludge and GO were previously observed to self-aggregate to form a hydrogel composite

with bioRGO and to show specific flocculation properties [45,49,83]. Thus, a change in the particle size (**c**) was also used as evidence of the formation of bioRGO.

The following three observations were checked to verify the occurrence of biologically reduced GO (pre-requisite of **hypothesis 1**):

a) Increased I_D/I_G ratio

To determine the degree of reduction of bioRGO, Raman spectroscopy was performed. The level of defects in bioRGO was measured using Raman spectroscopy and calculated by measuring the intensity ratio of the D peak at 1,347 cm^{-1} (I_D) and the G peak at 1,581 cm^{-1} (I_G). An I_D/I_G ratio of zero means no defects at all, and a higher ratio means higher defect content in the bioRGO and shows a characteristic signature of RGO.

Samples at day 0, 1, and 15 were taken to carry out Raman analysis on the trials with viable anaerobic sludge with GO and sterilized sludge with GO.

b) Increased presence of redox-active compounds

Previously, linear sweep voltammetry and cyclic voltammetry (CV) demonstrated higher electrochemical activity of anaerobic sludge amended with carbon-based materials (GO and biochar) [45,84]. Hence, supernatants from anaerobic sludge with and without GO were analyzed by CV.

c) Formation of bioRGO-sludge complex

An optical microscope (Eclipse Ti-S, Nikon, Tokyo, Japan) and a laser particle size analyzer (LS 13 320, Beckman Coulter Inc., Brea, USA) were used to compare the change in sludge floc size distribution in the control without GO addition and when GO was dosed.

Table 2-1: List of evidence of GO reduction and associated tasks to perform.

Evidence of GO reduction	Performed tasks
Increase in the I_D/I_G ratio	Raman spectroscopy during day 0 and 1
Formation of bioRGO-sludge complex	Particle size characterization via laser particle size analyzer and optical microscopy
Increased presence of redox-active compounds	Cyclic voltammetry

2.2. Research objective 2

Long-term BMP experiments for evaluating the effects of GO on the degradation kinetics at different rate-limiting conditions.

Objective 2 sought to modify the feeding strategy of batch systems to simulate continuously fed reactors by applying multiple re-feeds. Literature studies on GO impact on methane production are based on batch assays, in which contradictory results in terms of SMP and degradation kinetics are documented. However, the extension of the duration of the investigation by applying multiple feeds should allow a broader comprehension of the longer-term impact of GO. Similarly, it could also facilitate the determination of GO impact in continuous systems.

Moreover, GO addition seems to affect the anaerobic digestion process differently by stimulating or inhibiting certain AD steps (hydrolysis, acidogenesis, acetogenesis, and methanogenesis). By employing standard substrates, for which the rate-limiting steps are well known, conclusions can be drawn about which AD step is negatively or positively impacted by the GO addition. For example, Bueno-Lopez et al. [34] tested starch and glucose to assess the impact of GO on the methanogenic processes, and they found that GO presence (from 5 mg/L upward) hampered the hydrolysis stage.

Therefore, the following hypotheses made of three parts were formulated:

> *Hypothesis 2.1: An optimum concentration of GO exists at which the specific methane yield is significantly higher compared with a control, but achieving this optimum requires 1+ refeeding steps.*

> *Hypothesis 2.2: An optimum concentration of GO exists at which the kinetic parameters (i.e., hydrolysis rate, VFA conversion rate, maximum BMP rate, and lag-phase) are significantly improved (i.e., either regarding higher rates or shortened lag-times) compared with a control. Achieving such optimum GO concentration requires 1+ refeeding steps.*

> *Hypothesis 2.3: GO addition has a stimulating effect on substrates in which the methanogenesis step is considered to be rate-limiting.*

It was assumed that the microbial community needs a certain time to adapt to the added GO, which consumes electrons during its bioreduction, and the same electrons thus become unavailable for methane formation. The rationale for temporally expanding the studies (**hypothesis 2.1** and **2.2**) was based on three potential reasons:

i)   The biological reduction of GO consumes electrons from the supplied substrate, which would otherwise be available for methane production [35].

ii)   The introduction of the nanomaterial acts as an environmental stressor, causing at least an initial inhibition of the bacterial activity (cell death, wrapping, and trapping) [68].

iii)   The adsorption properties of the graphene material might also contribute to lower cumulative methane production because the soluble organic matter might be adsorbed and are thus less available for methane production [71].

Such negative impacts on the anaerobic culture and its performance are thus limited to the initial phase when GO is amended for the first time. Extending the investigation period by subsequentially refeeding the batch reactors (or choosing a continuous system) would provide the necessary time for the anaerobic culture to adapt. In this case, three fed-batch systems of 15 bottles each were used, which provided better statistical evidence for all kinds of treatment due to the high "n" (45 bottles). Besides, since all the GO is already reduced during the first feeding, all the substrate supplied thereafter would be available for methane production during the following feeding events.

Moreover, as described in hypothesis 2.3, it is hypothesized that GO improves the final AD step, i.e., methanogenesis. Two model substrates were employed to gain insights on the limiting step in the AD process due to the GO addition: glucose and microcrystalline cellulose (MCC). Glucose is known as an easily degradable substrate. No hydrolysis is needed and acidification is known to happen very fast, making it a substrate for identifying potential impacts of GO addition on the methanogenesis step. On the other hand, MCC degradation involves all the anaerobic digestion steps, with hydrolysis as its rate-limiting step. Differentiating between these two substrates and comparing their performance allowed for identifying which typical limiting step (hydrolysis or methanogenesis) was favored or inhibited by the GO addition.

2.3. Research objective 3

Long-term BMP experiments for evaluating the effects of GO on degradation kinetics and recovery in overloading conditions.

Following the results obtained in **objective 2**, **objective 3** seeks to expand the understanding of GO-amended anaerobic systems. In particular, the addition of GO is here investigated as a measure to tackle the most common operation failure in AD systems: acidification with the increase in organic loading.

For mitigating the effects of acidification, carbon-based materials, such as BC and AC, have usually been applied to enhance the electron transfer among different microbial strains and avoid acidification [18,85–87]. Similarly, the use of GO in its bioreduced form (see pre-requisites of **hypothesis 1**) is expected to achieve the same (or superior) mitigation effect at an already lower concentration, as it leads to the formation of a conductive bioRGO gel-like structure that may provide overall better connectivity. For example, Wang et al. [86] used 20 g/L of BC, while Gökçek et al. [73] used only up to 30 mg/L of RGO for the recovery of acidified AD reactors. This suggests that the necessary dosage of GO could be much smaller than for AC or BC. Therefore, the following hypothesis was formulated:

> *Hypothesis 3: The presence of bioRGO in overloaded anaerobic reactors acts as a mitigator, and model-derived kinetic constants and stability parameters are significantly better compared with a control.*

To evaluate the effectiveness of GO in reducing the negative effects of high substrate dosage, a design of three different GO levels and three different ISRs was established, and first-order model-derived kinetics were considered. Compared to other mitigation strategies with carbon-based materials, the overloading conditions in this study will be applied only after an initial phase, where the bioRGO is formed and the enhanced degradation kinetics for GO-amended assays are confirmed.

2.4. Summary of research objectives and hypotheses

Table 2-2: Summary of the dissertation's objectives, hypotheses, and corresponding publications.

Research Objective	Hypothesis	Publication	Chapter
1: Evaluation of selected organic micropollutants (OMPs) removal in BMP assays with the addition of GO.	*1: The presence of bioRGO significantly improves the biotransformation of selected OMPs and the specific methane yield when compared with a control, i.e., without GO addition.*	**Paper I** Ponzelli, M., Zahedi, S., Koch, K., Drewes, J.E., Radjenovic, J. (2022), *Journal of Environmental Chemical Engineering*, 10, 108373	**3**
2: Long-term BMP experiments for evaluating the effects of GO on degradation kinetics at different rate-limiting conditions.	*2.1: An optimum concentration of GO exists at which the <u>specific methane yield</u> is significantly higher compared with a control, but achieving this optimum requires 1+ refeeding steps.* *2.2: An optimum concentration of GO exists at which the <u>kinetic parameters</u> (i.e., hydrolysis rate, VFA conversion rate, maximum BMP rate, and lag-phase) are significantly improved (i.e., either regarding higher rates or shortened lag-times) compared with a control. Achieving such optimum GO concentration requires 1+ refeeding steps.* *2.3: GO addition has a stimulating effect on substrates in which the <u>methanogenesis step</u> is considered to be rate-limiting.*	**Paper II** Ponzelli, M., Radjenovic J., Drewes, J.E., Koch, K. (2022), *Bioresource Technology*, 360, 127642	**4**
3: Long-term BMP experiments for evaluating the effects of GO on degradation kinetics and recovery in overloading conditions	*3: The presence of bioRGO in overloaded anaerobic reactors acts as a mitigator, and model-derived kinetic constants and stability parameters are significantly better compared with a control.*	**Paper III** Ponzelli, M., Nguyen, H.H., Drewes, J.E., Koch, K. (2023), *Sustainability*, 15 (3), 2224	**5**

3. Rapid biological reduction of graphene oxide: Impact on methane production and micropollutant transformation

Author contributions: Michele Ponzelli was responsible for planning and conducting the research, data analysis, and manuscript preparation. The experiments were conducted by Michele Ponzelli. Jelena Radjenovic performed the transformation products analyses. Soraya Zahedi introduced the BMP tests to Michele Ponzelli. Jelena Radjenovic, Konrad Koch, and Jörg E. Drewes supervised the study. The manuscript was reviewed by Jelena Radjenovic, Konrad Koch, Jörg E. Drewes, and Soraya Zahedi.
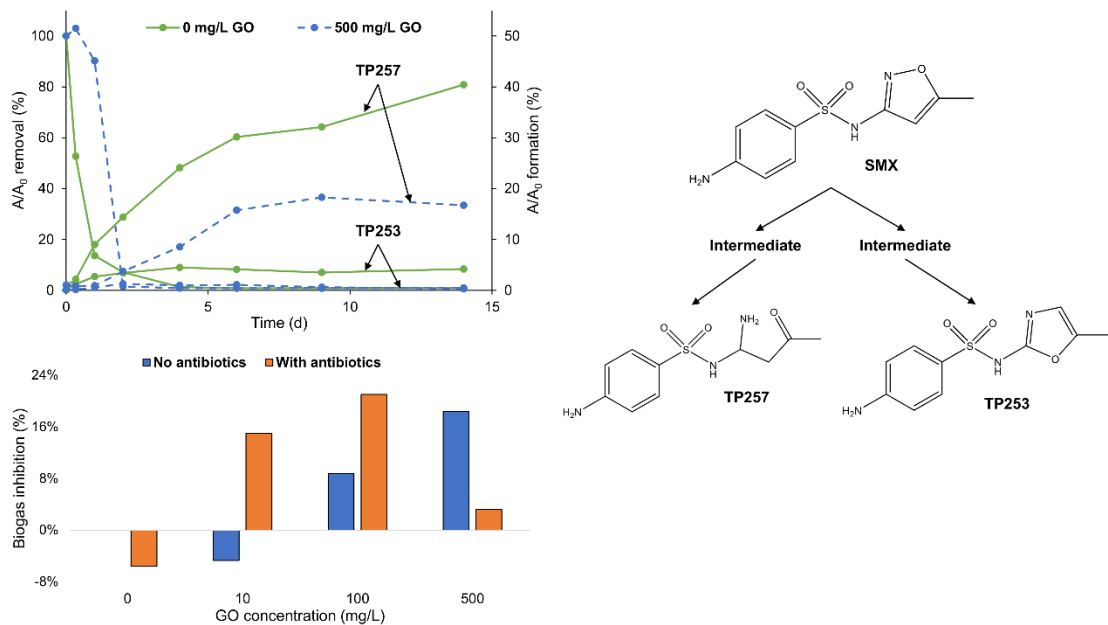
Figure 3-1: Graphical abstract Paper I (*Rapid biological reduction of graphene oxide: Impact on methane production and micropollutant transformation*).

Abstract

This study investigates the impact of graphene oxide (GO) addition to anaerobic sludge and the formation of biologically reduced GO (bioRGO) on both the anaerobic transformation of organic contaminants and the corresponding biogas production. A hydrogel-like material of anaerobic digestate and bioRGO was formed on the first day after GO addition. Raman spectroscopy showed an increase in the I_D/I_G ratio from 0.74 to 1.01, confirming the reduction of GO due to anaerobic respiration. The anaerobic removal of model antibiotics sulfamethoxazole and trimethoprim was unaffected by the GO addition. Yet formation of bioRGO inhibited the formation of the identified transformation products (TPs) of sulfamethoxazole, TP253 and TP257. Furthermore, the formation of TP253 and TP257 biotransformation products of sulfamethoxazole in sterilized sludge confirmed that their removal was likely achieved via intracellular enzymes that had enough thermal stability to remain active after the sterilization. For trimethoprim, no transformation products could be detected using the employed analytical method. The production of methane was generally inhibited up to 18% due to the presence of high GO levels (>100 mg/L) (288 vs. 353 mL CH_4/g VS).

3.1. Introduction

Climate change and population growth are putting increased pressure on the implementation of technologies that address the water-energy nexus and enable water, energy, and cost recovery. Conventional wastewater treatment plants (WWTPs) employing aerobic activated sludge processes might become obsolete due to their high energy demand, large amounts of sludge produced, and loss of nutrients [88]. Novel anaerobic wastewater treatment technologies can offset the energy and greenhouse gas costs of the activated sludge process and even become net energy producers [89]. They offer an opportunity to recover valuable soil amendment, drastically reduce the quantity of the produced sludge, and can facilitate the implementation of decentralized wastewater treatment [90]. Nevertheless, anaerobic processes suffer from long start-up times, low removal rates of organic pollutants, and susceptibility to disruptions by the organic overload [10].

The addition of low-cost conductive materials (e.g., granular activated carbon, biochar, magnetite, graphene-like materials) to anaerobic systems is an attractive strategy to promote the interspecies electron transfer (IET) between fermentative bacteria and the methanogens, and thus

enhance the degradation of organics and methane production [91,92]. Microbial reduction of graphene oxide (GO) to bio-reduced graphene oxide (bioRGO) has drawn significant interest due to the changes it induces in the morphology and behavior of the anaerobic consortia [45,93], with some studies reporting the self-aggregation of the bacteria in a hydrogel-like structure [26,45]. Microbial reduction of GO can be achieved by single bacterial strains, such as *Escherichia coli* [24], *Shewanella* [94], as well as by mixed microbial communities [22] and anammox bacteria [25] too. However, working with laboratory-adapted sludge may not represent the anaerobic culture present in the full-scale digestor. In order to investigate the impact of GO on the behavior of the real culture of the anaerobic digester, experiments in this study were conducted using freshly sampled sludge.

Regarding the impact of the bioRGO on methanogenesis, several studies reported an inhibiting effect at high GO concentrations (i.e., 500-1,440 mg/L) [68,71], likely due to the consumption of the electrons by GO reduction instead of methane formation [35]. Yet, graphene material amended to anaerobic digestate leads to higher methane production yields and rates, with up to 51.4% more when a concentration of 120 mg/L is applied [95]. It is unclear whether GO exerts toxic effects on the microorganisms. For example, Liu et al. [75] observed loss of *E. coli* viability with GO addition (40 mg/L). On the contrary, Guo et al. [77] reported a significant enhancement in *E. coli* and *Staphylococcus aureus* cell growth and biofilm formation with the addition of GO, even up to a concentration of 500 mg/L. Perreault et al. [96] demonstrated that the antibacterial activity of GO is size-dependent, with smaller GO sheets having a higher density of defects inducing higher oxidative stress to the cells.

In addition, bioRGO was observed to enhance the biotransformation and reduction of a range of organic and inorganic contaminants, such as dyes [26,50], nitroaromatics [50,51,61] and halogenated aromatics [48,51]. However, the fate of trimethoprim (TMP) and sulfamethoxazole (SMX), two antibiotics commonly used in human and veterinary medicine, in the anaerobic digestion with bioRGO was not explored yet. They are typically administered together and were selected due to their inclusion in the third Watch List under the EU Water Framework Directive (Directive 2008/105/EC) [97]. Moreover, high concentration levels of SMX (above 5 mg/L) are known to negatively affect the anaerobic microbial population, while 0.5-5 mg/L level might positively affect the anaerobic digestion performance [98–100]. In this study, environmentally

relevant concentrations were selected for both SMX and TMP (0.2 µM, i.e., 61 and 70 µg/L, respectively) [101,102].

In this study, we investigated the impact of GO addition in the range from 10 to 500 mg/L of GO (i.e., 0.9 - 46.8 mg GO per g of volatile solids, VS) on methane production and biotransformation of TMP and SMX. Moreover, the microbial reduction of GO to bioRGO and changes in the sludge morphology were characterized using Raman spectroscopy, optical microscopy, and particle size analysis. The removal of contaminants by abiotic effects (e.g., adsorption onto the GO and the sludge matrix) was checked by controlling with an aqueous GO solution and sterilized sludge. Although sludge sterilization may change sludge characteristics, it is still used to allow an indication of contaminant adsorption. To gain insight into the biotransformation pathway of the selected contaminants, several transformation products (TPs) were tentatively identified.

The hypothesis tested in this study is whether the presence of bioRGO can significantly improve the biotransformation of the two selected antibiotics and the methane production compared to a control. Compared to previous approaches, this study followed the biochemical methane potential (BMP) guidelines set by Holliger et al. [103], which include the use of a standard substrate and specific termination criteria. Additionally, the main novelty of this work is the investigation of the GO impact on the anaerobic biotransformation of antibiotics, and their TPs behavior, which is relevant for novel anaerobic wastewater treatment processes, such as anaerobic membrane bioreactor (AnMBR), up-flow anaerobic sludge blanket (UASB), anaerobic biofilm reactors, and similar reactor configurations.

3.2. Materials and methods

3.2.1. Materials and chemicals

The GO was provided from Graphenea (San Sebastián, Spain) as a 4 g/L aqueous dispersion, with a flake size <10 µm. Analytical standards for SMX and TMP and microcrystalline cellulose (MCC) were purchased from Merck (Madrid, Spain). Isotopically labeled standards SMX-d4 and TMP-d3 were purchased from LGC Standards (Barcelona, Spain). All reagents used for sample preparation and analysis were of analytical grade.

3.2.2. Experimental setup

The inoculum used in the experiments was collected from the anaerobic digester of the WWTP in Girona, Spain, working at mesophilic temperature (35°C) and treating primary and secondary sludge. The content of total solids (TS) and volatile solids (VS) of the inoculum was 1.9% and 1.2%, respectively. The experiments were conducted with MCC as substrate. As recommended when using MCC, the inoculum substrate ratio (ISR) was set to 2 based on VS [103].

To study the impact of the GO and the presence of contaminants on the formation of methane, BMP tests were conducted with inoculum, substrate (MCC), 0, 10, 100, and 500 mg/L of GO, and with and without the addition of antibiotics. BMP tests were performed in triplicate using sealed 240 mL bottles with 150 mL of working volume. The sludge characteristics are summarized in **Table 0-1**, Supporting material. GO, MCC, and antibiotics were added to the inoculum prior to incubation, and pH control was not controlled. Before sealing the BMP bottles, the headspace was flushed with nitrogen gas for one minute to guarantee anaerobic conditions. All the bottles were stored in a temperature-controlled incubator at 35 °C. All bottles were placed on an orbital shaker at 50 rpm to ensure sufficient mixing. Accumulated methane was determined by measuring the biogas production and methane content once a day for the first 10 days and every 3-4 days thereafter. Biogas volume was measured with a pressure sensor (PM7097, ifm electronic, Barcelona, Spain) at the bottle headspace. After each measurement, the bottle headspace was vented to ambient pressure. CH_4 concentration was measured using an infrared sensor (GIR-3000, Gastron Co., Gyeonggi-do, Korea). According to the previously published guidelines, the results were normalized to temperature, pressure, and water vapor partial pressure [104]. Cumulative gas productions were calculated by subtracting the endogenous methane production obtained from blanks, i.e., assays containing only inoculum. Relative standard error bars based on the triplicate measurements were calculated according to [105].

To evaluate the impact of the GO addition on the removal of target antibiotics, experiments were performed using an additional set of BMP bottles. Such extra bottles were not included in the determination of methane production. SMX and TMP were added simultaneously at the initial concentration of 0.24 μM each to have amounts comparable to environmental concentrations observed in sewage sludge [29,30]. Samples (~2 mL) were withdrawn at designated time intervals.

After sampling, the bottles were purged with a gentle nitrogen stream to remove the oxygen from the headspace. Prior to analysis, the samples were centrifuged and filtered using a 0.2 µm hydrophilic polytetrafluoroethylene (PTFE) membrane filter (Millex, Merck, Madrid, Spain). To evaluate the adsorption of the contaminants on the GO, experiments were performed using 500 mg/L of GO solution in milli-Q water. Additional experiments with the sludge sterilized by autoclaving at 120 ºC for 20 min were performed to evaluate the adsorption of the antibiotics on sterilized sludge. **Table 3-1** summarizes all the different experimental settings investigated. To identify possible TPs formed during anaerobic biotransformation, experiments were performed by adding SMX and TMP separately at higher initial concentrations (i.e., 40 µM) to anaerobic sludge and varying concentrations of GO (i.e., 0, and 500 mg/L). The formation of the identified TPs was later confirmed in the experiments conducted at lower initial concentration of antibiotics (i.e., 0.24 µM).

Table 3-1: Summary of the different experimental settings (n=3, †: n=6). The following abbreviations are used: microcrystalline cellulose (MCC); sterilized sludge (SS); control assays without antibiotics (CTRL); assays with antibiotics (ANT).

Inoculum	Substrate	Antibiotics	GO concentration (mg/L) and name			
			0	10	100	500
Absent	None	0.24 µM	-	-	-	500
Present	None	None	Blank	-	-	-
		0.24 µM	SS*	-	-	-
	MCC	None	CTRL	CTRL10	CTRL100	CTRL500
		0.24 µM	ANT†	ANT10†	ANT100†	ANT500†

3.2.3. Analytical methods

The target antibiotics were analyzed in the selected reaction monitoring (SRM) mode using a hybrid triple quadrupole-linear ion trap mass spectrometer (5500 QTRAP, Applied Biosystems, Waltham, USA) with a Turbo Ion Spray source, coupled to a liquid chromatograph (Waters Acquity Ultra-Performance™, Waters Corporation, Milford, USA), according to the previously published method [101]. To correct the matrix interferences, the quantification was performed

using isotopically labeled standards (i.e., SMX-d4 and TMP-d3). Tentative identification of the TPs of antibiotics was performed by full-scan mode of analysis, isolation of the protonated molecular ions, collision induced dissociation (CID) MS^2 experiments in the positive electrospray mode, and mass spectral comparison with the parent compound, as well as with the literature data.

According to the Standard Methods, TS and VS were analyzed [106]. Total and soluble (filtered at 0.45 µm) chemical oxygen demand (COD) were analyzed using LCK114 test kits (Hach Lange, Germany). Ammonium (NH_4^+) concentration was measured via ion chromatography (IC) (Dionex ICS-5000, Thermo Fisher Scientific, Waltham, USA), and total alkalinity concentration was measured via titration (855 Robotic Titrosampler, Metrohm, Filderstadt, Germany). pH and conductivity were measured using a pH meter (GLP21 Crison, Hach Lange, Barcelona, Spain) and a conductometer (GLP 31+ Crison, Hach Lange, Barcelona, Spain). The size of the sludge flocs was evaluated using an inverted optical microscope (Eclipse Ti-S, Tokyo, Nikon) and a laser diffraction particle size analyzer (LS 13 320, Beckman Coulter Inc., Brea, USA). A dispersive spectrometer (Jobin-Yvon LabRam HR 800, Horiba, Madrid, Spain) coupled with an optical microscope (Olympus BXFM, Olympus Iberia, Barcelona, Spain) was used for Raman characterization. The CCD detector was cooled at -64°C, and a 532 nm laser line was used with a dispersive grating of 600 lines mm^{-1} and a laser power at sample of 0.5 mW. The Raman spectroscopy analysis was performed for the sludge inoculum with 500 mg/L of added GO on days 0, 1 and 15, to verify the formation of the bioRGO. Moreover, Raman spectroscopy was also performed on the sterilized sludge inoculum with 100 mg/L of added GO to verify if any formation of bioRGO occurs without the viable microbial community. To investigate the redox activity of the sludge supernatant, cyclic voltammetry (CV) experiments were performed with the fresh anaerobic inoculum and inoculum on day 15 of the experiments conducted in the presence of 500 mg/L of GO, using a three-electrode set-up, with glassy carbon as the working electrode, platinum electrode as the counter electrode, and 3 M Ag/AgCl reference electrode (BASi, Lafayette, USA). The CV was performed using a 5 mV/s scan rate ranging from -1.5 to +1.5 V vs. Ag/AgCl, using a BioLogic multi-channel potentiostat/galvanostat VMP-300.

3.2.4. Gompertz model and statistical analysis

A modified Gompertz kinetic model was used to get more information on the methanogenic process, allowing the determination of the maximum methane production rate (R_{MAX}) and the lag-phase length (λ) [107].

$$B(t) = B_\infty \cdot e^{-e^{\left(\frac{R_{MAX} \cdot e}{B_\infty}(\lambda - t) + 1\right)}}$$ (*Equation 1*)

Such parameters were calculated through iteration using the MS Excel solver function. The objective function was the relative standard square error (RSS), set as minimum. The relative root means square error (rRMSE) and the coefficient of determination R^2 were used to assess the model's fitness and efficiency [108]. Initial iteration values of infinite methane production (B_∞), R_{MAX}, and λ are set at 1. All variables are constrained to non-negative values (≥ 0), and ultimate BMP (B_∞) is constrained to values less than or equal to 414 mL CH_4/g VS. This upper limit represented the maximum (100%) theoretical BMP for MCC (($C_6H_{10}O_5)_n$), as provided by the *Online Biogas App* (OBA) [109].

Moreover, two-way analyses of variance (ANOVA) are carried out using Origin2021 software (OriginLab Corporation, Northampton, Massachusetts, US) to evaluate statistical differences among the different experimental conditions, considering significant values of $p < 0.05$.

3.3. Results and discussion

3.3.1. Characterization of the bioRGO-amended inoculum

Raman spectroscopy measurements confirmed the biological reduction of GO to bioRGO (**Table 3-2**). The level of defects in the initial GO and bioRGO was calculated by measuring the intensity ratio of the D peak at 1347 cm^{-1} (I_D) and the G peak at 1581 cm^{-1} (I_G) obtained using Raman spectroscopy (**Figure 3-2**). The I_D/I_G ratio of zero represents no defects, and a higher ratio means higher content of graphene defects. At the beginning of the experiments, the measured I_D/I_G ratio was 0.74 for the initial anaerobic sludge (AS) with added GO. This ratio increased to 1.01 after 1 day of anaerobic incubation, evidencing a rapid microbial reduction of GO to bioRGO and the

formation of defects (**Table 3-2**). Similar rapid (< 1 day) reduction was reported previously for pure anaerobic cultures amended with GO like *Shewanella* [20], *E. Coli* [21], *Geobacter sulfurreducens* [23], and others [26,45]. However, only Shaw et al. [25] demonstrated biological reduction from the mixed microbial community, but only after 9 days. Moreover, the I_D/I_G ratio decreased to 0.82 on day 15, indicating further changes in the structure of bioRGO. This may be due to an increased ordering of the sp^2 bonded graphitic domains and reduction of oxygen moieties in the graphitic lattice [110,111]. The same sample presents a peak at the D+D' (around 2900 cm^{-1}), which also confirmed the formation of RGO [25]. In the experiments with the sterilized sludge (SS) and added 100 mg/L of GO, the I_D/I_G ratio remained relatively unchanged, with I_D/I_G ratios of 0.71 and 0.68 on day 1 and day 15, respectively (**Figure 3-2b**, **Table 3-2**). This result confirms that the microbial reduction of GO was occurring only in the presence of a biologically-active microbial community.

Table 3-2: Peak intensities and relative I_D/I_G ratios for GO-amended anaerobic sludge (AS) and sterilized sludge (SS) samples.

	AS+GO			SS+GO		
	I_D (1347 cm^{-1})	I_G (1581 cm^{-1})	I_D/I_G	I_D (1347 cm^{-1})	I_G (1581 cm^{-1})	I_D/I_G
Day 0	98.89	134.06	0.74	98.89	134.06	0.74
Day 1	130.29	129.40	1.01	94.56	133.81	0.71
Day 15	109.68	132.97	0.82	91.21	134.21	0.68
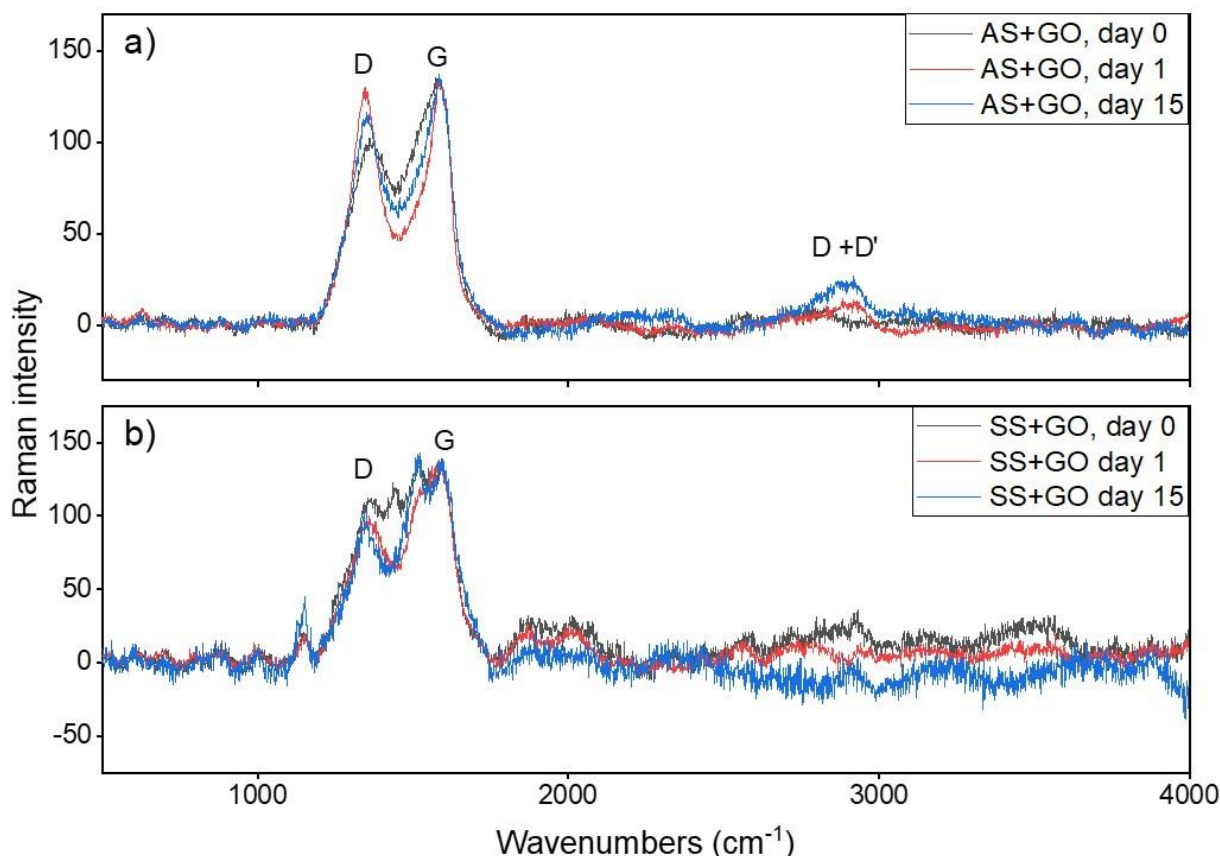
Figure 3-2: Raman spectra of **a)** anaerobic sludge (AS) with graphene oxide (GO) added on day 0, 1, and 15, and **b)** sterilized sludge (SS) amended with GO on day 0, 1 and 15.

The particle size analysis of AS with 500 mg/L of GO added showed a progressive increase in the floc size, with the measured mean particle diameters of 75 µm and 195 µm on day 1 and 15 of the experiment, respectively (**Figure 3-3a**). On the other hand, control samples (i.e., sludge without GO) showed no change in particle size, obtaining 51.3 and 57.5 µm on days 1 and 15. In addition, for samples with GO, a right shift of the differential volume peak towards higher particle diameters was noted, and for the sample on day 15, the volumetric distribution curve showed a higher percentage (≥25%) of particles with an estimated diameter >200 µm. However, it is important to note that this size distribution measurement of the suspended particles was based on the principles of light scattering and gives only an indicative size for non-spherical particles, such as sludge flocs, as their irregular size and shape makes them difficult to measure and quantify. From the optical microscope images of the sludge (**Figure 0-1**), it was evident that the formation of bioRGO led to a significant increase in the sludge floc size. For example, the observed floc

diameters of 63-131 µm for anaerobic inoculum were increased with 500 mg/L of GO to 325-689 µm after 1 day of anaerobic treatment and up to 1,223 µm after 15 days.
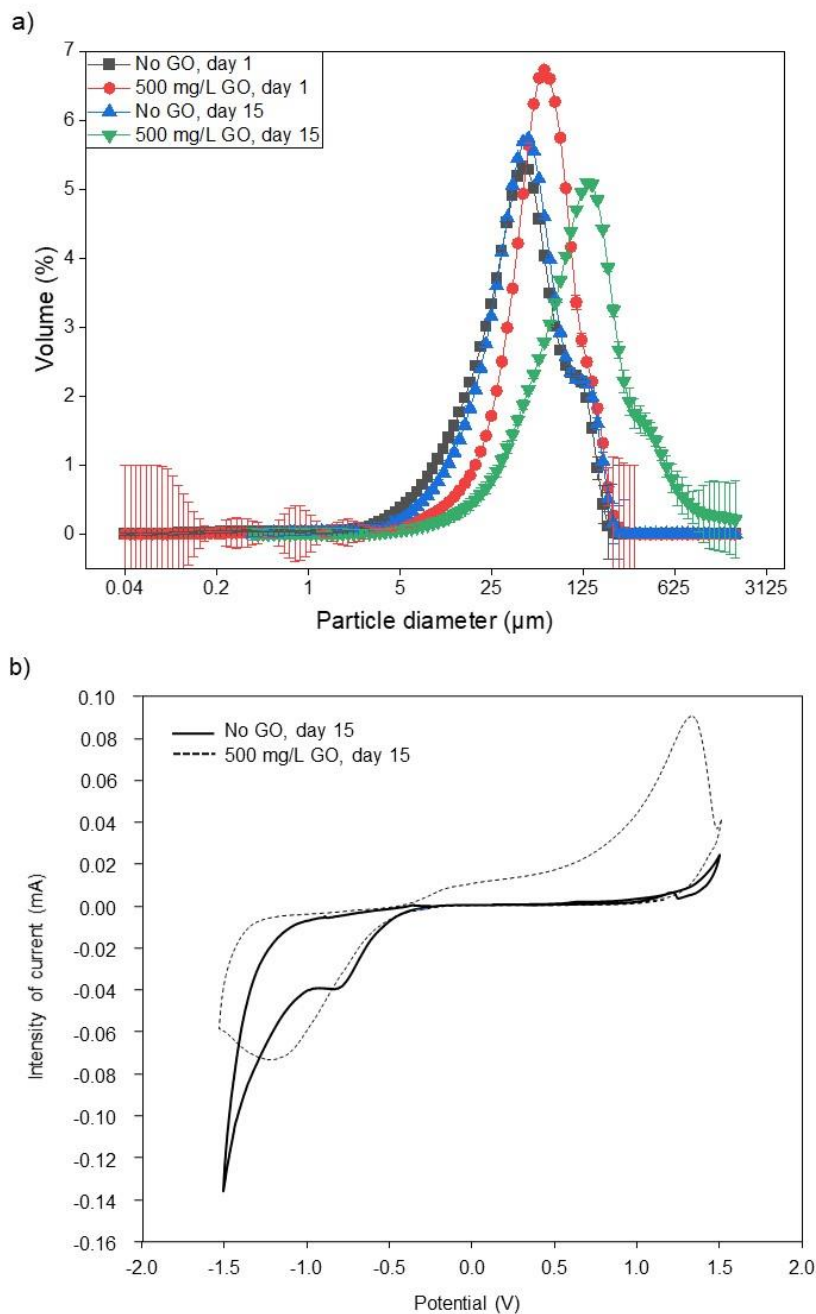
Figure 3-3: **a)** Log scale of the particle size distribution for the sample with and without added GO at 500 mg/L on day 1 and day 15. The results are presented as mean values of three replicates with their standard deviations, and **b)** Cyclic voltammetry (CV) of anaerobic sludge with and without 500 mg/L of GO on day 15.

Figure 3-3b illustrates the cyclic voltammetry (CV) measurements obtained for the anaerobic sludge inoculum samples on day 15 of the BMP tests conducted in the absence and presence of 500 mg/L of GO. The positive scan of the supernatant of the anaerobic inoculum did not show any anodic peaks, whereas in the reverse scan there was a reduction peak at -0.6 V vs. the Standard Hydrogen Electrode (SHE). In the supernatant from the sample with the bioRGO, two peaks appeared in the CV scan, at 1.5 V and -1 V/SHE, indicating the presence of redox-active compounds in the supernatant of bioRGO-modified sludge. In addition, the larger area of the CV from the bioRGO assay indicates a larger capacitance of this supernatant compared with the unmodified anaerobic inoculum. This can be explained by the higher content of the capacitive material (e.g., electron shuttles) formed in the bioRGO inoculum, likely due to the enhanced activity exoelectrogens [112]. Increased capacitance with bioRGO was previously observed in the CV measurements obtained from the GO-amended *Geobacter sp.* strain R4 [45].

It was demonstrated that the added GO was already bioreduced by the mixed anaerobic culture within a few days. This bioRGO is highly redox-active and tends to form a hydrogel with a larger floc size. Whether the presence of the bioRGO impacts the overall anaerobic digestion process is discussed in the next section.

3.3.2. Impact of bioRGO on the biogas production

The specific methane production (SMP) curves from each condition investigated are depicted in **Figure 3-4**. Dixon's test revealed the presence of two outliers with a significance level ($p < 0.05$) for both the conditions with the addition of 100 mg/L of GO, with and without antibiotics (**Figure 0-2**). These two were excluded from further data analysis. For all the conditions tested, an initial lag phase of about two days was noticed, which is quite common when microcrystalline cellulose is used as a substrate [113]. The two straight dotted lines of **Figure 3-4** represent the minimum and maximum BMP of cellulose, i.e., 340-395 mL CH_4/g VS, which should be achieved to validate the test results [114]. In the experiments without added GO, the SMP reached 354 ± 31 and 373 ± 26 mL CH_4/g VS in the absence and presence of antibiotics, respectively. Thus, the addition of SMX and TMP at low initial concentrations of 0.24 µM did not significantly influence biogas production. The addition of GO at lower concentrations (10 mg/L, i.e., 0.9 mg GO/g VS) did not impact the SMP in the absence of antibiotics by 5%, but led to a decreased performance when antibiotics were present (i.e., 15% inhibition) (**Figure 3-5**). The presence of 100 mg/L of GO (9.4

mg GO/g VS) inhibited the anaerobic digestion process in both the absence (9% inhibition) and presence of antibiotics (21% inhibition). Thus, although the addition of antibiotics did not impact methane production, their simultaneous presence with the GO led to a more pronounced inhibiting effect within the range of 10-100 mg/L GO. In the experiments with 500 mg/L of GO (46.8 mg GO/g VS), biogas production decreased by 18% without antibiotics. However, in the presence of antibiotics (ANT500), the inhibition at 500 mg/L GO was only 3%, resulting in an overall higher amount of methane formed (i.e., 342 mL CH_4/g VS) compared to CTRL500 (i.e., 289 mL CH_4/g VS), which had no antibiotics. Thus, while GO addition inhibits biogas formation linearly, similar to previously reported findings [71], exposure of sludge to low µM concentrations of antibiotics impacts the response of the microbial community to the addition of an external electron acceptor (i.e., GO). In the presence of antibiotics, the highest inhibition of the process by GO addition was observed at 100 mg/L of GO. The literature previously reported a bell-shaped impact of GO on biogas production and microbial activity [31,68]. For example, Wang et al. reported a bell-shaped impact of GO addition on the activity and extracellular polymeric substances (EPS) production of annamox bacteria [31].
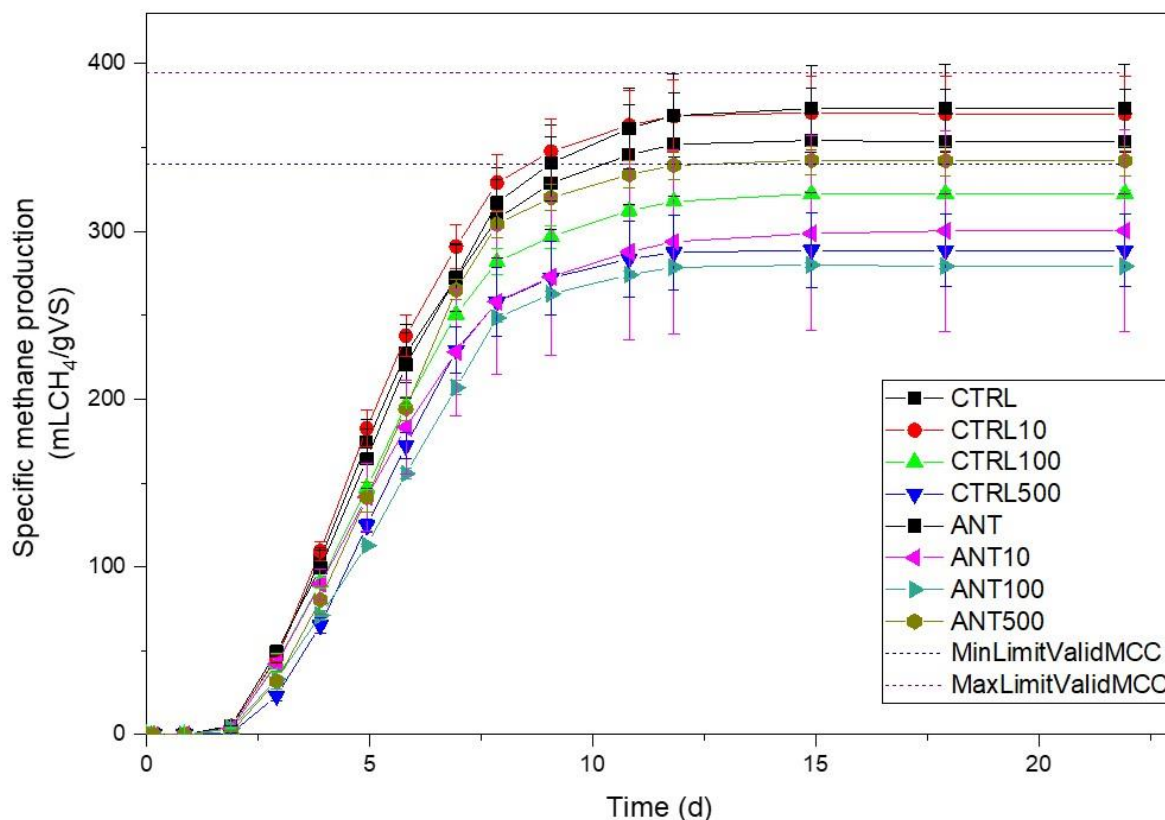
Figure 3-4: Specific methane production (SMP) of AS with different GO dosages, with and without added antibiotics (at 0.24 µM initial concentration). See **Table 3-1** for details. The results are presented as mean values of triplicate measurements (where applicable) with standard deviations. The straight dotted lines represent the minimum and maximum validation BMP of cellulose, i.e., 340 and 395 mL CH_4/g VS

Therefore, the result of the BMP tests demonstrates that the GO addition impacts the performance of anaerobic sludge. As illustrated in **Figure 3-5**, increasing the GO concentrations led to increased biogas inhibition. On the other hand, when antibiotics were amended, the biogas inhibition behaved in a bell-shaped way. Hence, it is unclear which level of GO concentration might not have an inhibiting impact on the anaerobic activity and if BMP tests are the proper method to comprehensively elucidate its impact on anaerobic sludge. Furthermore, two-way ANOVA analysis did not reveal any significant ($p < 0.05$) differences in biogas production between the assays containing antibiotics and the ones without.
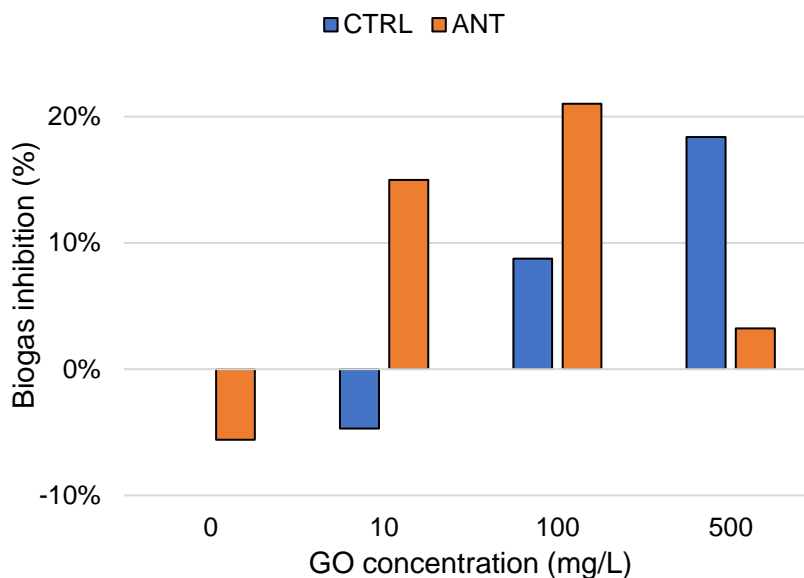
Figure 3-5: Biogas inhibition for the different GO levels without and with antibiotics (CTRL and ANT, respectively), compared to the control assay with no GO and antibiotics. The results are presented as mean values of triplicate measurements (where applicable) with standard deviations.

As already mentioned, the bioreduction of GO might indeed limit the number of electrons otherwise available for methane production during the first feeding phase [35]b. Once the bioreduction GO is completed, it is hypothesized that GO might not consume more electrons thereafter. Continuously or with multiple refeed set-up, it might be helpful to determine the real impact of GO reduction on the methane yield after the initial phase.

3.3.2.1. Gompertz model and statistical analysis

As it can be inferred from **Figure 0-3**, the experimental values of the methane production perfectly fit the Gompertz model achieving an R^2 of 1.0 ± 0.0 and an rRMSE of 0.0% for all tested assays (**Table 0-2**).

Moreover, the two-way ANOVA analysis revealed no significant ($p < 0.05$) differences for B_∞ and R_{MAX} across the different experimental conditions. However, further statistical tests on the lag-phase length λ revealed a significant difference ($p < 0.05$) between conditions containing 500 mg/L vs. 0 mg/L of GO and 500 mg/L vs. 10 mg/L of GO (**Figure 3-6**). Therefore, it can be suggested that high GO concentrations (500 mg/L) could play a major role in inducing significant delays in biogas production.
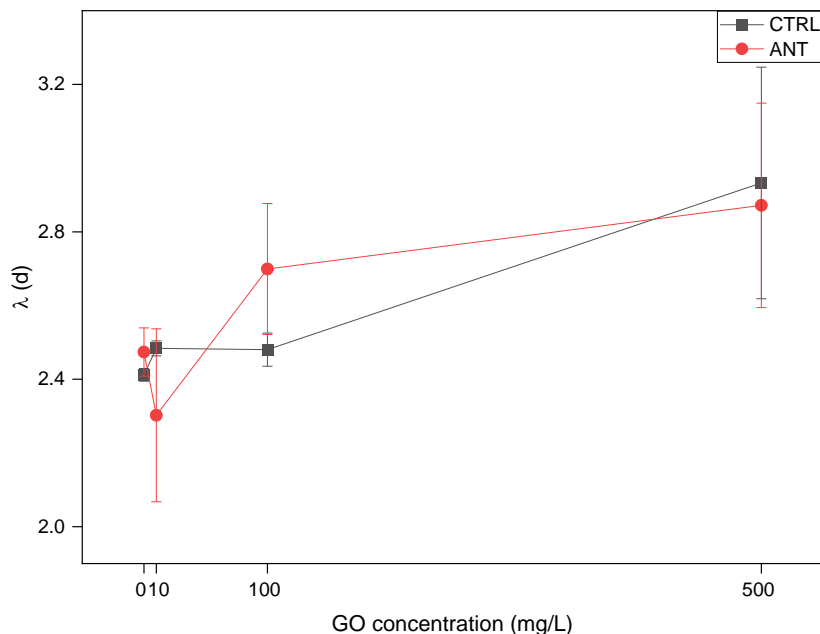
Figure 3-6: Lag-phase length for condition without (CTRL) and with antibiotics (ANT) at four GO levels (i.e., 0, 10, 100, 500 mg/L). Error bars represent standard deviations (n=3).

3.3.3. Impact of bioRGO on the removal of organic pollutants

Figure 3-7 shows the observed removals of SMX and TMP in the presence of different GO concentrations (0, 10, 100, and 500 mg/L) and the control experiments conducted with the sterilized sludge and only GO solution (500 mg/L) to understand their removal due to adsorption onto sludge and GO nanosheets, respectively. In the control experiments with sterilized sludge, both SMX (**Figure 3-7a**) and TMP (**Figure 3-7c**) were rapidly removed in the first few days. In the case of SMX, complete removal was obtained already in the first 24 h, similar to the experiments conducted with biologically-active anaerobic sludge (**Figure 3-7b**). Even though the sludge underwent sterilization procedures (i.e., 120 ºC, 20 min), the removal of SMX in the experiments with sterilized sludge was likely due to biotransformation and not adsorption onto sludge, as explained further below. The decrease in TMP concentration with sterilized sludge (**Figure 3-7c**) was similar to the biologically-active anaerobic sludge (5d) results, and TMP was entirely removed after three days. The gradual decrease in TMP concentration in the experiments with sterilized sludge also suggests biotransformation as the dominant removal mechanism, as adsorption would lead to a more abrupt decrease in concentration. Although autoclaving is considered as an efficient sludge sterilization technique, more so than for instance inhibition of

42

sludge with sodium azide [115], this study indicated that the biological activity of the sludge was maintained resulting in biotransformation of both TMP and SMX, likely due to the presence of liberated intracellular enzymes that maintained their activity after autoclaving.
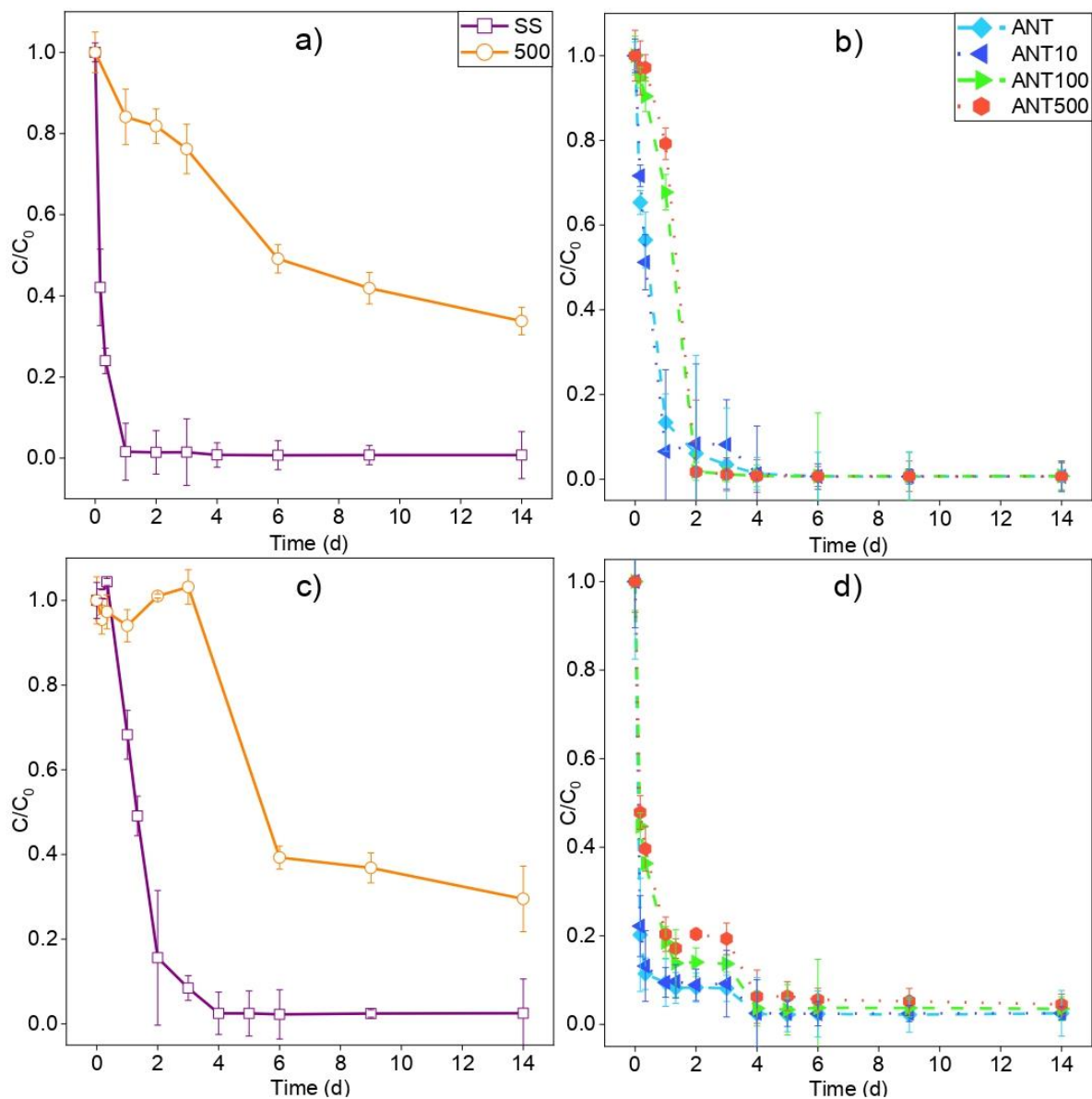
Figure 3-7: Concentrations (C) of sulfamethoxazole (SMX) (a, b) and trimethoprim (TMP) (c, d) normalized to the initial value (C_0) measured in the experiments conducted with anaerobic sludge with 0, 10, 100, and 500 mg/L of GO added, sterilized sludge (SS) and 500 mg/L of GO (500). See **Table 3-1** for details. The results are presented as mean values of triplicate measurements with standard deviations.

The concentration of TMP in the 500 mg/L GO solution remained unchanged in the first 3 days and then decreased to reach ~60% removal on day 6 of the experiment. SMX disappearance was more gradual in the presence of GO only, reaching around 65% removal by day 14. Both TMP and SMX can interact with graphene nanosheets of GO/RGO via π-π electron donor-acceptor interactions, electrostatic interactions, and hydrogen bonding [116–118]. TMP was present as uncharged species at an experimental pH of 7.2 (pK_a = 7.4, [119]) and strong π-π interactions were previously determined as the dominant adsorption mechanism of an uncharged TMP molecule at RGO nanosheets [118]. The decrease observed in the TMP adsorption onto GO between day 3 and 6 is likely a consequence of mild reduction and wrinkling of GO nanosheets at 35 ºC, which was the temperature maintained in all experiments. Variations in the wrinkling of the graphene nanosheets can have a pronounced effect on the energy distribution of their adsorption sites and thus impact their interaction with SMX and TMP [117]. SMX was present as an anion (pK_{a1} = 1.4, pK_{a2} = 5.8, [120]), and may have been adsorbed more gradually to GO and partially reduced GO nanosheets due to the somewhat decreased π-π interactions, as GO has a negative charge within the range of pH 3 to 11 [121]. Previously, SMX adsorption in the GO dispersion was observed to occur already within the first few hours [122,123].

In the experiments with biologically-active anaerobic sludge, SMX and TMP were rapidly removed in the first two days of the experiment and were not affected by the GO addition (**Figure 3-7b, Figure 3-7d**). Similar results on rapid removal of SMX and TMP by mixed anaerobic communities were previously explained by the carbon-rich environment in the BMP assays, which facilitates their removal through co-metabolic degradation processes [60,123,124]. Thus, the presence of bioRGO did not further enhance the anaerobic biotransformation of the target antibiotics. However, the addition of GO had an impact on the amounts of the formed transformation products (TPs) of SMX.

For TMP, no TPs could be identified in any of the conducted experiments, including the target search for the previously reported products of TMP anaerobic transformation, e.g., formed by anaerobic demethylation [125]. Two TPs were identified for anaerobic degradation of SMX, including the protonated molecular ions, $[M+H]^+$ of 254 (TP253) and $[M+H]^+$ 258 (TP257). Product TP253 exhibited the identical MRM transitions as the parent compound (i.e., m/z 254→m/z 156.1, and m/z 254→m/z 92) but eluted at an earlier retention time (t_R) of 3.4 min

compared with the t_R of SMX (5.5 min) (**Figure 3-8, Figure 0-4**). This, together with the identical mass spectra as compared to SMX (**Figure 3-8a**), indicated a rearrangement in the isoxazole moiety in the SMX molecule to form TP253 (**Figure 3-8b**). This rearrangement in TP253 was reported in a recent study on SMX transformation by sulfate-reducing and methanogenic communities [126]. In the same study, the authors observed another product with the nominal mass of 255 Da (molecular ion at *m/z* 256), formed by the cleavage of the N-O bond and isoxazole ring opening. Based on the obtained mass spectrum of TP257 (**Figure 3-8c**), this product was likely formed via a similar pathway but involved further hydrogenation of the double bond in the isoxazole moiety. Such TPs are common in anaerobic environments and are formed by sulfate-reducing bacteria and methanogenic cultures [126–128]. Thus, the anaerobic biotransformation of SMX proceeded via isomerization and N-O bond cleavage and reduction of the isoxazole moiety (**Figure 0-5**), similar to previously reported data [126].
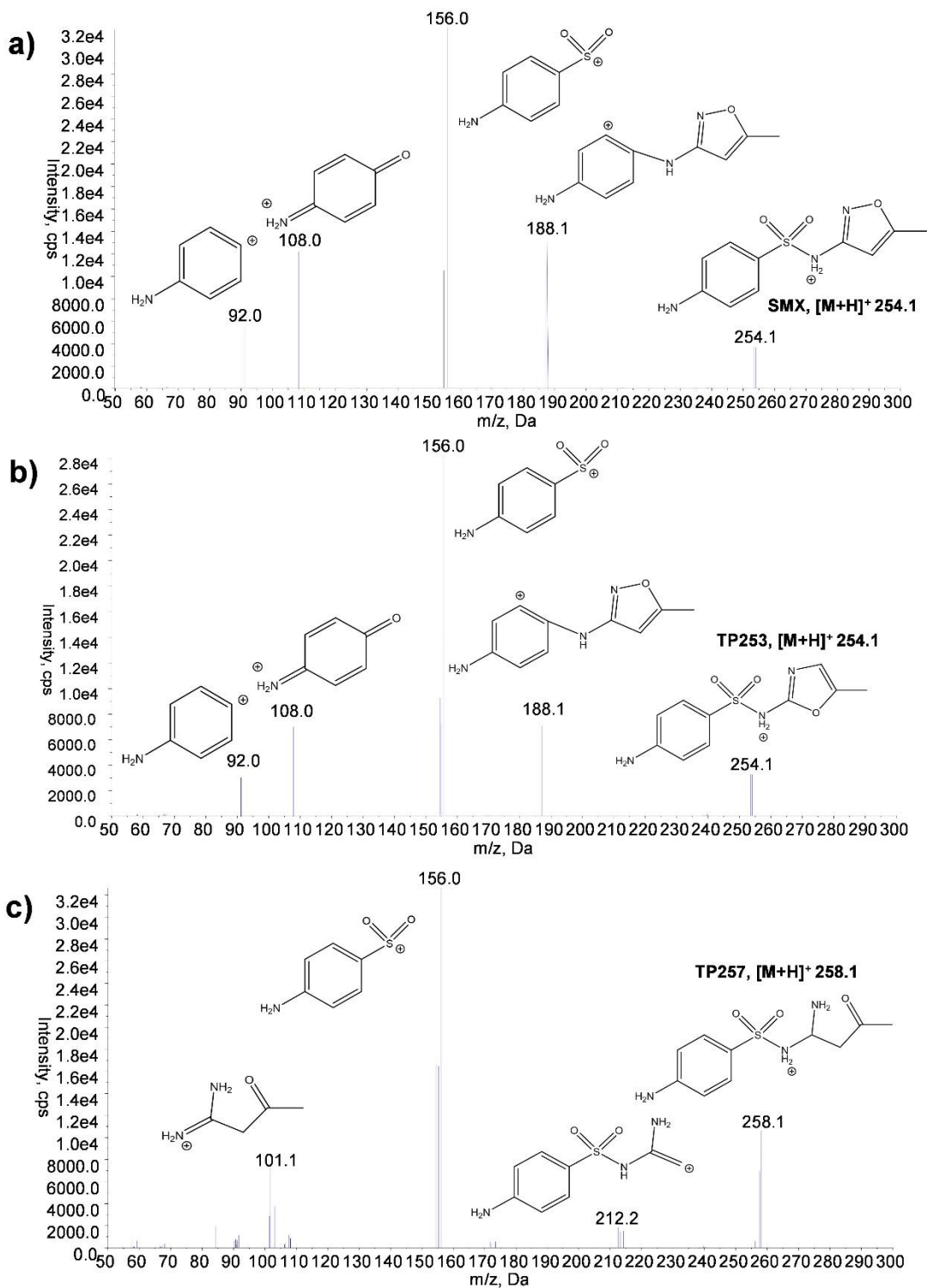
Figure 3-8: Product ion spectra of **a)** sulfamethoxazole (SMX) and its transformation products (TPs): **b)** TP253, and **c)** TP257 and proposed fragment ion structures.

Although the addition of GO did not impact the SMX removal kinetics of the parent compound, it had a pronounced inhibiting impact on the formation of TP253 and TP257 (**Figure 3-9**). For example, the amount of TP253 (estimated based on the peak area of the *m/z* 254 and normalized to the initial peak area of SMX) reached approximately 4% of the initial amount of SMX in the absence of GO, whereas the addition of 500 mg/L of GO lowered this value to a maximum of 1% (**Figure 3-9a**). Similar behavior was observed for TP257, which reached 40% of the initial amount of SMX in the absence of GO, but only 16% in the presence of 500 mg/L of GO. The presence of 100 mg/L of GO gave similar results as in the case of AS without GO for both TP253 and TP257. This inhibiting effect of GO addition on the formation of TP253 and TP257 may have been a consequence of the consumption of the available electrons by the GO being the external electron acceptor. Yet the removal kinetics of the parent compound remained unchanged and the inhibiting effect of GO in the biotransformation of SMX could only be noted after its TPs were identified and their formation profiles determined. Furthermore, both TP253 and TP257 were also detected in the experiments conducted with the sterilized sludge. TP253 was rapidly formed and reached up to 12% of the initial amount of SMX within the first 24 h of the experiment, indicating that this compound was likely the primary biotransformation product of SMX. This result is surprising considering that viable sludge formed significantly lower quantities of TP253. Considering that the autoclaving treatment led to sludge lysis, it is likely that the formation of TP253 was enhanced by the liberation of specific intracellular enzymes. Intracellular enzymes were previously reported to play a significant role in the anaerobic biotransformation of antibiotics and other organic pollutants [129,130]. A recent study indicated a lower metabolic potential for the biotransformation of antibiotics via extracellular enzymes than via intracellular enzymes [129]. In the biotransformation of ciprofloxacin by the anaerobic sulfate-reducing bacteria, cytochrome P450 catalyzed hydroxylation and desethylation reaction in piperazinyl ring [130]. Nevertheless, it should be noted that denaturation of the cytochrome P450 enzyme is expected to occur at temperatures above 90ºC [131], and its contribution to the biotransformation of SMX, as well as the elucidation of key intracellular enzymes that were active in the sterilized sludge, require further study. From the qualitative profiles of TP253 and TP257 presented in **Figure 3-9**, it can be observed that the appearance of new products does not occur simultaneously with the disappearance of the parent compound. Thus, anaerobic biotransformation of SMX likely included also other intermediate products that precede the formation of TP273 and TP257, and that could

not be identified in the present study. The exception to this behavior is the experiment with the sterilized sludge, where a sharp decrease in SMX concentration is followed by a sharp increase in the amount of the formed TP253.
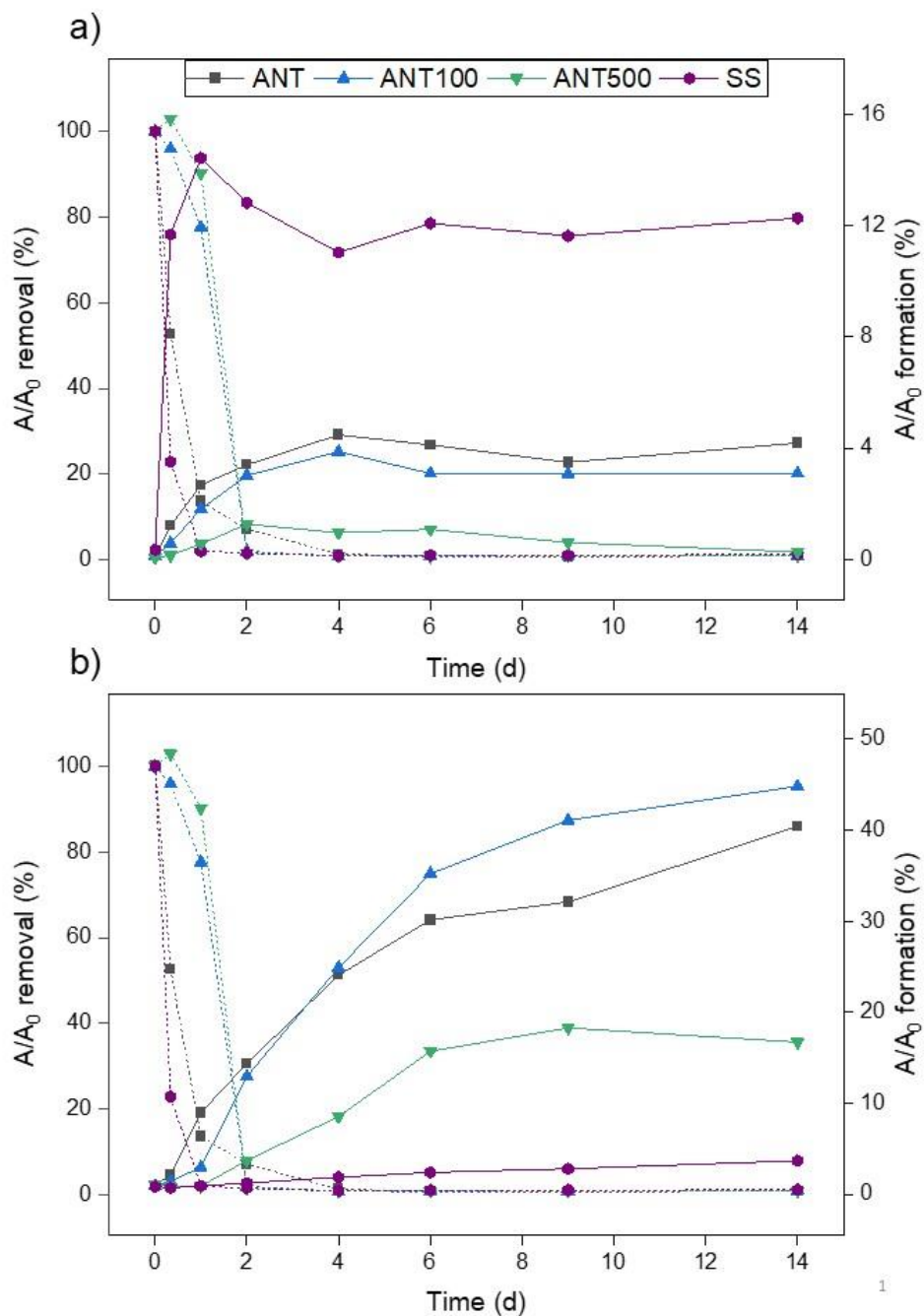
Figure 3-9: Peak areas of: a) Transformation product 253 (TP253), and b) Transformation product 257 (TP257), obtained from the extracted ion chromatograms (XICs) and normalized to the initial value of peak area of sulfamethoxazole (SMX). Normalized concentrations of the parent compound (SMX) are presented in dotted lines for comparison. See **Table 3-1** for details.

3.4. Conclusions and outlook

Rapid microbial reduction of GO to bioRGO occurred after one day of incubation with mixed anaerobic sludge. However, the formation of bioRGO negatively impacted the BMP (up to 21%) and did not influence the removal of selected antibiotics. Nevertheless, the addition of incremental amounts of GO led to a proportional decrease in the amounts of the identified biotransformation products of SMX, TP253 and TP257, formed via isomerization and N-O bond cleavage and reduction of the isoxazole moiety. Thus, although it was not evident from the removal kinetics of the parent compound, the anaerobic biotransformation of SMX was affected by the bioRGO presence. Furthermore, these products were measured in the sterilized sludge, indicating a prominent role of intracellular enzymes liberated upon the autoclaving in the anaerobic biotransformation of SMX. Thus, the results point out the necessity of a comprehensive evaluation of the impact of GO on the biotransformation of organic pollutants, including the analyses of their biotransformation products. Moreover, it is noted that BMP tests are not suitable to properly evaluate the impact of bioRGO on biogas production and organic micropollutants removal. Future studies should extend the investigation period to continuous systems.

3.5. Acknowledgements

3.6. Appendix – Supplementary material

The supplementary material of this article can be found in Appendix C of this thesis.

4. Enhanced methane production kinetics by graphene oxide in fed-batch tests

Author contributions: Michele Ponzelli was responsible for planning and conducting the research, data analysis, and manuscript preparation. The experiments were conducted by Michele Ponzelli. Konrad Koch, Jelena Radjenovic, and Jörg E. Drewes supervised the study. The manuscript was reviewed by Konrad Koch, Jelena Radjenovic, and Jörg E. Drewes.
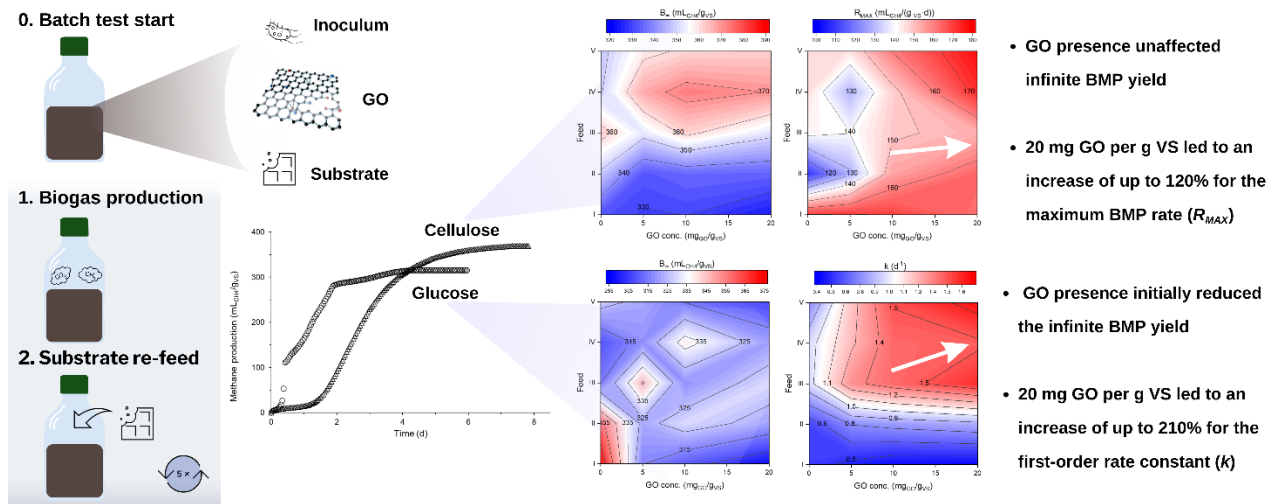
Figure 4-1: Graphical abstract Paper II (*Enhanced methane production kinetics by graphene oxide in fed-batch tests*).

Abstract

The study aims to prove that the addition of graphene oxide (GO) improves anaerobic digestion (AD) kinetic performance. Classical batch tests were modified to a fed-batch strategy at four GO levels while using two substrates (glucose and microcrystalline cellulose (MCC)). First-order and modified Gompertz models were respectively applied to evaluate the kinetic performance. The results showed significantly ($p < 0.05$) improved kinetic from the third refeeding step for both substrates. 20 mg GO per g of volatile solids (VS) led to an increase of up to 210% for the first-order rate constant (k) and up to 120% for maximum biochemical methane potential (BMP) rate (R_{MAX}) compared to control for glucose and MCC, respectively. The findings of this work suggest the implementation of GO in continuously operated systems to accelerate the AD process.

4.1. Introduction

Climate and recent geopolitical events are dictating the agenda of European governance towards a rapid transition in its energy source suppliers. Switching from fossil fuel consumption to renewables is leading the debates both at a climate change level, to meet the stringent greenhouse gas reduction target, and at the economic and energetical level to cope with the skyrocketing gas prices and to gain own energy independence [4,132]. Biomethane production from anaerobic digestion (AD) of biodegradable materials, such as sewage sludge and the organic fraction of municipal waste, could play a crucial role in this transition. However, one of the main drawbacks of the anaerobic treatment process is the relatively slow ability to transform complex substrates into biogas. The anaerobic process is indeed rate-limited by the successful syntropy of the two main constituting microbial communities, the fermenters and the methanogens [14]. Their interactions and the successful production of the final product (i.e., methane and carbon dioxide) are intrinsically dependent on the interspecies electron transfer (IET) occurring among them [13]. A possible way to increase the IET efficiency is switching to direct IET (DIET) by introducing conductive materials into the mixed liquor [133,134]. Different studies report significant enhancement of AD performance for different generally carbon-based amended materials, such as biochar [135], activated carbon [136], and nano-graphene materials [70].

Notably, results for graphene materials are conflicting. For example, Dong et al. [71] documented a 7% and 12.6% methane production inhibition for graphene oxide (GO) with 54 and

52

108 mg of GO per gram of volatile solids (VS) in the inoculum (mg_{GO}/g_{VS}) during waste-activated sludge digestion. Similarly, Zhang et al. [68] recorded inhibition from 2% to 17% with 0.155 to 15.5 mg_{GO}/g_{VS} for swine manure. On the other hand, an improvement of 17.6% in the cumulative methane yield was noticed during the co-digestion of sewage sludge and food waste when 1.1 g_{GO}/g_{VS} was added [70]. Even Kundu et al. [137] reported a 1.35-fold increase for 13.7 g_{GO}/g_{VS} addition in the AD of lemon waste.

The controversial results for GO addition in AD systems might be explained by the occurrence of its reduction mediated by the microbial community. The biological reduction of GO is a prerequisite for achieving DIET-related enhancement [22]. Once GO undergoes such a reduction process, its defects, represented by the presence of oxygen functional groups, can indeed be partially restored through microbial respiration [20,82]. Thus, it is hypothesized that such DIET-related enhancement can be observed only at the 1+ refeeding step. For example, in Ponzelli et al. (Preprint) [138], although the biological reduction of GO under anaerobic conditions occurred, the expected improvement of the biogas production was not observable. It was assumed that the microbial community needs a certain time to adapt to the additive, while the additive may also consume electrons during its bioreduction, making them not available for methane formation. Therefore, the initially limited methane production is based on three potential reasons: i) the biological reduction of GO consumes electrons from the supplied substrate, which would otherwise be available for methane production [35]; ii) introduction of the nanomaterial acts initially as an environmental stressor, causing the inhibition of bacterial activity including cell death, wrapping, and trapping [68]; or iii) high adsorption properties of the graphene material might also contribute to lower cumulative methane production, because the soluble organic matter might be adsorbed, and is thus less available for methane production [71]. Such negative impacts on the anaerobic culture seem thus to be limited to the initial phase only when GO is amended for the first time. Extending the investigation period by subsequentially refeeding the batch reactors (or choosing a continuously operated system) would provide the necessary time to the anaerobic culture for adaptation to the additive and to turn the stressor into a stimulator. Moreover, antimicrobial properties of GO seem to be linked to oxidative mechanisms present only for small size GO sheets [96]. Contrarily, no bacterial inactivation for suspended growth systems was reported, but only cell trapping with impermanent effects.

In this study, the feeding strategy has been modified to simulate continuously fed reactors in batch experiments by applying multiple refeeds once the plateau phase of biogas production is reached [139]. Therefore, low-cost GO is added to anaerobic sludge to evaluate its impact on the degradation kinetics of two model substrates, glucose and microcrystalline cellulose (MCC), over multiple refeeds. Furthermore, the intrinsic difference between the two selected substrates may allow a better understanding of the stimulating/antagonistic effect of GO addition on the limiting step in the AD process. Glucose is known as an easily degradable material. No hydrolysis is needed and acidification is known to happen very fast, making it a substrate to identify potential impacts of GO addition on the methanogenesis step [81]. On the other hand, MCC degradation involves all the AD steps, with hydrolysis as its rate-limiting step [103]. Differentiating between these two substrates and comparing their performance allows the identification of which limiting step is favored or inhibited by the GO addition.

4.2. Materials and methods

4.2.1. Materials and chemicals

The GO was provided from Graphenea (San Sebastián, Spain) as a 4 g/L aqueous dispersion, with a flake size <10 µm. Powder MCC (CAS 9004-34-6) (Alfa Aesar, Karlsruhe, Germany) and D-glucose (CAS 50-99-7) (VWR International GmbH, Ismaning, Germany) were employed as model substrates.

4.2.2. Experimental setup and operation

Biochemical methane potential (BMP) experiments were carried out using three automatic methane potential test system II systems (AMPTS II, Bioprocess Control, Lund, Sweden). The experiments were conducted with glucose and MCC as substrates. The inoculum used in the experiments was collected from an anaerobic digester of the Garching wastewater treatment plant (Germany), working at mesophilic temperature (38°C), treating a mixture of primary and secondary sludge. The inoculum was characterized by total solids (TS) and VS content of 19.5 ± 0.4 g_{TS}/kg and 12.3 ± 0.2 g_{VS}/kg (mean $\pm$ standard deviation, n=3). For glucose and MCC, the TS content was 990.6 ± 0.6 g/kg and 998.5 ± 1.5 g/kg, respectively, and the VS/TS ratio was 100% in both cases. The inoculum substrate ratio (ISR) was set to 2 based on VS for both substrates, as

recommended by the guidelines [103]. The operating conditions of the AMPTS are described elsewhere [113].

A factorial design with three factors and multiple levels was selected to perform the experiments. The factors are the type of substrate, the GO concentration (applied only at the beginning of the experiment), and the number of feeds. **Table 4-1** outlines the employed levels for each factor.

Table 4-1: Summary of the experimental conditions and their codes.

	GO conc. (mg_{GO}/g_{VS})			
Substrate	0	5	10	20
None	Blank	-	-	-
MCC	C-0	C-5	C-10	C-20
Glucose	G-0	G-5	G-10	G-20

All the tested conditions were conducted in quintuplicate (n=5), including blanks (i.e., assays containing only inoculum), employed to determine the endogenous gas production from the inoculum itself. The working volume in each assay was only 250 mL (out of 500 mL total) because of observed overflow events in preliminary tests owing to the formation of hydrogel. Since the goal of this study was to evaluate the impact of GO during different feeds, the BMP termination criterion (i.e., <1% cumulative methane production over three consecutive days) was usually not achieved [140]. In contrast, an extended starvation period during the plateau phase is even assumed to be antagonistic to the activity of the microbial community. The refeed happened approximately every week for both substrates to avoid starvation, where only the substrate was added to the assays. It was hypothesized that the unavailability of the substrate could cause a longer lag-phase at the following refeed, altering the kinetic parameters provided by the models. A total of five subsequent feeds have been carried out and are indicated by roman numbers. Cumulative gas production was calculated by subtracting the endogenous methane production obtained from blanks. Blanks were run for the entire experimental period, without any opening or flushing between the different feeds.

4.2.3. Analytical methods

TS and VS of inoculum, glucose, and MCC were analyzed according to standard methods [106].

4.2.4. Kinetic models

Two kinetic models were adopted to estimate kinetic parameters based on the specific methane production (SMP) curve obtained from the AMPTS II (see **Table 4-2**). The first-order one-step model is commonly adopted to predict and assist operators in designing and operating full-scale plants [141,142]. It was selected here due to its simplicity and to gain insights into the kinetic constant.

Table 4-2: Description of the adopted kinetic models.

Model	Parameters	References
First-Order One-Step $B(t) = B_\infty\left(1 - e^{-kt}\right)$	B_∞ = Infinite BMP yield (mL/g) k = First-order rate constant (1/d) t = Time (d)	[81,143]
Modified Gompertz $B(t) = B_\infty \cdot e^{-e^{\left(\frac{R_{MAX}\cdot e}{B_\infty}(\lambda-t)+1\right)}}$	B_∞ = Infinite BMP yield (mL/g) R_{MAX} = Maximum BMP rate (mL/g/d) λ = Lag time (d) t = Time (d)	[107]

The modified Gompertz model is a sigmoidal curve, initially used to describe bacterial growth, consisting of a lag-phase, exponential phase, and a stationary phase [107]. Compared to the first-order models, the Gompertz model describes those substrates that exhibit an initial phase with low or absent biogas production (i.e., lag phase), which is frequently reported for complex substrates as MCC [144]. Moreover, the Gompertz model can provide insights into the maximum methane production rate and the lag-phase duration. As for the first-order model, this obtainable information on rate constant and lag-phase duration is helpful to determine the synergistic or antagonistic effect of GO addition to anaerobic systems and compare GO-amended conditions with control ones or similar literature studies.

Initial iteration values are set according to indications by Brulé et al. [143]. All variables are constrained to non-negative values (≥ 0), and infinite BMP (B_∞) is constrained to the theoretical

BMP of the corresponding substrate, i.e., values less than or equal to 372 and 414 mL_{CH4}/g_{VS} for glucose ($C_6H_{12}O_6$) and MCC (($C_6H_{10}O_5)_n$), respectively.

4.2.5. Statistical parameters and analysis

Kinetic parameters were calculated through iteration using the MS Excel solver function. The objective function was set to minimize the relative standard square error (RSS). The relative root means square error (rRMSE) and the coefficient of determination R^2 were used to assess the model's fitness and efficiency [108]. Analysis of the residuals, i.e., the differences between experimental and model data, were also calculated to evaluate the closeness of the model to reality.

Moreover, a two-way analysis of variance (ANOVA) was carried out using Origin 2021 software (OriginLab Corporation, Northampton, Massachusetts, US) to evaluate statistical differences among the different experimental conditions, and values of $p < 0.05$ were considered significant.

4.3. Results and discussion

The study was conducted to systematically evaluate the impact of GO addition in batch tests following a fed-batch strategy. The results are divided into two sets according to the two different investigated substrates. The first set is focused on the experiments with glucose, where the first-order model is applied. The second set represents the results of the experiments with cellulose, where the modified Gompertz model is used. Moreover, a preliminary section on the goodness of the fit is presented.

4.3.1. Model efficiency

The main goal of this study was to evaluate the degradation kinetics of two model substrates with very different digestion behavior. Thus, two widely applied models have been chosen: the first-order one-step model for glucose and the modified Gompertz for MCC. As shown in **Figure 4-2**, the first-order model fits well with the methane production curve from glucose degradation. The condition G-0 (III) serves as a representative example and shows a high R^2 of 0.98 and a low

rRMSE of 4.9%, confirming the generally high goodness of the fit for glucose with the first-order model. Assay C-0 (III) for MCC modeled by modified Gompertz perfectly describes SMP curve with an R^2 of 1.0 and an rRMSE of only 1.5%. Very similar behavior was observed for the other tested conditions (see **Table 4-3** and **Table 4-4**). These examples generally confirm the appropriateness of the two selected models.
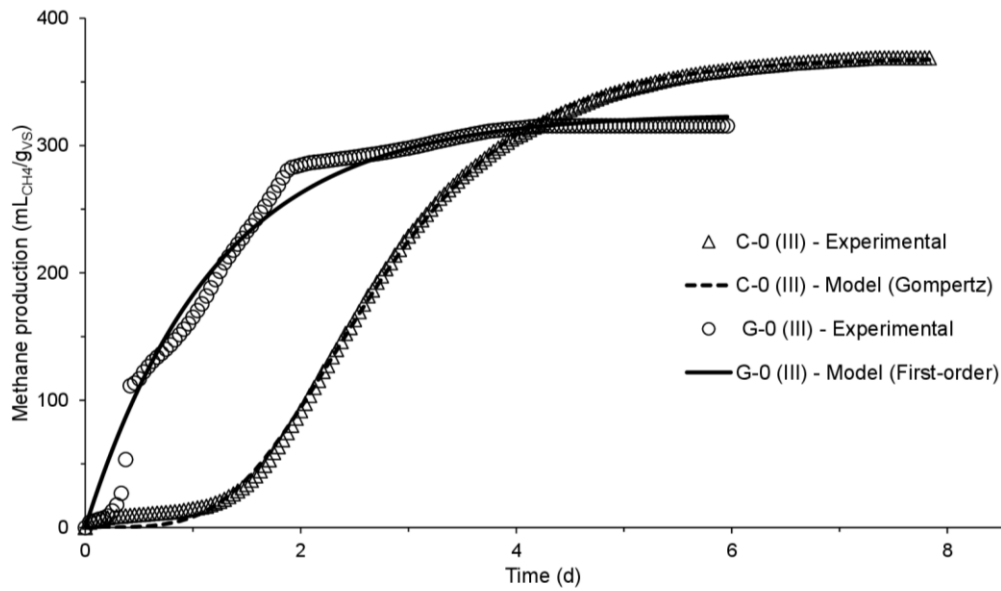
Figure 4-2: Mean experimental values (symbols) and model data (line) of methane production for positive control of cellulose (C-0) and glucose (G-0) during feed III.

Table 4-3: Experimental, and kinetic parameters obtained from first-order one-step model for assays supplied with glucose. To evaluate the goodness of fit, the coefficient of determination (R^2) and the relative root mean square error (rRMSE) are also indicated. Standard deviation of five replicates is reported (n=5), if not indicated differently ([†]: n=4, [‡]: n=3).

			Model data			
		Experimental SMP	Glucose – First-order one-step		Model fit	
			B_∞	k	R^2	rRMSE
Sample	Feed	mL_{CH4}/g_{VS}	mL_{CH4}/g_{VS}	1/d	-	%
	I[†]	360.6 ± 12.2	372 ± 0	0.56 ± 0.04	0.98 ± 0.00	5.6 ± 0.6
	II	334.6 ± 5.7	358 ± 6	0.58 ± 0.02	0.98 ± 0.00	5.6 ± 0.6
G-0	III[†]	311.6 ± 7.1	314 ± 8	0.96 ± 0.10	0.97 ± 0.01	5.5 ± 0.6
	IV[†]	301.8 ± 9.2	308 ± 4	0.96 ± 0.11	0.98 ± 0.01	3.8 ± 0.8
	V[†]	304.7 ± 12.7	329 ± 7	0.76 ± 0.08	0.98 ± 0.00	5.1 ± 0.4
	I	289.6 ± 6.4	315 ± 5	0.49 ± 0.03	0.97 ± 0.00	6.6 ± 0.1
	II	331.6 ± 15.9	322 ± 16	0.76 ± 0.06	0.97 ± 0.01	6.7 ± 0.8
G-5	III	349.6 ± 19.4	346 ± 16	1.33 ± 0.06	0.97 ± 0.00	4.5 ± 0.5
	IV	324.3 ± 6.0	318 ± 5	1.22 ± 0.06	0.98 ± 0.00	3.7 ± 0.2
	V	315.9 ± 8.2	322 ± 9	1.19 ± 0.05	0.98 ± 0.00	5.0 ± 0.6
	I	277.8 ± 4.1	308 ± 4	0.44 ± 0.01	0.97 ± 0.00	7.0 ± 0.2
	II	318.6 ± 5.6	330 ± 7	0.80 ± 0.06	0.97 ± 0.01	6.1 ± 0.6
G-10	III[†]	326.3 ± 7.3	317 ± 7	1.43 ± 0.09	0.98 ± 0.00	3.5 ± 0.2
	IV[†]	341.9 ± 16.1	339 ± 15	1.43 ± 0.05	0.99 ± 0.00	2.8 ± 0.2
	V	314.8 ± 3.3	314 ± 4	1.50 ± 0.10	0.99 ± 0.00	3.7 ± 0.7
	I	266.2 ± 12.9	298 ± 12	0.42 ± 0.03	0.97 ± 0.00	7.6 ± 0.4
	II	311.4 ± 6.1	321 ± 10	0.84 ± 0.09	0.97 ± 0.00	5.7 ± 0.5
G-20	III	334.1 ± 23.6	329 ± 20	1.57 ± 0.13	0.98 ± 0.00	3.1 ± 0.3
	IV	322.4 ± 8.9	319 ± 8	1.46 ± 0.07	0.99 ± 0.00	2.4 ± 0.3
	V[†]	308.1 ± 7.2	307 ± 5	1.65 ± 0.20	0.99 ± 0.00	3.3 ± 0.5

Table 4-4: Experimental, and kinetic parameters obtained from the modified Gompertz model for assays supplied with MCC. To evaluate the goodness of fit, the coefficient of determination (R^2) and the relative root mean square error (rRMSE) are also indicated. Standard deviation of five replicates is reported (n=5), if not indicated differently ([†]: n=4, [‡]: n=3).

		Model data				
		Experimental SMP	**MCC – Modified Gompertz**			**Model fit**	
			B_∞	R_{MAX}	λ	R^2	rRMSE
Sample	**Feed**	mL_{CH4}/g_{VS}	mL_{CH4}/g_{VS}	$mL_{CH4}/(g_{VS}\cdot d)$	d	-	%
C-0	I	332.8 ± 4.2	332 ± 4	170.4 ± 1.6	0.77 ± 0.03	1.00 ± 0.00	1.3 ± 0.1
	II	344.8 ± 5.9	349 ± 6	109.4 ± 5.9	1.40 ± 0.1	1.00 ± 0.00	0.8 ± 0.1
	III	364.0 ± 9.8	363 ± 11	142.3 ± 9.1	1.32 ± 0.09	1.00 ± 0.00	1.8 ± 0.6
	IV	353.3 ± 13.4	349 ± 16	146.0 ± 15.2	1.09 ± 0.16	1.00 ± 0.00	2.3 ± 1.0
	V	352.1 ± 11.7	348 ± 11	146.5 ± 21.7	0.94 ±.14	1.00 ± 0.00	2.5 ± 1.0
C-5	I	331.6 ± 10.3	329 ± 9	170.9 ± 5.3	0.73 ± 0.02	1.00 ± 0.00	1.2 ± 0.1
	II	333.1 ± 7.5	333 ± 7	128.7 ± 16.4	1.32 ± 0.04	1.00 ± 0.00	2.0 ± 1.1
	III[†]	353.9 ± 12.1	353 ± 11	140.2 ± 10.1	1.43 ± 0.17	1.00 ± 0.00	2.1 ± 0.5
	IV[‡]	365.6 ± 10.0	367 ± 16	129.5 ± 10.0	1.43 ± 0.15	1.00 ± 0.00	1.8 ± 0.4
	V	358.7 ± 9.8	358 ± 11	145.0 ± 20.8	1.09 ± 0.17	1.00 ± 0.00	2.2 ± 0.4
C-10	I	330.1 ± 5.1	330 ± 5	169.4 ± 2.8	0.69 ± 0.02	1.00 ± 0.00	1.1 ± 0.1
	II	345.4 ± 9.4	335 ± 8	154.7 ± 4.7	1.30 ± 0.11	1.00 ± 0.00	3.1 ± 0.8
	III[†]	367.6 ± 8.9	362 ± 13	148.8 ± 10.2	1.25 ± 0.12	1.00 ± 0.00	3.3 ± 1.1
	IV[†]	372.4 ± 10.1	373 ± 3	147.7 ± 11.5	1.27 ± 0.08	1.00 ± 0.00	3.1 ± 0.9
	V	364.8 ± 16.0	361 ± 17	160.3 ± 21.9	0.95 ± 0.15	1.00 ± 0.00	2.6 ± 0.4
C-20	I	326.6 ± 11.2	324 ± 10	162.5 ± 7.1	0.63 ± 0.03	1.00 ± 0.00	1.6 ± 0.1
	II	344.3 ± 19.2	334 ± 19	163.8 ± 13.7	1.19 ± 0.04	1.00 ± 0.00	2.7 ± 0.2
	III	359.5 ± 8.6	352 ± 8	152.6 ± 6.0	1.17 ± 0.10	1.00 ± 0.00	2.6 ± 0.6
	IV	375.7 ± 23.9	370 ± 25	172.3 ± 5.5	1.43 ± 0.24	1.00 ± 0.00	3.3 ± 0.5
	V	368.3 ± 19.1	362 ± 17	177.4 ± 35.2	0.94 ± 0.07	1.00 ± 0.00	2.8 ± 1.0

4.3.2. Effects of GO addition on the degradation kinetics of glucose

The first-order one-step model was applied to evaluate the kinetic parameters obtained from batch assays supplied with glucose. As illustrated in **Figure 4-3a**, the GO presence initially reduced the infinite BMP yield B_∞ (i.e., during feed I and II). Otherwise, no differences between GO-amended assays and the control condition (G-0) for B_∞ were noticed during subsequent feedings. The limited methane yield in the first feeding events may be explained by the reported entrapment effect of the additive [96]. Previous studies also reported dose- and time-dependent cytotoxicity effects of graphene materials on bacterial communities [75,77]. Thus, the trapping and toxic effects mitigate over time, resulting in similar B_∞ values across all conditions from feed III on.

In terms of the first-order degradation rate constant *k*, no impact was noticed during feed I and II. Instead, from feed III to V, all GO-amended assays (i.e., G-5, G-10, and G-20) showed values above 1.2 d^{-1}, significantly higher than G-0 (0.96-0.76 d^{-1}). Such findings might confirm the formulated hypothesis that digestion performance inhibition for GO-amended assays occurs only during initial periods. Thereafter, an improvement in degradation kinetics is apparent, with a comparable methane yield of control ranging between 308 and 329 mL_{CH4}/g_{VS}.

Although the BMP termination criteria were not fulfilled in most tests, it should be mentioned that the calculated infinite BMP yield B_∞ reached values in line with the reference value of 305-355 mL_{CH4}/g_{VS} (**Figure 4-3a** and **b**), which represent the refined validation criterion of 82.1% and 95.4% of the theoretical BMP of glucose (i.e., 372 mL_{CH4}/g_{VS}) [140]. As illustrated in **Figure 4-3a** and **b**, GO presence seems to affect B_∞ during feed I negatively. After that, GO-added assays achieved B_∞ values comparable to the control condition. One unexpected finding is the high B_∞ of 372 ± 0 mL_{CH4}/g_{VS} (corresponding to the upper model constraint) obtained for G-0 during feed I. A similar observation has been reported by Koch et al. [145] for cellulose. The authors concluded that residual organic matter in the inoculum was degraded in the assay with substrate owing to an improved C/N ratio by adding carbon-rich substrate, while this was not the case in the inoculum-only assay.

61
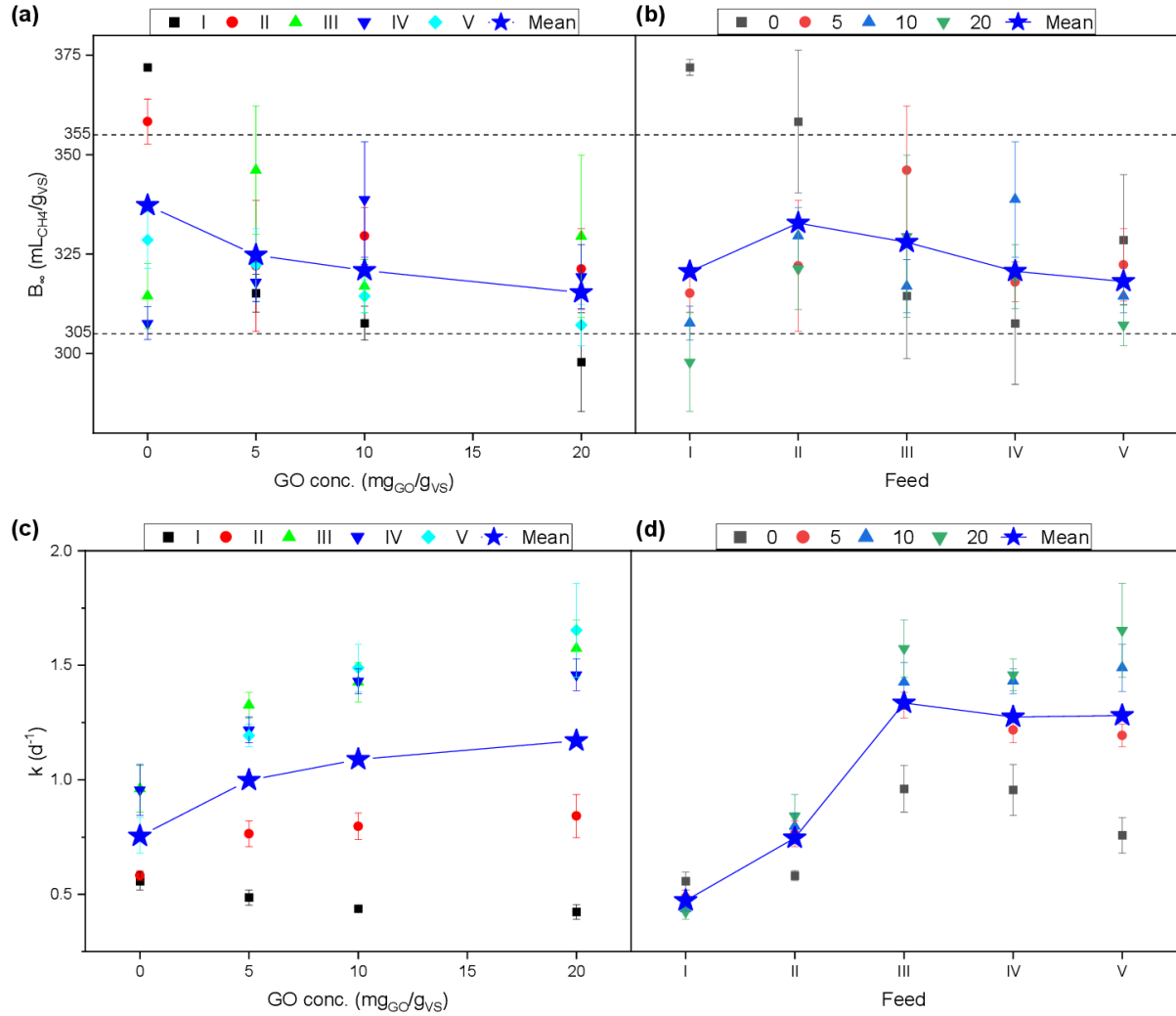
Figure 4-3: Plots of each condition supplied with glucose during the five feeds and for the four GO levels (0, 5, 10, and 20 mg_{GO}/g_{VS}) for the infinite BMP yield B_{∞} (**a**, and **b**), and the first-order rate constant k (**c**, and **d**). Star symbols indicate the mean of all assays for each abscissa position. Horizontal dotted lines in (**a**) and (**b**) stand for the refined validation criterion of 82.1% and 95.4% of the theoretical BMP of glucose (i.e., 372 mL_{CH4}/g_{VS}) from Holliger et al. (2021). Error bars represent standard deviation (n=5).

From **Figure 4-3d,** it is evident how higher degradation kinetics were achieved from feed III on for GO-supplied assays, while the control condition (i.e., G-0) exhibited significantly lower values. Moreover, considering the trend of the mean values (stars signs) of **Figure 4-3c,** a maximum for k is obtained for GO concentrations even higher than 20 mg_{GO}/g_{VS}. However, considering each feed, two-way ANOVA showed that G-10 is not performing significantly different from G-20, but was significantly different from G-5 (until feed III). Thus, even a concentration of 10 mg_{GO}/g_{VS} is enough to achieve significantly faster degradation.

The findings from this section suggest a stimulating role of GO in promoting AD performance in fed-batch systems using easily degradable feedstock, like glucose.

4.3.3. Effects of GO addition on the degradation kinetics of cellulose

Experimental results of methane production obtained with MCC-supplied assays were simulated using the modified Gompertz model. **Figure 4-4a** showed that regardless of the GO level applied, the infinite BMP yield B_∞ was statistically unaffected during each feed, varying from about 324 to 373 mL_{CH4}/g_{VS}. There was no initial inhibition of GO-amended tests for MCC-supplied assays compared to glucose. Thus, the initial inhibition may not be attributed to the bioreduction of GO consuming some of the electrons only, but probably to other underlying mechanisms. For instance, the hydrolysis of MCC is carried out by the synergetic reactions of microbial secreted endo- and exo-enzymes (α-amylase and oligo-1,6-glucosidase), not involved in glucose degradation [146]. The rate-limiting step defines the kinetics of methane formation. For glucose, this is likely the methanogenesis, and the methanogens seem to be inhibited by the presence of GO initially. In contrast, the rate-limiting step for MCC is hydrolysis performed by bacteria, which do not seem to be negatively impacted by the GO.

On the other hand, the maximum BMP rate R_{MAX} was significantly improved when a GO concentration higher than or equal to 10 mg_{GO}/g_{VS} was added to the system (**Figure 4-4c**). It is important to remark that R_{MAX} has a lower kinetic explanatory power than k of the first-order model, which is determined from the slope of all data points, while R_{MAX} is the single point of maximum methane production. It is, however, interesting to observe that condition C-5 showed both lower R_{MAX} and longer lag-phase duration λ, indicating an antagonistic impact of low GO concentration (i.e., 5 mg_{GO}/g_{VS}) on methane formation (**Figure 4-4c** and **e**). At the same time, this was not valid for the corresponding condition with glucose: G-5. This finding is consistent with Zhang et al. [68], who found a greater inhibition of methane production at low GO levels (5 mg/L).
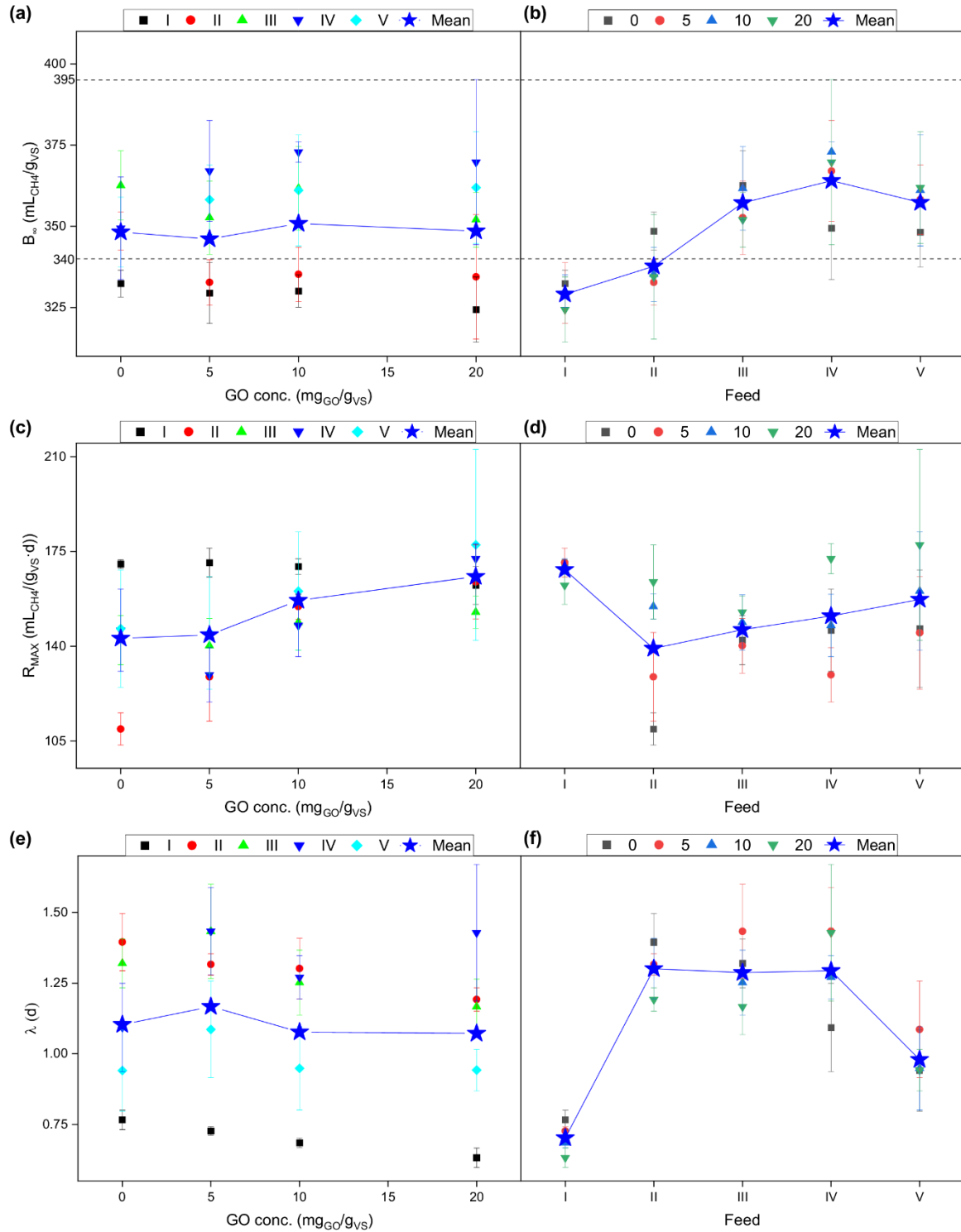
Figure 4-4: Plots of each condition supplied with MCC during the five feeds and for the four GO levels (0, 5, 10, and 20 mg$_{GO}$/g$_{VS}$) for the infinite BMP yield B$_\infty$ (**a**, and **b**), the maximum BMP rate R$_{MAX}$ (**c**, and **d**), and the lag-phase length λ (**e**, and **f**). Star symbols indicate the mean of all assays for each abscissa position. Horizontal dotted lines in (**a**) and (**b**) stand for the refined validation criterion of 82.1% and 95.4% of the theoretical BMP of MCC (i.e., 414 mL$_{CH4}$/g$_{VS}$) from Holliger et al. (2021). Error bars represent standard deviation (n=5).

From **Figure 4-4b**, a rising trend of B_∞ during the subsequent feeds is visible, which ultimately reached a stable value from feed III on. Likely, microorganisms adapted to the same substrate supplied over time [145]. A nitrogen inhibition due to low C/N in the inoculum sample might also be accounted for interpreting the higher R_{MAX} noticed during feed I (**Figure 4-4d**) [147]. Overall, higher R_{MAX} values were found at higher GO concentrations. This finding aligns well with a previous observation of Lin et al. [148], who found a linear correlation between kinetic parameters and the applied graphene concentration. Even Quintana-Najera et al. [149] noticed a significant increase of R_{MAX} for increasing biochar addition during the co-digestion of cellulose and *Chlorella vulgaris*. Both additives, graphene and biochar, are also carbon-based and known to promote DIET. In contrast, Zhang et al. [68] found a bell-shaped methane production inhibition over 0.6-16 mg_{GO}/g_{VS}. The statistical analysis carried out for this study revealed that at least an amount of 10 mg_{GO}/g_{VS} is needed to achieve a significantly higher R_{MAX} than the control. Besides, conditions C-10 and C-20 do not show any significant difference for each feed. Therefore, the 10 mg_{GO}/g_{VS} level might be a possible optimum for R_{MAX} improvement. However, the extension of GO concentration to values greater than 20 mg_{GO}/g_{VS} is needed to verify such a claim and to check whether an inhibition may occur at higher GO amounts.

Regarding the lag-phase duration λ, except for point C-20 during feed V, which has a p-value of 0.038 (close to the selected one of 0.05), a significant difference among the four tested GO levels was absent (**Figure 4-4e** and **f**). Hence, no apparent impact of GO was noticed on the lag-phase duration. Contrarily, highly significant differences can be noticed between feed I (i.e., 0.70 d) and the subsequent ones (i.e., feed II, III, IV, and V), which showed mean λ values of 1.30, 1.29, 1.29, and 0.98, respectively. A plausible explanation for such shorter λ during the I. feed might be the presence of undegraded substrate present in the inoculum. The higher R_{MAX} detected during feed I may also support this explanation (**Figure 4-4d**).

4.3.4. Outlook

The adoption of the two models allowed the estimation of methane production kinetic emphasizing the beneficial effect of GO addition on the degradation kinetics of two different substrates. The experimental results revealed that GO concentration above 10 mg_{GO}/g_{VS} improved the kinetic

parameters while showing no inhibitory effect on the methane yield compared to the control from 1+ refeeding steps.

The reported inhibition of the AD process was, in most cases, an observation of a one-time application that could be overcome in non-batch systems. The applied fed-batch system is quasi between a batch test and a continuously operating system. These promising results should culminate in continuous experiments with GO. Besides, further research may supply other (real) substrates, test higher GO concentrations (for some parameter could be beneficial), analyze the potential shift in the microbial community, or investigate intermediates products of AD. Enhancement in biogas production with the addition of GO to glucose assays may be a promising strategy for treating high-strength food-processing wastewaters like the sugar industry, characterized by a high content of rapidly-degradable organic material.

4.4. Conclusions

Fed-batch tests with glucose and MCC revealed that GO concentrations greater than or equal to 10 mg_{GO}/g_{VS} are critical for accelerating methane production rates. However, this improvement only occurs after 1+ feed steps. Overall, this study demonstrates that the addition of GO at low quantities can accelerate the AD process in fed-batch systems.

4.5. Acknowledgments

5. Improved Recovery of Overloaded Anaerobic Batch Reactors by Graphene Oxide

Author contributions: Michele Ponzelli was responsible for planning and conducting the research, data analysis, and manuscript preparation. The experiments were conducted by Hiep H. Nguyen. Konrad Koch and Jörg E. Drewes supervised the study. The manuscript was reviewed by Konrad Koch and Jörg E. Drewes.

Abstract

Anaerobic digestion reactors may suffer from acidification when overloading occurs. Carbon-based materials are amended to mitigate the souring effects of excessive loading. This study aims to test if graphene oxide (GO) helps overloaded anaerobic reactors recover faster. Batch tests were conducted following a fed-batch strategy at different GO levels (0, 10, and 20 mg GO per g of volatile solid (VS)) and different inoculum substrate ratios (ISRs) of 2, 1, and 0.75 based on VS. While an ISR of 2 was initially applied, the ISR was decreased to 1 and 0.75 in two parallel sets of experiments to simulate overloading conditions at the fourth feeding cycle. Lastly, an ISR of 2 was restored in all assays. First-order model kinetic constants confirmed a significant ($p < 0.05$) effect by GO from the third feed on. Although the GO-amended assays did not alleviate the acidification effects, during the final phase the kinetic constants reached values similar to or even above the controls (without GO). Moreover, a GO concentration up to 20 mg_{GO}/g_{VS} had no impact on FOS/TAC. Overall, this study broadens the understanding of the design and operation of anaerobic reactors amended with GO.

5.1 Introduction

Towards the road to defossilization and the increased use of sustainable sources in the energy sector, renewable gas represents a key cornerstone in this transition [150]. Renewable gas and nutrient-rich digestate to be applied as fertilizer are the main outputs of the anaerobic digestion (AD) process, where organic matter is stabilized and resources are recovered. Digesters are among the most reliable and affordable technologies to deal with feedstocks characterized by high organic content, such as municipal organic waste or sewage sludge [151]. However, AD comprises different sequential steps to degrade the organic matter and produce biogas, which requires long retention times (ca. 20–30 days). These steps can generally be classified as hydrolysis, acidogenesis, acetogenesis, and methanogenesis. All of them are performed by different microorganisms (bacteria, archaea, but also fungi) with different kinetics. The overall cooperation and synergy of such microbial communities are based on a delicate syntropic balance that, if altered, can lead to reactor failure, often recognized as acidification [13]. An imbalance in the AD operation can occur when the organic loading rate (OLR) is too high for the microorganisms to handle cooperatively. Fermentative bacteria are known to be much faster than methanogens [10].

Thus, they convert organic material into volatile fatty acids (VFAs), among others, at a rate higher than methanogens convert those into methane (CH_4). In cases of excessive loading, VFAs accumulate within the reactor, and environmental conditions turn acidic as methanogens cannot keep up with their conversion [10]. Furthermore, pH values lower than 6.8 are detrimental for methanogens, inhibiting their activity and ultimately leading to the failure of the process [152].

Thanks to their electric properties, carbon-based materials, such as biochar, granular or powder-activated carbon (AC), are recently being applied to enhance the electron transferability among the different microbial strains by direct interspecies electron transfer (DIET), leading to shorter retention times and avoiding acidification [18,85–87]. Similarly, graphene oxide (GO) is also recently being investigated as it resembles graphene, the material with the highest conductivity known, except for the presence of oxygen functional groups [19,153]. However, GO possesses oxygen functional groups in its hexagonal honeycomb carbon plan, making it less conductive than pristine graphene. Conversely, GO is less costly than graphene and can restore its layer composition through physical, chemical, or biological reduction [20,82]. Furthermore, compared to AC or biochar, the necessary dosage is reported to be much smaller [19,154].

Compared with other mitigation strategies, GO will be added at the beginning of the experiment rather than at the moment of acidification due to overloading [155]. It is hypothesized that GO can act as a mitigator against overloading conditions only when GO is in its biologically reduced form. One of the main advantages of using GO in an anaerobic batch reactor is its ability to increase the rate of substrate conversion and act as a support for immobilizing microorganisms [22,156]. The research gap here investigated is the lack of understanding of the impact of GO addition in overloaded anaerobic batch reactors.

This study aims to determine the ability of GO-amended anaerobic reactors to recover from the effects of excessive loading. The ability will be assessed by comparing model-derived kinetic constants and stability parameters to a control and among different GO concentrations and inoculum substrate ratios (ISRs) applied. Given the quasi-continuous operation in fed-batch mode, the highly sophisticated and automated systems, and the factorial design of the experiment employed, this systematic study offers robust insights into the impact of GO in overloaded anaerobic assays.

5.2 Materials and Methods

5.2.1 Materials and Chemicals

A 4 g/L aqueous dispersion of GO with flake sizes < 10 µm and pH 2.2–2.5 was supplied by Graphenea (San Sebastián, Spain). D-glucose powder (CAS 50-99-7) (VWR International GmbH, Ismaning, Germany) was used as the test substrate.

5.2.2 Experimental Setup and Operation

Biochemical methane potential (BMP) experiments were performed using three Automatic Methane Potential Test System II systems (AMPTS II, Bioprocess Control, Lund, Sweden) using glucose as substrate. The inoculum used in the experiments was collected from the anaerobic digester of the Garching wastewater treatment plant (Garching, Germany). The digester is fed with a mixture of primary and secondary sludge and operated at a mesophilic temperature of around 38 °C. The inoculum was characterized by total solids (TS) and volatile solids (VS) contents of 24.5 $\pm$ 0.1 g_{TS}/kg and 15.9 $\pm$ 0.1 g_{VS}/kg (mean $\pm$ standard deviation, $n = 3$). For glucose, the TS content was 998.7 $\pm$ 0.1 g/kg, and the VS/TS ratio was 100%. AMPTS operating conditions are described elsewhere [156,157].

The experiments were designed according to a factorial design with three factors (feed, GO concentration, and ISR) and multiple levels. As shown in Table 5-1, a total of nine conditions were tested, each carried out in five replicates ($n = 5$). GO was added only at the beginning of the experiment, and the concentrations of 0, 10, and 20 mg_{GO}/g_{VS} were chosen according to literature values [73,156]. Roman numbers were adopted to indicate the five subsequent feeding cycles.

Table 5-1: Experimental conditions according to the combination of GO and ISR levels.

	ISR		
GO Concentration (mg_{GO}/g_{VS})	**2**	**1**	**0.75**
0	0–2	0–1	0–0-75
10	10–2	10–1	10–0.75
20	20–2	20–1	20–0.75

The three ISRs were chosen according to comparable literature studies that simulated overloading conditions [73,158,159]. However, it is important to highlight that the ISR of 1 and 0.75 (representing the overloading conditions) were applied to the target assays only during feed IV (failure phase). Instead, feeds I, II, III, and V (recovery phase) were performed at an ISR of 2, as recommended for normal operating conditions [103].

Since the objective of this investigation was for comparison purposes among the tested conditions rather than for the determination of the BMP of a given substrate, the guidelines for BMP tests were slightly adapted [140]. The BMP termination criteria of daily methane production lower than 1% for three consecutive days was replaced with less than 0.3 mL_{CH4}/d for two days. Cumulative methane production is expressed as gross instead of the net since blanks (assays containing only inoculum) were not carried out. In fact, the scope of the study was not to assess the exact BMP yield from each tested condition but to gain insights from their comparisons.

5.2.3 Analytical Methods

The TS and VS of inoculum and glucose were analyzed according to standard methods [106]. For each of the nine conditions, one of the five replicates was used to grab samples for FOS/TAC measurement at two specific times. The first was at day 2 of feed IV (i.e., at the beginning of the failure cycle), and the second was at the end of feed V (when the digestion process reached the plateau phase). While FOS ("Flüchtige Organische Säuren") represents the volatile fatty acids content expressed as $mg_{CH3COOH}$/L, TAC ("Totales Anorganisches Carbonat") indicates the alkaline buffer capacity expressed as mg_{CaCO3}/L [160]. Their ratio is generally considered an operational indicator of anaerobic digester status. A FOS/TAC ratio below 0.3–0.4 suggests a stable process, while above 0.8, the process can be considered unstable [151,161,162]. The FOS/TAC ratio was determined with the Titralab AT1000&KF100 Series (Hach, Germany) following the Nordmann method [163]. Of course, the assays, from which the liquid samples were taken, were not considered for the average methane production calculations.

5.2.4 Kinetic Model

Designers and operators widely employ kinetic models to forecast and evaluate the potentiality of anaerobic digesters in full-scale scenarios [141,142]. The selection of a model depends on the substrate's degradation behavior. The methane production of glucose degradation is reported to start immediately (no initial lag-phase), which is typical for more complex substrates that involve hydrolysis processes (e.g., microcrystalline cellulose or sewage sludge) [156,164,165]. Thus, to assess the impact of GO and ISR ratios on the kinetics constants, a first-order model was applied [81].

$$B(t) = B_\infty(1 - e^{kt}) \qquad\qquad (\textit{Equation 2})$$

where,

- $B(t)$ = methane yield at time t (mL_{CH4}/g_{VS});
- B_∞ = ultimate methane yield (mL_{CH4}/g_{VS});
- k = first-order rate constant (d^{-1}); and
- t = time (d).

Iterations were performed using the MS Excel solver function, where the objective function was the minimization of the relative standard square error (RSS). Besides, as lower limits, the k and ultimate methane yield (B_∞) variables were constrained to positive values, and initial values were set following the recommendation of Brulé et al. [143]. Moreover, B_∞ was upwardly limited to the maximum theoretical BMP of glucose ($C_6H_{12}O_6$), i.e., 372 mL_{CH4}/g_{VS}.

5.2.5 Statistical Parameters and Analysis

To understand the efficiency and the fitness level of the proposed kinetic models with the experimental data, the relative root means square error (rRMSE) and the coefficient of determination R^2 were respectively used [108].

Furthermore, given the factorial design of the experiments conducted, three-way analyses of variance (ANOVA) were carried out using Origin 2021 software (OriginLab Corporation, Northampton, MA, USA) to estimate statistical differences among the different experimental

conditions. A *p*-value < 0.05 was used as the significance level, and the Bonferroni test was adopted to compare the means and control the overall Type I error.

5.3 Results

5.3.1 Model Accuracy

To assess the ability of GO to attenuate the effects of low ISRs (i.e., high substrate dosage) during the degradation of glucose, the first-order model was applied. The suitability of the model was evaluated through the R^2 and rRMSE values. Except for conditions with the lowest ISR of 0.75 during feed IV (failure phase), R^2 and rRMSE were greater than 0.97 and lower than 7%, respectively, for all conditions tested, confirming the overall suitability of the model (Table 0-1). The relatively lower model performance for ISR 0.75 can be explained by the overloading effect, which caused an anomalous methane production behavior. In Figure 5-1, the experimental and model values of the methane production of ISR 0.75 and 2 are compared for feed IV. While for assay 0–2, the model aligns very well with the experimental data (R^2 of 0.99 ± 0.00 and rRMSE of 3.1 ± 0.4), this is not the case for 0–0.75, confirmed by the low R^2 of 0.91 ± 0.06 and the high rRMSE of $11.6 \pm 2.4\%$ achieved.
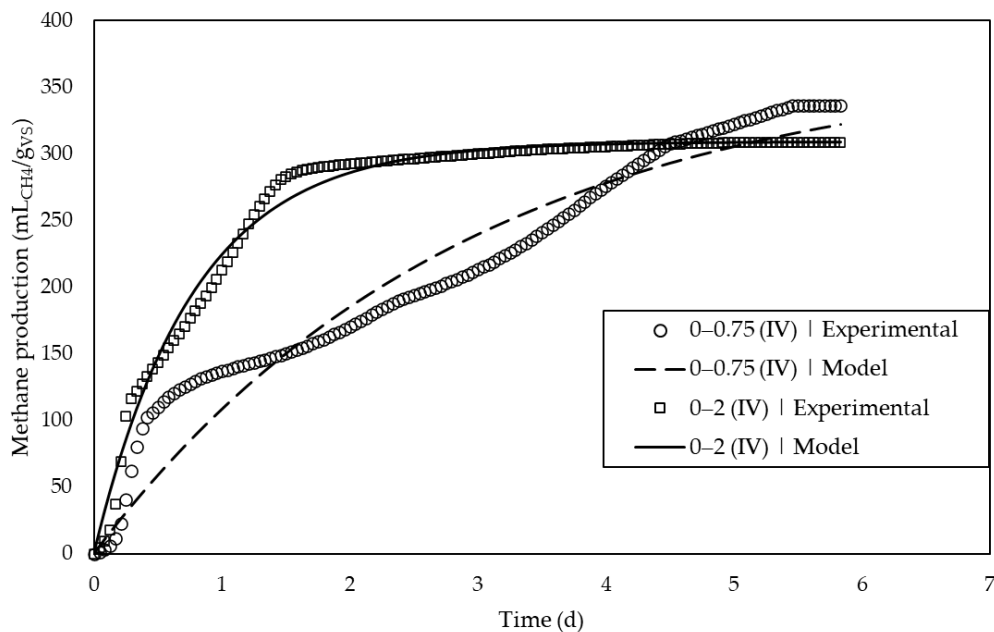
Figure 5-1: Comparison of experimental cumulative methane yield of conditions 0–0.75 (empty dots) and 0–2 (empty squares) during feed IV and their corresponding model-derived values (dashed and solid line, respectively).

5.3.2 Impact of GO and ISRs on the Kinetic Parameters

5.3.2.1 Ultimate Methane Yield B_∞

The kinetic parameters obtained from the first-order model, namely B_∞ and k, were used to evaluate the impact of GO concentration on the anaerobic reactor's capabilities to counteract stress conditions. After an initial feeding strategy at an ISR of 2 for all assays until feed III, feed IV was conceived as a failure phase where higher substrate dosages were applied.

Figure 5-2 illustrates that at feed I, high B_∞ values were observed across all conditions because no blanks were included; hence, the reported values are the gross gas productions of both substrate and inoculum. Moreover, significantly lower B_∞ values were observed when GO was present. Both aspects have already been reported in a similar previous study [156]. From feed II on, the B_∞ values dropped to around 305 mL_{CH4}/g_{VS} and were kept stable and maintained within the range of 305–355 mL_{CH4}/g_{VS}, representing the refined validation criteria [140]. It is noteworthy that it can be expected that the background production from the inoculum itself, usually measured in blanks, is

74

getting smaller in fed-batch systems with each new feed. Although increases can be observed at feed IV for the conditions with lower ISRs, the B_∞ values were still within the proposed range.
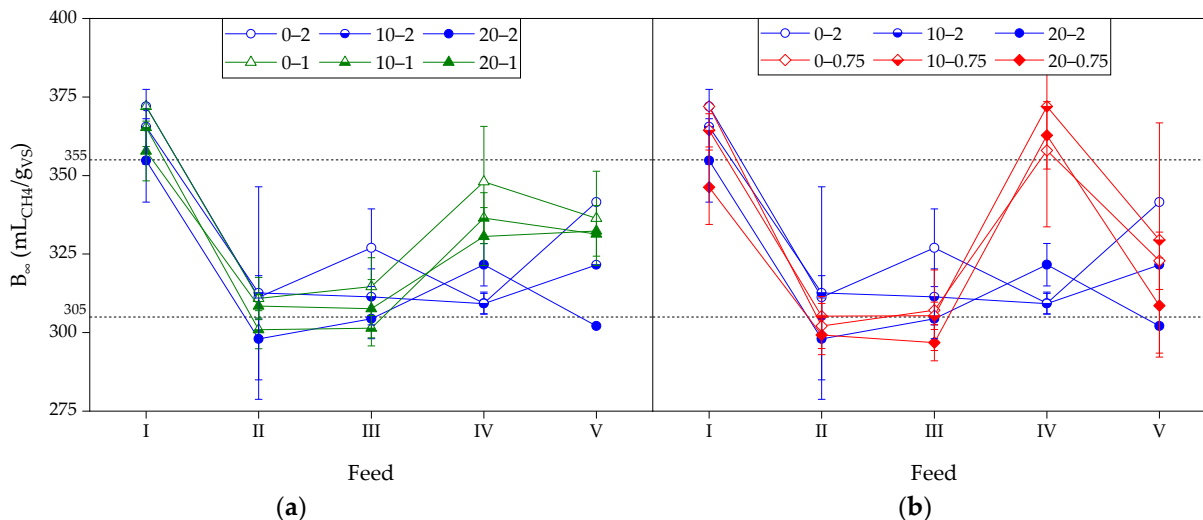
Figure 5-2: Average of the ultimate methane yield B_∞ obtained from first-order model corresponding to three GO levels (0, 10, and 20 mg_{GO}/g_{VS}), and: (a) conditions with ISRs of 2 and 1; (b) conditions with ISRs of 2 and 0.75. Horizontal dotted lines show the refined validation criterion of 82.1% and 95.4% of the theoretical BMP of glucose (i.e., 372 mL_{CH4}/g_{VS}) according to the validation criteria proposed by Holliger et al. [140]. Error bars represent the standard deviations of replicates (n = 5, where applicable).

Finally, regardless of the GO concentrations applied, at feed V (recovery phase at an ISR of 2), all conditions yielded similar B_∞ values (no significant differences from three-way ANOVA) (Table 0-2). Thus, both conditions with ISRs of 0.75 and 1 recovered comparably.

The absence of significant differences ($p < 0.05$) among the conditions for B_∞ is evident in Figure 5-3 (and in Table 0-3). It shows the incremental differences in the B_∞ values for the GO-amended condition compared to the control (no GO) for each considered ISR. The B_∞ values were generally close to or below 0%, indicating a slightly lower B_∞ for GO-amended assays compared to their respective conditions without GO (for each considered feed).
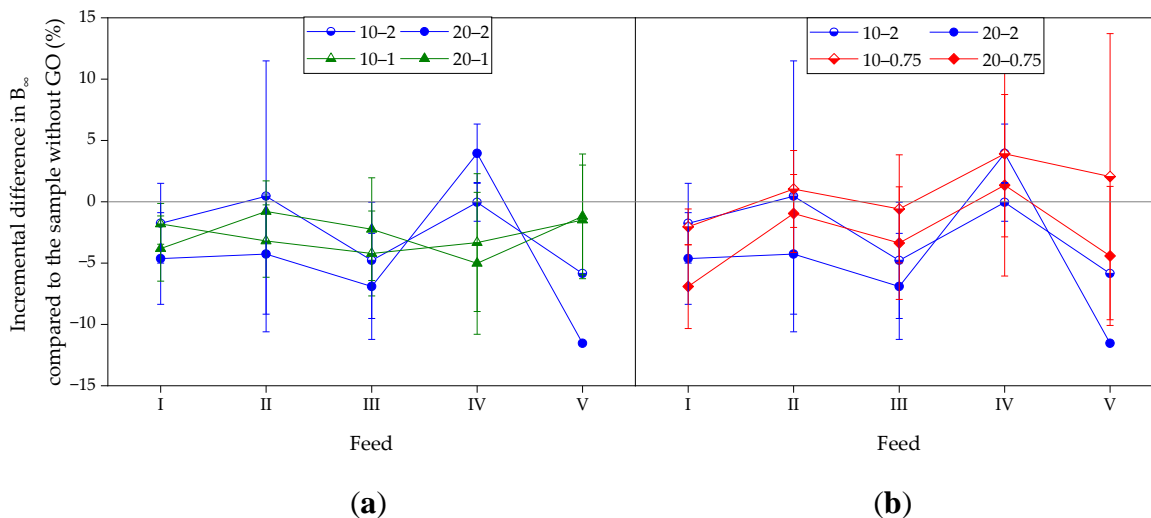
Figure 5-3: Average incremental difference in the ultimate methane yield B_∞ compared to the respective (same ISR) condition without GO for each feed. (a) 10 and 20 mg_{GO}/g_{VS} of ISR 2 and 1 conditions compared with their respective control (0–2 and 0–1); (b) 10 and and 20 mg_{GO}/g_{VS} of ISR 2 and 0.75 conditions compared with their respective control (0–2 and 0–0.75). Error bars represent the standard deviations of replicates (n = 5, where applicable).

Figure 5-4 provides further details on the impact of GO and the high ISR of feed IV on the methane production behavior for 20–0.75. Initially (20–0.75 (I)), it can be seen how the methane production curve has a low steepness and a longer time needed to reach the plateau. Such limited methane production was assumed to be related to lower electron availability, used for the biological reduction of GO, happening during the first day [35,45,138]. However, during the recovery phase (20–0.75 (V)), the methane production curve perfectly overlaps the previous feeding cycles II and III curves, where an ISR of 2 was applied. As already seen in Figure 5-2 and Figure 5-3, the capacity of GO to fasten methane production is kept even after an intense loading stress.
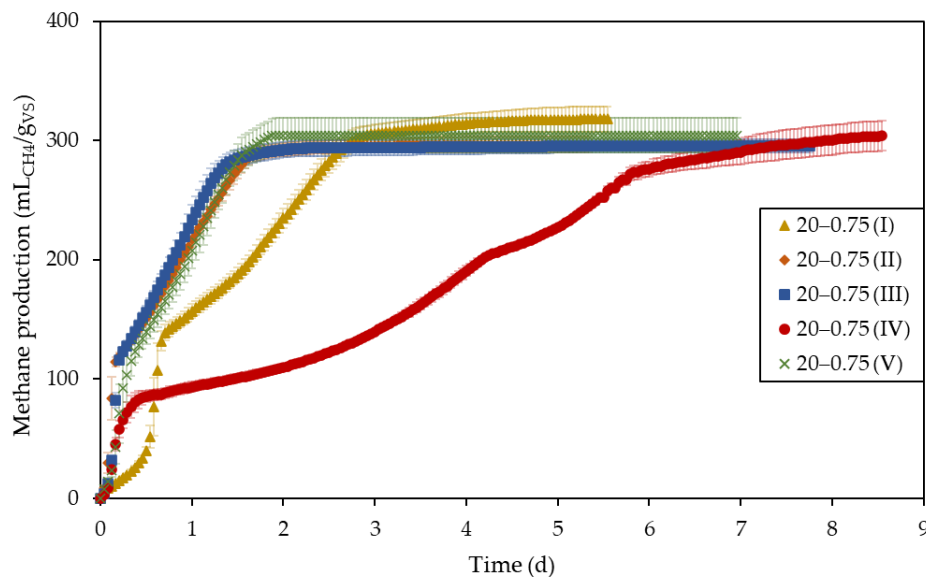
Figure 5-4: Average cumulative methane yield over time for the condition of 20 mg$_{GO}$/g$_{VS}$ and ISR of 0.75 (applied only at feed IV). Roman numbers indicate the feeding cycle. Error bars represent the standard deviations of replicates (n = 5, where applicable).

5.3.2.2 First-Order Rate Constant k

Another model-derived kinetic parameter extracted to evaluate the impact of GO on overloaded anaerobic assays is the kinetic constant k.

Regardless of the GO level considered during feed I, the kinetic constant was only around 0.55 d^{-1}, two times smaller than in feed II (ca. 1.5 d^{-1}) (Figure 5-5). A potential explanation of such low k values in the first batch test might be a potential ammonia inhibition and the necessary adaptation to the easily degradable substrate [147]. However, for each tested ISR, GO presence significantly improved k from feed III on (Table 0-6), confirming findings from a similar previous study [156]. At feed IV, the dosage of a higher amount of substrate caused the kinetic constants to drop to 0.51–0.61 d^{-1} for an ISR of 1 and 0.20–0.34 d^{-1} for an ISR of 0.75. Meanwhile, k values for ISR of 2 kept similar to feed III with values ranging from 1.30–1.55 d^{-1}. Remarkably, the enhanced kinetics due to GO addition were preserved even after the loading shock (feed IV) for assays with an ISR of 1. Conditions 10—1 and 20—1 during feed V achieved values of 1.78 d^{-1} and 1.76 d^{-1}, significantly higher than 0—1 (1.56 d^{-1}). However, the same behavior was not observed for the ISR of 0.75. The assay 0—0.75 achieved a k value of 1.67 d^{-1}, significantly higher than 1.43 d^{-1} and 1.31 d^{-1} of conditions 10—0.75 and 20–0.75, respectively (Table 0-7).
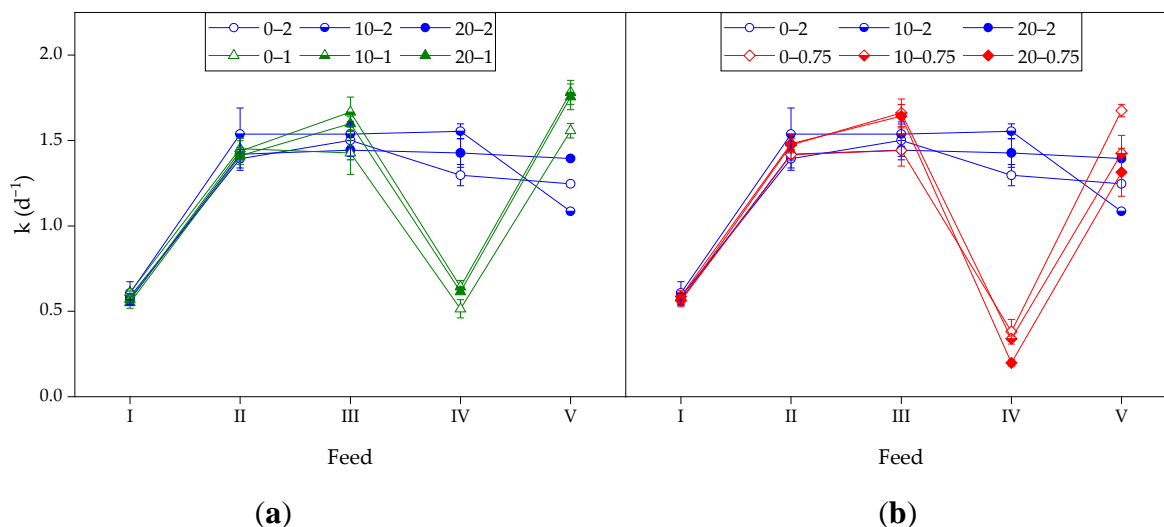
Figure 5-5: Average first-order rate constants k obtained from first-order model corresponding to three GO levels (0, 10, and 20 mg$_{GO}$/g$_{VS}$), and: (a) conditions with ISRs of 2 and 1; (b) conditions with ISRs of 2 and 0.75. Error bars represent the standard deviation of replicates (n = 5, where applicable).

In Figure 5-6, a relative increase in the kinetic constant *k* for GO-amended conditions compared to controls can be seen from feed III. During feed IV, where ISRs of 1 and 0.75 were applied, the impact of the increased substrate availability differed for the two ratios. For ISR 1 (Figure 5-6a), the faster kinetics for conditions 10–1 and 20–1 were preserved both during the failure phase (feed IV) with *k* values of 25% and 20% higher than 0–1, respectively, and during the recovery phase (feed V) with *k* values of 14% and 13% higher than 0–1, respectively. On the other hand, for an ISR of 0.75, the first-order rate constants were consistently smaller than the control without GO (0–0.75) during both feeds IV and V. Conditions 10–0.75 and 20–0.75 achieved −11% and −48%, respectively, during feed IV, and −14% and −22%, respectively, during feed V.
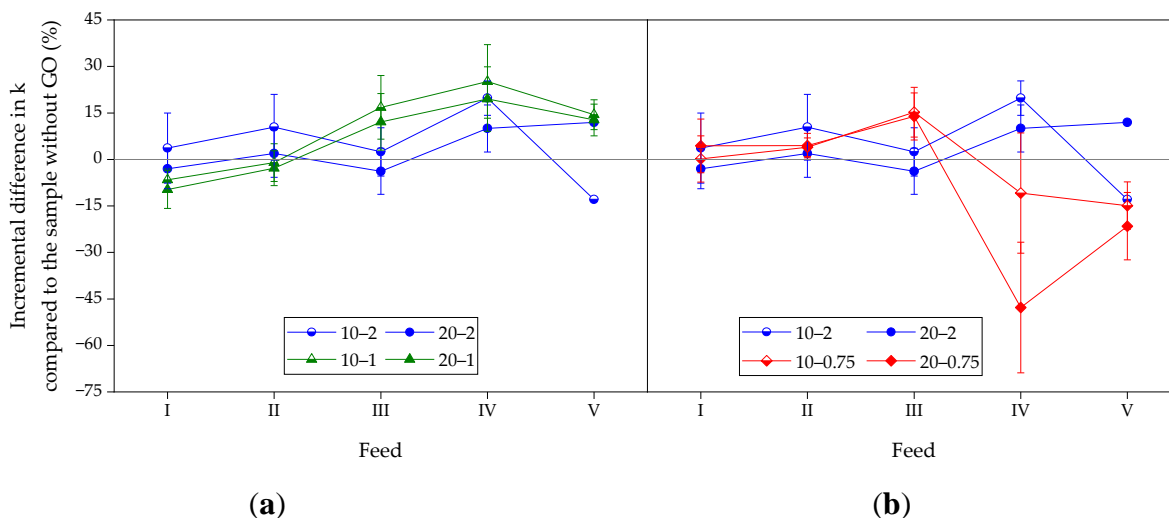
Figure 5-6: Average incremental difference in the first-order rate constant k compared to the respective (same ISR) condition without GO for each feed. Schemes follow another format. (a) 10 and 20 mg_{GO}/g_{VS} of ISR 2 and 1 conditions compared with their respective control (0–2 and 0–1); (b) 10 and 20 mg_{GO}/g_{VS} of ISR 2 and 0.75 conditions compared with their respective control (0–2 and 0–0.75). Error bars represent the standard deviation of replicates ($n = 5$, where applicable).

5.3.3 Impact of GO and ISRs on the pH and FOS/TAC

pH and FOS/TAC measurements were also carried out in this study to gain further insight into the reactor stability during (and after) the overloading phase. As described in Figure 5-7a, at day 2 of the failure phase (feed IV), the lower the ISR applied, the lower the pH values due to the higher VFA concentration present. Interestingly, GO presence affected the pH values, too.

The addition of GO (pH of ca. 2.2) caused a long-term impact on the pH, resulting in significantly lower values than in control assays (i.e., without GO) (Table 0-8). In fact, pH values remained lower for GO-amended assays even after four feeds. Nonetheless, at the end of feed V, all conditions, except 20–0.75 (pH of 7.2), exhibited no significant difference in their pH values, ranging from 7.3–7.5 (Table 0-9).

Moreover, a GO concentration of up to 20 mg_{GO}/g_{VS} had no impact on the FOS/TAC, as the three-way ANOVA revealed no significant differences (Table 0-10). However, it should be highlighted that the FOS/TAC is an indirect estimation of the alkalinity ratio carried out through titration. Since the GO-amended assays had a lower pH, a lower starting pH meant a lower TAC value (Figure 5-7d) and a higher FOS for the control (no GO) (Figure 5-7c). The GO addition might consequently help in the VFA degradation, which often becomes the rate-limiting step in

AD after applying a high organic loading (low ISR) with an easily degradable substrate [166]. This would finally also link back to the observed higher k values, which—in this case with glucose as substrate—were not reflecting the hydrolysis as the rate-limiting step but rather the VFA degradation.
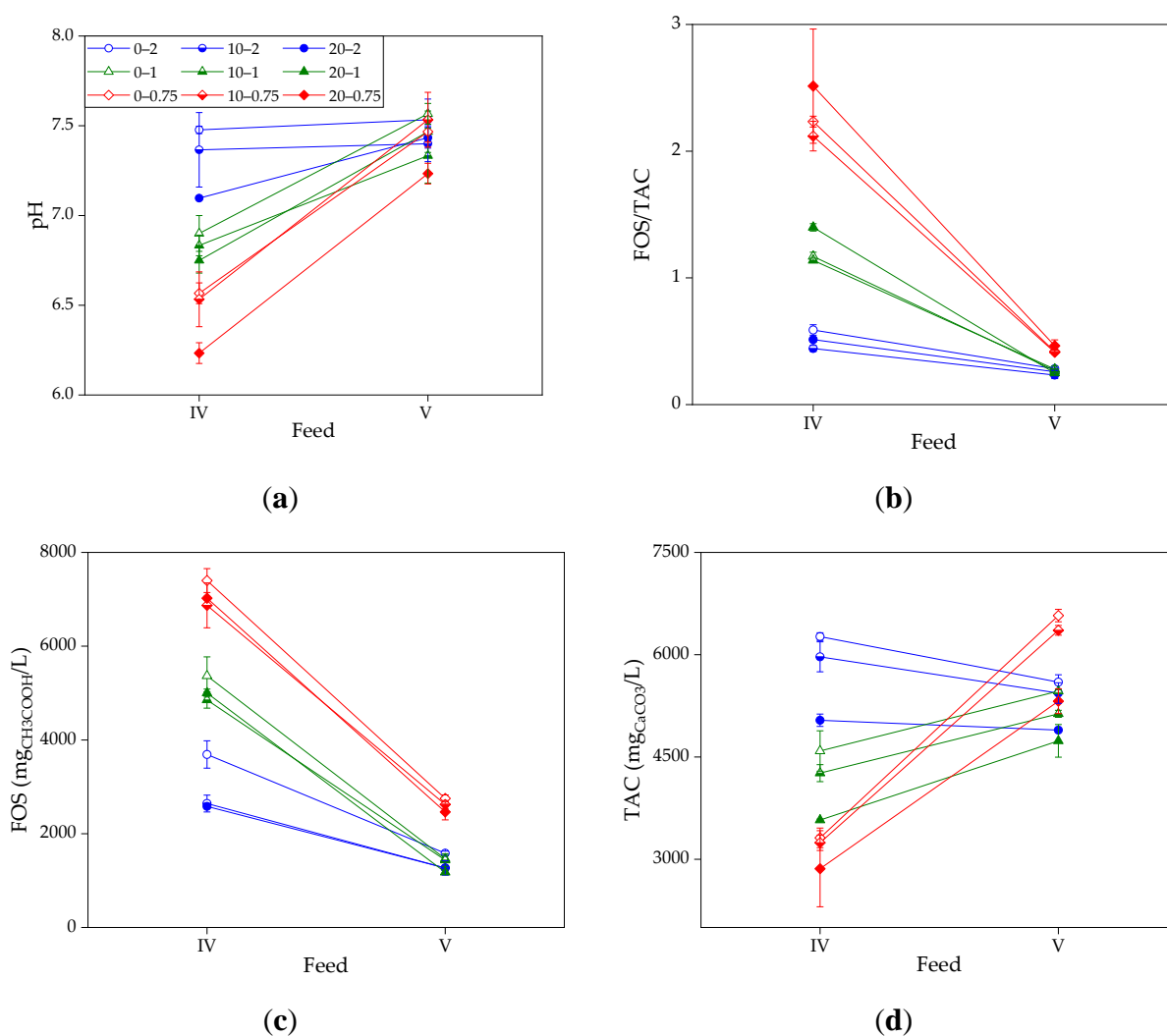
Figure 5-7: Average values of (a) pH value, (b) FOS/TAC, (c) FOS, and (d) TAC at day 2 of feed IV and the end of feed V. Error bars represent the standard deviations of replicates ($n = 3$).

5.4 Discussion

Previous studies have already reported the more efficient conversion of VFA and the faster kinetics owing to the presence of carbon-based materials in overloaded batch assays. For example,

Wang et al. [86] used biochar at 20 g/L to recover a severely acidified AD system. They observed that biochar addition was helpful for a more rapid methanogenesis recovery due to DIET. Similarly, the GO added in this investigation may allow the same DIET capabilities as the faster VFA degradation could be observed indirectly through the FOS/TAC measurements. However, compared to Wang et al., who used 1.53 $g_{biochar}/g_{VS}$, in this study, only 10 to 20 mg_{GO}/g_{VS} were used. Therefore, GO addition may bring the beneficial effects of carbon-based material in DIET establishment already at significantly smaller concentrations.

Gökçek et al. [73] adopted similar concentrations of 0, 10, 20, and 30 mg/L (i.e., 0, 1, 2, and 3 mg/g_{VS}), but of already reduced GO (RGO). Adding RGO had a beneficial effect, leading to higher and faster methane production in overloaded anaerobic digesters. Still, the use of GO (and its consequent biologically reduced form), as in the present study, seems to be preferred over RGO in terms of its production effort [167]. In contrast to the biological reduction of GO, the reduction of GO to RGO entails the use of physical (thermal energy), chemical (strong oxidant), or their combination (photochemical) methods [168].

One aspect that requires attention is the long-lasting acidifying effect due to the GO addition observed. Although no significant differences were noticed among the average pH values of each condition at the end of feed V (except for 20–0.75), during the AD process (day 2 of feed IV), those differences were amplified and became significant (even for an ISR of 2, Figure 5-7a). Low pH values can severely inhibit the process. However, the lower pH may even represent a silver lining in adopting GO as an additive. A lower pH (caused by the GO presence) shifts the equilibrium from inhibiting ammonia to ammonium (NH_4^+). In fact, the high ammonia concentrations found in typical anaerobic digesters were reported to cause a prolonged inhibition role in the AD process [169,170]. This condition is generally referred to in the literature as "inhibited steady state conditions" [171]. Thus, the system may benefit from the presence of GO due to the lowered pH. Future investigations should, therefore, also focus on the impact of GO on the ammonia concentration in the AD system.

Similarly, a closer inspection is needed to understand the VFA distribution. Previous studies suggested the critical role of propionate acid in anaerobic reactors supplemented with nanomaterial (i.e., nano-zero valent iron-modified biochar) [172]. The analysis of AD intermediates combined

with 16sRNA gene sequencing could be decisive in clearly assessing the contribution of GO (or bioRGO) toward DIET in engineered nanosystems.

5.5 Conclusions

The impact of GO addition (0, 10, and 20 mg_{GO}/g_{VS}) in overloaded anaerobic reactors (ISRs of 2, 1, and 0.75 based on $VS_{inoculum}$) was studied. The results showed that the addition of low GO amounts contributed to the acceleration of degradation kinetics obtained from the first-order model under standard operation conditions (i.e., an ISR of 2). Moreover, during and after an overloading situation (lower ISR), the kinetic constant k ended up at similar values as the control (no GO) or even above. Overall, this study contributed to the area of recovering acidified AD processes using novel carbon-based nanomaterials as additives.

Author Contributions

Funding

6. Summary of research outcome and hypothesis testing

This chapter summarizes the principal research objectives of the current dissertation and the respective hypotheses with their testing. Finally, Table 6-1 outlines the results of the hypotheses testing.

6.1. Research objective 1

Objective 1 of this thesis aimed to demonstrate that adding GO in batch reactors can enhance the biotransformation and removal of persistent OMPs while increasing the specific methane production. This can be achieved only if GO undergoes a biological reduction process (bioRGO) first. The formation of bioRGO results in an enhanced electron transfer and faster degradation of organic material. Thus, to evaluate the validity of **objective 1**, the following hypothesis was formulated:

> ***Hypothesis 1***: *The presence of bioRGO significantly improves the biotransformation of selected OMPs and the specific methane yield when compared with a control, i.e., without GO addition.*

As reported in *Paper I* (see Chapter 1), a rapid microbial reduction of GO to bioRGO occurred after one day of incubation with mixed anaerobic sludge, as evidenced by an increase in the I_D/I_G ratio from 0.74 to 1.01, measured using Raman spectroscopy. Also, CV and particle size measurements confirmed biological reduction with increased redox activity and formation of larger flocs. Although bioRGO formation occurred rapidly, it had no impact on the removal of selected antibiotics (i.e., SMX and TMP removal efficiencies reached 90% in 48 hours), and it suppressed the formation of the identified biotransformation products of SMX. Moreover, the biogas production was inhibited by up to 21% with 100 mg/L of GO compared with the control condition (0 mg/L of GO).

Therefore, **hypothesis 1** is <u>partially rejected</u>: bioRGO formation was achieved, but no improved OMP removal or biogas enhancement occurred. However, the study demonstrated that

the presence of bioRGO impacted the biotransformation of SMX by suppressing the formation of the identified sulfamethoxazole TPs.

6.2. Research objective 2

The second objective of this thesis was to demonstrate that the extension of the investigation period (from a single feed to multiple feeds) in batch tests amended with GO positively influenced the degradation kinetics at different rate-limiting conditions. **Hypothesis 2** was subdivided into three parts:

> *Hypothesis 2.1: An optimum concentration of GO exists at which the specific methane yield is significantly higher compared with a control, but achieving this optimum requires 1+ refeeding steps.*

> *Hypothesis 2.2: An optimum concentration of GO exists at which the kinetic parameters (i.e., hydrolysis rate, VFA conversion rate, maximum BMP rate, and lag-phase) are significantly improved (i.e., either regarding higher rates or shortened lag-times) compared with a control. Achieving such optimum GO concentration requires 1+ refeeding steps.*

> *Hypothesis 2.3: GO addition has a stimulating effect on substrates in which the methanogenesis step is considered to be rate-limiting.*

As it is evidenced in Chapter 4 (*Paper II*), GO addition in batch systems had an unequivocal positive effect. Since the third feeding cycle, the kinetics values of the two standard substrates tested significantly improved from 10 mg_{GO}/g_{VS}. Similarly, the specific methane yields were comparable across all the tested conditions. Therefore, **hypothesis 2.1** is <u>partially accepted</u>, and **hypothesis 2.2** is <u>accepted</u>.

Hypothesis 2.3 is <u>accepted,</u> too. Assays employing the use of glucose, which is rate limited by the methanogenesis step (hydrolysis for cellulose), showed a particular increase in the degradation rate constant k. Namely, a 210% increase in k value was observed for GO concentrations of 20 mg_{GO}/g_{VS}, compared with the control (i.e., 0 mg_{GO}/g_{VS}).

6.3. Research objective 3

Objective 3 followed the promising findings of the long-term study of **objective 2**. This third research objective intended to attest that GO improves the recovery of overloaded anaerobic batch reactors. The following hypothesis was formulated:

> **Hypothesis 3**: *The presence of bioRGO in overloaded anaerobic reactors acts as a mitigator, and model-derived kinetic constants and stability parameters are significantly better compared with a control.*

Similar to *Paper II*, *Paper III* research (see Chapter 5) was conducted using a fed-batch strategy at different levels of GO but using also different ISRs to simulate the overloading conditions. The study showed that while GO did not alleviate the acidification effects, during the final phase the kinetic constants reached values similar to or even above the controls. Therefore, **hypothesis 3** is <u>partially accepted</u>.

Table 6-1: Summary of hypotheses testing.

Hypothesis	Outcome
1: The presence of bioRGO significantly improves the biotransformation of selected OMPs and the specific methane production when compared with a control.	Partially rejected
2.1: An optimum concentration of GO exists at which the specific methane yield is significantly higher compared with a control, but achieving this optimum requires 1+ refeeding steps.	Partially accepted
2.2: An optimum concentration of GO exists at which the kinetic parameters (i.e., hydrolysis rate, VFA conversion rate, maximum BMP rate, and lag-phase) are significantly improved (i.e., either regarding higher rates or shortened lag-times) compared to a control. Achieving such optimum GO concentration requires 1+ refeeding steps.	Accepted
2.3: The GO addition has a stimulating effect on substrates, in which the methanogenesis step is considered to be rate-limiting.	Accepted
3: The presence of bioRGO in overloaded anaerobic reactors acts as a mitigator, and model-derived kinetic constants and stability parameters are significantly better compared with a control.	Partially accepted

7. Overall discussion

The impact of GO addition on the removal and biotransformation of selected OMPs and biogas production was investigated in this thesis. Anaerobic batch assays were employed to evaluate both aspects.

7.1. Effects of GO addition

7.1.1. Effects on OMPs removal and biotransformation

In contrast to previous research [50,56], the removal of the two OMPs tested (i.e., SMX and TMP) in this work was unaffected by the GO presence at different concentration levels (10, 100, 500 mg/L) (**Paper I**). Yet, GO addition clearly influenced the formation of the two identified SMX biotransformation products, namely, TP253 and TP257. As an example, formation of TP257 reached 40% of the initial concentration of SMX (estimation based on the peak area of the *m/z* 258 and normalized to the initial peak area of SMX) at 0 mg/L of GO, but only 16% at 500 mg/L. It is here hypothesized that GO addition led to the formation of other byproducts (at the expense of the TP253 and TP257), but that these were simply not identified by the technique employed in the study (LCMS). Moreover, the presence of the two SMX TPs was detected in the sterilized assays, pointing to the activity of intracellular enzymes likely released due to cell lysis during the autoclaving and that preserved their activity.

Therefore, the experiments described in this thesis indicate that GO impacts the biotransformation of OMPs, but not necessarily enhances it, as it was reported in literature. The results also suggest that subsequent studies exploring the effects of GO on OMPs removal and biotransformation should look beyond the parent compound and focus also on the changes in the biotransformation pathways.

7.1.2. Effects on methane production

The effect of GO addition on methane production was studied in batch assays with single (**Paper I**), and multiple (**Paper II, Paper III**) fed strategies. The experiments confirmed an initial inhibition or no improvement for biogas yield or kinetic parameters at the early stage. However, it

was evidenced that from the third feeding cycle, concentration from 10 mg$_{GO}$/g$_{VS}$ led to significant enhancement of the kinetic parameters. When glucose was used as the substate, the first-order rate constant k for the assays supplied with 20 mg$_{GO}$/g$_{VS}$ reached a two-fold higher value compared with the control (i.e., 1.65 ± 0.20 d^{-1} vs. 0.76 ± 0.08 d^{-1}). Similarly, for cellulose-supplied assays, the maximum methane production rate R_{MAX} value increased up to 20% compared with the control (177.4 ± 35.2 mL$_{CH4}$/g$_{VS}$·d^{-1} vs. 146.5 ± 21.7 mL$_{CH4}$/g$_{VS}$·d^{-1}). Moreover, the calculated infinite BMP B$_\infty$ was unaffected for both substrates from the third feed on, and achieved values in the typical range, i.e., 305-355 mL$_{CH4}$/g$_{VS}$ for glucose, and 340-395 mL$_{CH4}$/g$_{VS}$ for cellulose. Thus, the effects of GO on methane production proved to have a silver lining for long-term scenarios.

7.2. Engineering and process considerations

As it was described in this thesis, the use of GO in anaerobic treatment systems may improve the rate of biological reactions and pollutants transformation. However, some aspects related to the use of GO in anaerobic wastewater treatment systems need to be considered at the engineering and process level.

Dosage, dispersion of GO, and reactor configuration. All of these are crucial aspects in a reactor amended with GO. For example, once the GO is added to a reactor, it is crucial to ensure that GO is retained within the reactor and not lost with the effluent. This can be achieved by designing the reactor to have appropriate retention times and by using appropriate methods for separating the (R)GO from the treated effluent. These aspects will be further discussed in Chapter 7.3 and 7.5.

Interaction of GO with microbes. As shown in this dissertation (**Paper I**) and in the literature, GO can aggregate with microbes in anaerobic wastewater treatment systems. In these systems, GO can potentially enhance the removal of pollutants by providing a surface for microbial attachment. However, the effectiveness of GO in anaerobic treatment systems is highly dependent on several factors, including the concentration of GO and the specific type of microbe and wastewater (e.g., municipal, industrial, sewage sludge, etc.) being treated. Another essential factor to consider concerning the interaction between GO and microorganisms are the environmental conditions,

such as pH, temperature. Additionally, the long-term toxicity of GO to the microbes should be evaluated.

Environmental impact, handling, and disposal of GO. Generally, GO can be found in a powder form or as a dispersion in a liquid (as it was employed within this dissertation), but it can also be formed into films or sheets. However, being a relatively new material, the risk and safety of its handling are not fully defined. For example, the environmental fate of wastewater or sewage sludge containing GO is also another critical factor to consider. Typically, after a dewatering process, anaerobic sludge can be applied as a soil amendment (varying according to countries' regulations). However, sludge containing GO might not be accepted for such practice, and regulations are yet to be developed. Thus, the choice of its disposal may be narrowed down to incineration only, which is a practice in contrast with a circular approach pursed in this thesis and in recent water treatment schemes. Moreover, incineration of sludge may substantially increase the overall cost of using GO in a biological treatment system, while its main advantage relies on being relatively inexpensive compared to advanced treatment systems. Nevertheless, when considering the environmental fate of GO, its biotransformation (and its biodegradation) has also to be taken into account (Figure 7-1). Recently, it was demonstrated that human enzymes and insects can biodegrade GO [173,174]. Even if the latter sounds promising for implementation of GO in biological processes, the long-term environmental impact of GO disposal is not well understood. It is unclear whether the GO is fully degraded by the microbial community, and if any RGO particles remain intact. This aspect would be of concern in terms of nanomaterials toxicity, and it would determine whether GO-amended sludge could be treated as usual or not. Consequently, it is crucial to consider associated potential risks and conduct appropriate environmental assessments for the safe handling and disposal of biologic material containing GO.
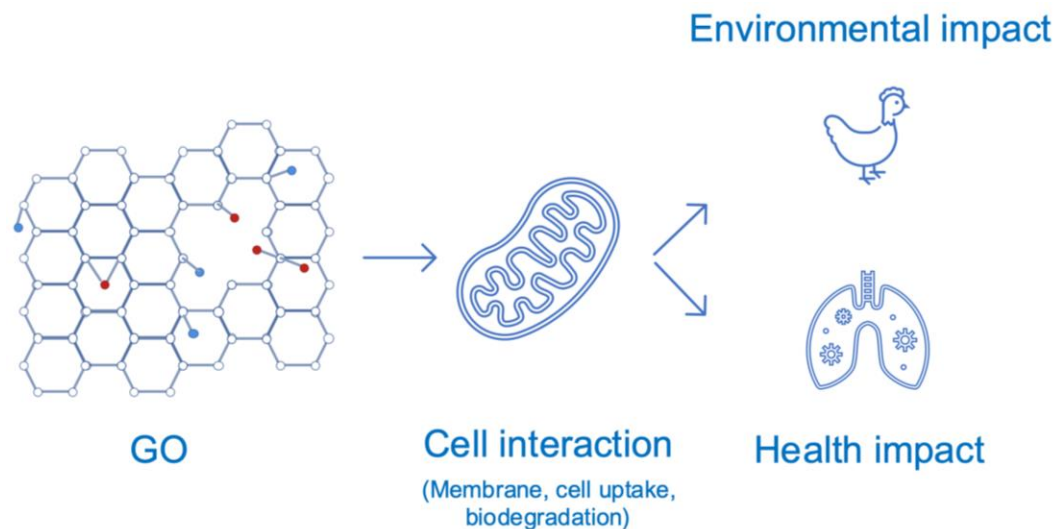
Figure 7-1: Health and environmental impact of GO (adapted from Graphene Flagship, Annual Report 2020 [175]).

Additionally, it should be noted that in all the performed experiments of this thesis (**Paper I**, **II**, and **III**), the formation of **hydrogel** (already reported in other studies) caused the overflow of some assays (Figure 7-2), which is linked with EPS excretion. The cause of increased EPS excretion in the GO-amended system seems to be explained by a combination of two main occurrences happening at the microbial level. The sharp edges of graphene cause cutting damage to membrane cells, leading to the release of intracellular material [75]. The formation of ROS due to GO bioreduction also leads to further environmental stress [77]. At the same time, as a microbial protective response, microorganisms tend to excrete greater amounts of EPS to adapt to the stress of the membrane and use the EPS as a shell for protection.
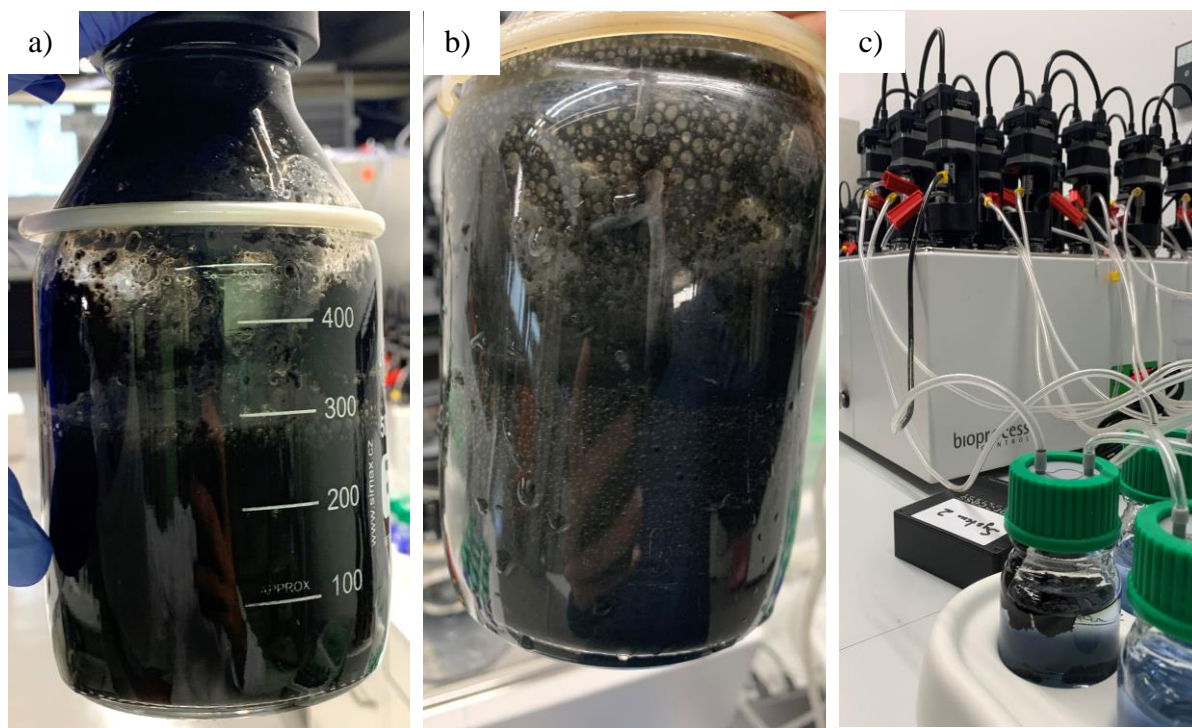
Figure 7-2: Formation of hydrogel (a, b) and consequent liquid overflow into the CO_2 trapping system (c).

Although this reported phenomenon of hydrogel formation and overflowing should be carefully studied and considered in prospective of scaling up the technology, increased EPS excretion is beneficial. The presence of EPS appears to play a fundamental role in protecting the bacterial cell from the antimicrobial effects of RGO, such as its atomically sharp edges that cause physical damage to the cell, but also to the formed or depleted reactive oxygen species that cause oxidative stress [39,77,95]. Furthermore, it was found that the GO sheet area assumed a central aspect for *Shewanella* inhibition and formation of an agglomerated GO-microorganisms complex (i.e. hydrogel) [78]. In particular, GO sheet area greater than $0.30\,\mu m^2$, and a relatively high degree of GO reduction (i.e., C/O ratio greater than 1.75, or I_D/I_G ratio > 1.01) were found crucial for rapid development of the hydrogel structure. Moreover, the lower presence of oxygen functional groups resulted in a more hydrophobic surface that in turn attracted further microbes leading to faster hydrogel formation.

7.3. Considerations on the reactor configuration

As can be inferred from **Paper II**, and **III**, a continuous-flow reactor configuration is proposed as being the optimal solution for retaining the nanomaterial, as it allows for a consistent flow of wastewater to be treated and for the GO to be added and retained within the reactor.

An anaerobic membrane bioreactor (AnMBR) configuration could be chosen over other configurations as it can effectively remove pollutants from wastewater while retaining the biomass – and the GO – within the reactor. A schematic representation of an AnMBR operated with an external membrane can be seen in Figure 7-3.
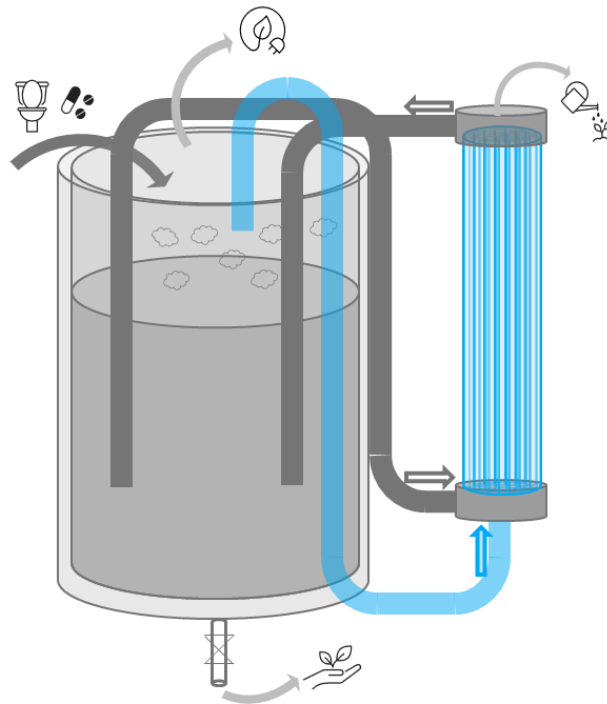
Figure 7-3: Schematic representation of the AnMBR with external membrane module.

However, when considering the operation of a continuous AnMBR amended with GO, some important engineering aspects need to be contemplated, including:

Dosage and dispersion of the GO. The appropriate dosage of GO will depend on the specific characteristics of the wastewater being treated and the biomass concentration present in the reactor (expressed as VS concentration). Concentration levels could be based on the batch experiments developed in this thesis, which were in the order of 5-50 mg_{GO}/g_{VS}. Proper GO dispersion is also

important to ensure that it is evenly distributed throughout the reactor. This aspect could be guaranteed by a continuous stirrer, and an internal recirculation system.

Membrane fouling and pore size. The combined presence of wastewater and GO can potentially foul the membrane. Thus, it is important to monitor the fouling of the membrane and perform regular maintenance to prevent excessive fouling. Also, the effect of GO on the minimization of fouling must be addressed, for instance by applying biogas sparging. On the other hand, the pore size of the membrane should be chosen such that it is able to retain the (R)GO from leaving through the permeate line. According to the particle size analysis of Chapter 1, where after 1 day only the GO reduction took place and the bioRGO-sludge particle size range increased from 63 - 131 µm to 325 - 689 µm (estimated via optical microscope), a microfiltration membrane (pore size of 0.1 - 10 µm) could be proposed.

Keeping target GO level. Some of the sludge leaves the reactor through the wasting line to maintain a specific biomass concentration and provide an SRT to the system. Moreover, GO seems prone to biodegradation, but the biodegradability rate depends on the operational conditions [173,174]. Thus, both aspects, i.e., the amount of (R)GO lost through the wasting line and the biodegradability rate, should be considered when operating the reactor. GO may need to be added regularly to maintain the target bioRGO concentration level.

Beyond treatment systems equipped with membrane, another possibility would be systems with magnetic particles impregnated into GO. This system, which already proven their capability in recovering overloaded anaerobic digesters [176], could offer another potential route for keeping the target GO level within the system. Similarly, systems with granular sludge such as UASB reactor, where bioRGO may facilitate the formation of these granules can also be considered.

7.4. Estimation of operating and capital costs

One concern is that the high cost of producing, and disposing biological material containing GO may make it less practical for use in large-scale treatment systems. Moreover, it is important to note that the cost of GO can vary depending on the supplier, the form (powder or as a surface on a substrate), quality, and quantity purchased. In general, small quantities (grams or less) can cost

anywhere from a few to several hundred dollars, while larger quantities (kilograms) can cost several thousand dollars or more.

As mentioned, given the conceptual stage of the experiments, a detailed estimation of the costs goes beyond the scope of this dissertation and is left out as it may not be reliable. However, listing and briefly discussing some of the potential advantages is possible. For instance, a major implication of a clear enhancement of the first-order rate constant k has a significant impact on the design of full-scale reactors. The degradation constant of the organic material (k) is indeed linked with the retention time. The first-order rate equation applied in Paper II and III is formulated as follows:

$$\frac{dC}{dt} = -kC \qquad \text{(\textit{Equation 3})}$$

Where C is the concentration of organic matter in the digester and t is time. Rearranging the equation and integrating it over the range of organic matter concentration, the following equation can be derived:

$$\theta = \int \left(\frac{C_0}{C}\right) e^{-kt} dC \qquad \text{(\textit{Equation 4})}$$

Where C_0 is the initial concentration of organic matter. When *Eq. 4* is evaluated over a range from C_0 to 0, the integral would lead to *Eq. 5*, which shows that the retention time is inversely proportional to k.

$$\theta = \frac{1}{k} \qquad \text{(\textit{Equation 5})}$$

Therefore, an increase in the k leads to a decrease in the retention time of the anaerobic digestor. As the retention time is a key parameter for the digestor design, this has a major implication when

it comes to determining the reactor size (i.e., its volume), or its capacity to handle organic material (i.e., organic loading rate, OLR). Hence, for an increased k the reactor size will be reduced, or, at the same volume, the OLR will be increased.

In Paper II, for the degradation of glucose during fifth feed, it was shown how between the condition with and without the k was doubled, i.e., 1.65 d^{-1} and 0.76 d^{-1} for G-20 and G-0, respectively. Although the study used a specific substrate (glucose), the advantages of such increased k are evident and can be reflected to the economics of the capital and operating expenses.

The increased kinetics then need to be benchmarked with the cost of adding GO to a full-scale anaerobic treatment process, like an AnMBR. However, not having scaled up the BMP experiments into such a reactor, a closer estimation can be made for a full-scale anaerobic digestor. Hence, as an hypothetical example, an addition of 10 mg_{GO}/g_{VS} (proved to be statistically significant for k increase) is considered for a municipal digestor with a volume of 2,480 m^3, a VS concentration of 15 g/kg [177], a GO cost of ca. €50-200/kg[1,2]. Thus, assuming a sludge density of 1,000 kg/m^3, addition of GO results in a cost ranging between €18,600 and €74,400. Presuming that addition of GO does not involve any further operational costs, and that GO is maintained within the digester, the benefits can be estimated with the higher OLR capacity given by the increased k. Moreover, new methods for graphene synthesis are likely to bring the price down in the near future as carbon-based waste material can be used. Thus, replacing graphite, which is the current industrial synthesis, with biowaste seems to be promising [178].

7.5. Opportunities for future research

Chapter 1 outlined a major prospect in this dissertation, which is the potential impact of GO on the biotransformation of OMPs, specifically antibiotics such as SMX and TMP. This could include further investigations into the formation and effects of bioRGO on the removal of these pollutants and the formation of biotransformation products, as well as the role of intracellular enzymes in this process.

---

[1] https://www.graphene-info.com/nanoxplore-plans-10000-ton-graphene-powder-facility
[2] https://bigthink.com/the-present/flash-graphene/

In Chapter 4, one main finding stands out for future perspectives. GO effects should preferably be investigated in long-term scenarios since the use of batch tests give limited insight into the behavior of the microbial community.

The third feed cycle has a particular significance. It represents the usual time needed to enter steady-state conditions. Although steady-state conditions are met at an infinite number of cycles, three times the retention time is conventionally adopted in literature [179,180]. Thus, the third feed cycle designates the beginning of steady-state conditions, where positive effects of GO are apparent.

As seen in **Paper II** (and **III**), the three automatic methane potential test systems provided high resolution measurements for the determination of the methane production profile (Figure 7-4a). Also, the generated first-order model had an excellent goodness of the fit with values of $R^2 < 0.97 \pm 0.01$, and rRMSE $< 7.6 \pm 0.4$. However, as can be observed in Figure 7-4**a** and **b**, deviations between the experimental points and the model curve are present and can be clearly distinguished. The SMP curve can be divided into:

- Phase 1 (0 d – 0.5 d): characterized by a short lag-phase and an exponential increase with a high slope.
- Phase 2 (0.5 d – 2 d): characterized by an intermediate slope.
- Phase 3 (2 d – end): similar to Phase 2, but with lower slope.

It might be interesting to correlate these three phases with the different AD stages. In fact, for glucose, the hydrolysis stage is negligible, and only acidogenesis, acetogenesis, and methanogenesis are present. It seems that during Phase 1, a fast and intense production of biogas is occurring. In the 0.25 d – 0.4 d timeframe (ca. 3.6 hours), 100 mL of CH_4 is produced (i.e., almost one third of the total BMP). Thereafter, methane production is abruptly stopped and proceeds with lower rates. It is possible to assume that the methanogens cannot keep up with the transformation of byproduct of the acidogenesis into methane due to the lower kinetics, or because of the increasingly acidic environment (inhibiting to methanogens) due to VFAs abundance.
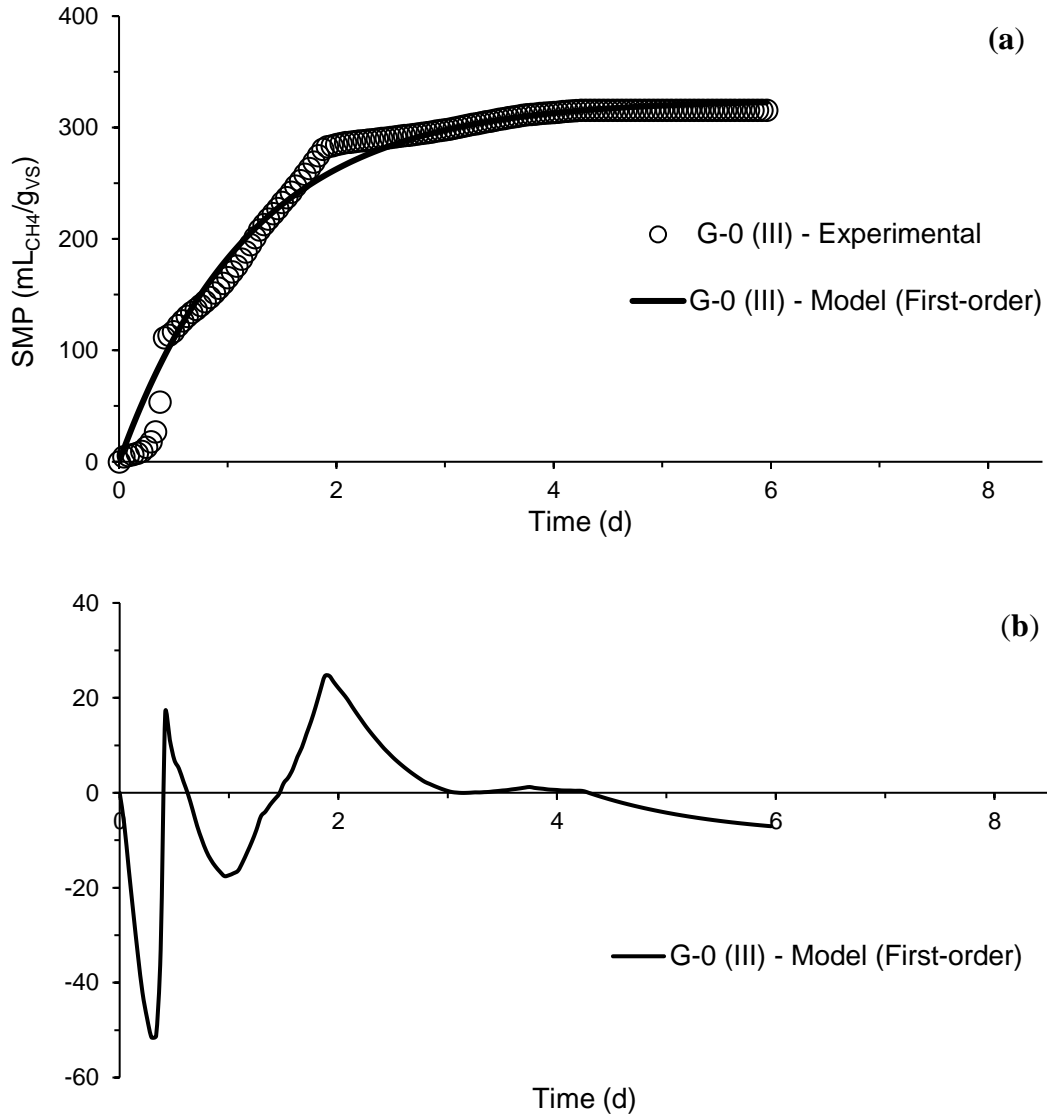
Figure 7-4: (**a**) Experimental and model SMP values for glucose during third feed in BMP test of Paper II, and (**b**) its analysis of residuals.

A more comprehensive model should be able to include these three phases. AD models available in literature have indeed tried to distinguish such phases, and two-, or three-steps models are available [143]. However, a big drawback of more complex models is the need to measure and calibrate more parameters into the model, such as the concentration of the included intermediates, e.g., VFAs or H_2 [181].

Besides, concerning the reactor configuration, Rodriguez-Narvaez et al. [182] highlight the need to rely on more than one single treatment for the removal of emerging contaminants, which also includes classes of OMPs. In fact, a single treatment technology like the only application of a

high surface carbonic material, such as graphene or RGO, will result in the removal of the contaminant only by adsorption. In this way, although the contaminant is no longer present in the aqueous matrix, it has not been transformed. Thus, the problem has simply shifted from the liquid to the solid phase.

Therefore, the combination of more than one treatment technology into a hybrid system might be desirable for completely removing the contaminant. A hybrid system, as in the case of bioRGO in an anaerobic environment, if, allows the adsorption of contaminant on the bioRGO on one hand, and on the other hand, anaerobic transformation of the contaminant, enhanced by the electronic exchange capacity offered by the present conductive material.

In fact, biological DIET methanogenic bacteria have been found in anaerobic reactors where biomass can aggregate. An example of such a reactor is the upflow anaerobic sludge blanket (UASB), where evidence of the DIET mechanism between bacteria and methanogens was first reported [17]. In fact, the sludge granules that are formed within an UASB reactor configuration allow to shorten the inter-microbial distance and make the electron transfer possible without the need of diffusive electron carriers such as hydrogen or formate. Otherwise, a carbon-based support matrix can be used for three main reasons:

- Provide a support medium for the microorganisms to grow.

- Enhance the electron transfer by using a conductive material.

- Adsorb potentially toxic compounds such as persistent pollutants or heavy metals (HM).

Overall, future research should evolve around comprehensive and detailed studies. Although the dissertation aimed at its application to wastewater systems, only the first steps were moved in this direction. Currently, the applicability of GO might be limited to specific industrial processes. The use of GO in real wastewater facilities needs further evaluation in the field of its life cycle assessment and its interaction with the microorganisms [19]. Also, special consideration should be given to the fulfillment (and even exceedance) of water discharge limits criteria[3]. Finally, the lasting impact of GO on the solid part requires careful and targeted investigations.

---

[3] https://ec.europa.eu/environment/archives/enlarg/handbook/water.pdf

8. Conclusions

The thesis explored the performance of a hybrid anaerobic nano-engineered system in terms of organic pollutant biotransformation and formation of biogas.

GO application was implemented in anaerobic batch environments. Studies aimed to confirm the bioRGO formation and assess its impact on OMPs biotransformation and biogas production. The results revealed the following main conclusions:

- The biological reduction of GO occurs within a day. This reduction process causes the formation of a bioRGO-sludge gel-like structure.

- Anaerobic inoculum sampled from full-scale anaerobic digesters (treating sewage sludge) is enough to achieve bioRGO formation.

- Inhibition of the biogas yield due to GO addition is limited to the initial phase.

- While not impacting the kinetics of SMX and TMP removal, 50 mg_{GO}/g_{VS} have suppressed the biotransformation pathway of SMX with lower concentrations observed for the identified TP253 and TP257.

- GO concentrations higher than 10 mg_{GO}/g_{VS} significantly increased anaerobic substrate degradation rate constants. Those kinetic constants were obtained from models showing high goodness of the fit. In particular, values of $R^2 > 0.98$, and $rRMSE < 7.6\%$ for glucose (first-order model), and R^2 of 1.0, and $rRMSE < 3.3\%$ for cellulose (modified Gompertz model).

- Continuous operating systems should be pursued for future investigations as the negative effect of GO addition (microbial environmental stress, biogas yield inhibition) are restricted to the early stage.

Appendix A

Conference proceedings

Ponzelli, M., Zahedi, S., Drewes, J.E., Koch, K., Radjenovic, J., Anaerobic degradation of persistent pollutants using bio-reduced graphene oxide (oral presentation). IWA ecotechnologies for wastewater treatment (ecoSTP21), June 2021, Milan, Italy.

Ponzelli, M., Radjenovic, J., Drewes, J.E., Koch, K., The impact of graphene oxide on methane production kinetics (30 min oral presentation). Nowelties final conference, May 2022, Dubrovnik, Croatia.
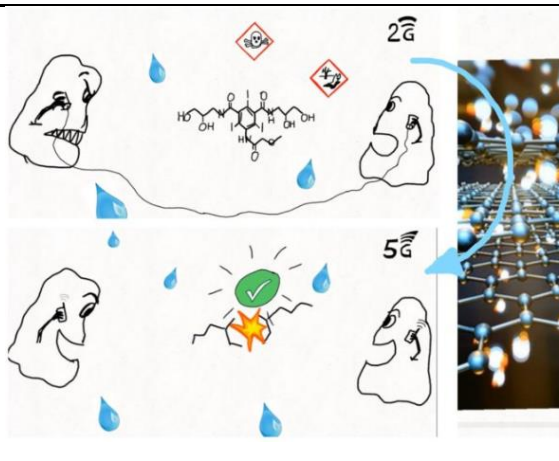
Ponzelli, M., Casabella, O., Pijuan, M., Radjenovic, J., Removal of pharmaceuticals during long-term operation of anaerobic membrane reactor treating municipal wastewater (poster presentation). The 12th IWA Micropol & Ecohazard conference, June 2022, Santiago de Compostela, Spain.

Appendix B

Outreach activities

For facilitating the comprehension and the diffusion of the conducted research to a broad audience, blog article and videos were published on social media platforms and on the project website (https://nowelties.eu/). A digital book collecting all the 100+ blogs was also created[4].

A collection of the most relevant outreach activities can be found below.

Title, URL, date and format	Cover picture
Graphene: The Microbes' 5G Network https://nowelties.eu/graphene-the-microbes-5g-network/1702/ 28.02.2020 – Web article	
15 seconds Research Executive Agency challenge #MyJobinResearch https://twitter.com/REA_research/status/1272802286281150464 16.10.2020 – Twitter video	

---

[4] https://nowelties.eu/wp-content/uploads/2022/09/Nowelties-Book-of-Blog-EU-MSCA-logos.pdf

Water reuse: How safe is it?

https://www.aigues.net/water-reuse-how-safe-is-it/

13.10.2020 – Web article

The Microbes 5G Network

https://youtu.be/i8SklIojiVo

05.03.2021 – YouTube video
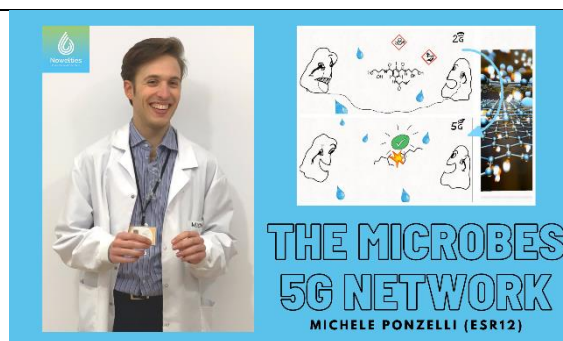
Water reuse to the rescue? From emerging contaminants to emerging heroes

https://www.youtube.com/watch?v=cy_Cl5E9iDk

14.03.2021 – YouTube video

A Day in the Lab

https://www.youtube.com/watch?v=BEh2IWvlaY

E

09.07.2021 – YouTube video
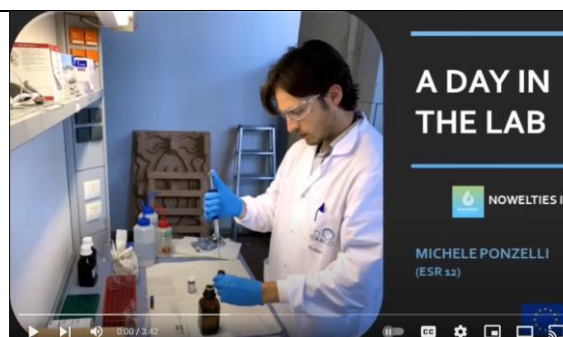
Appendix C

Supplementary material Paper I
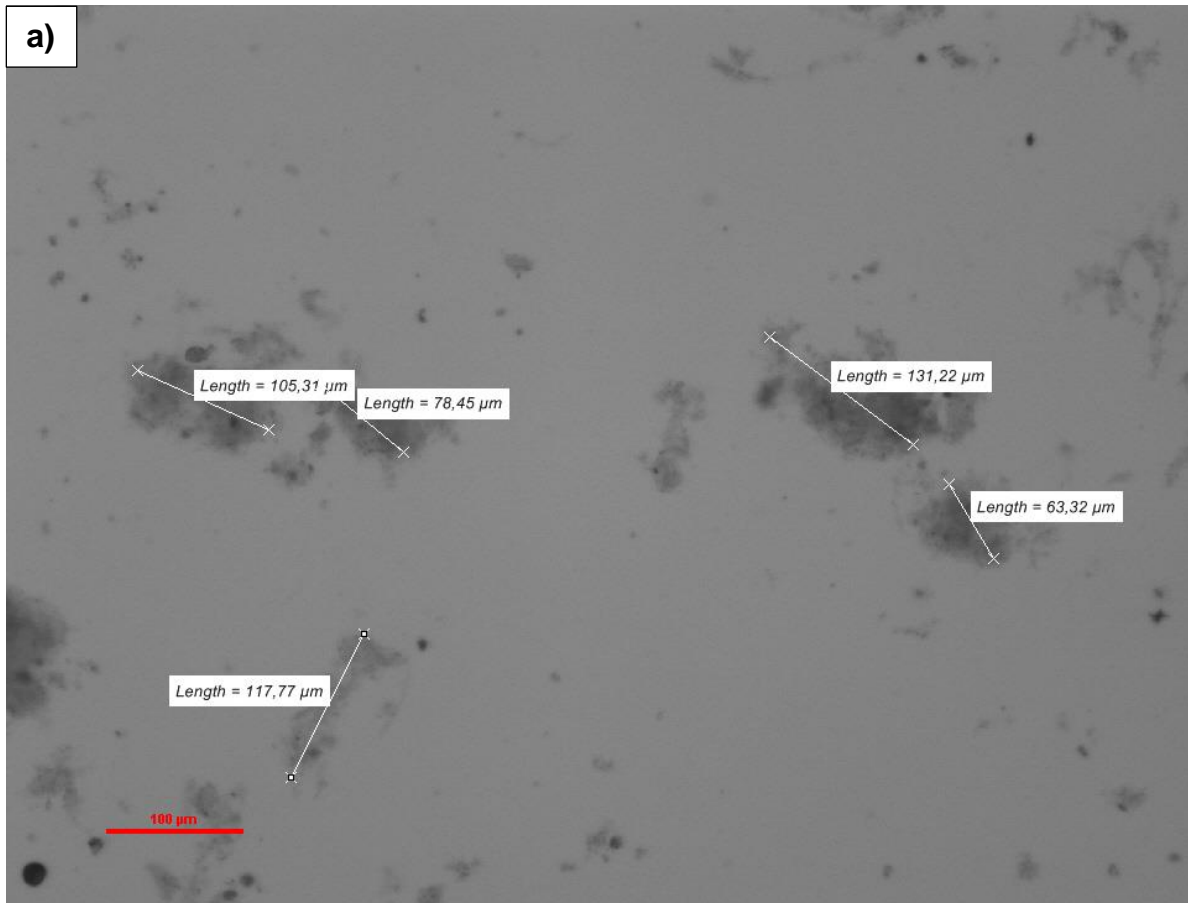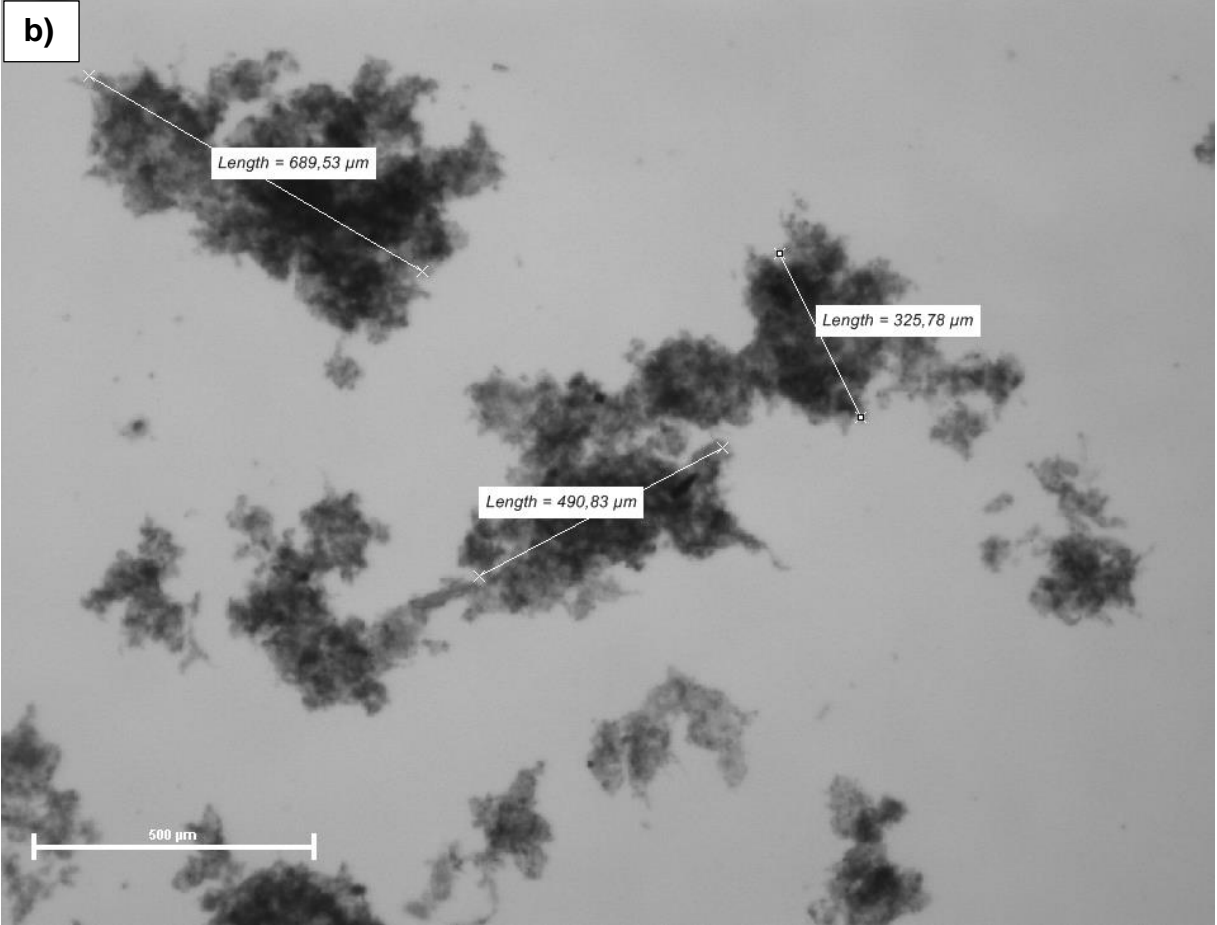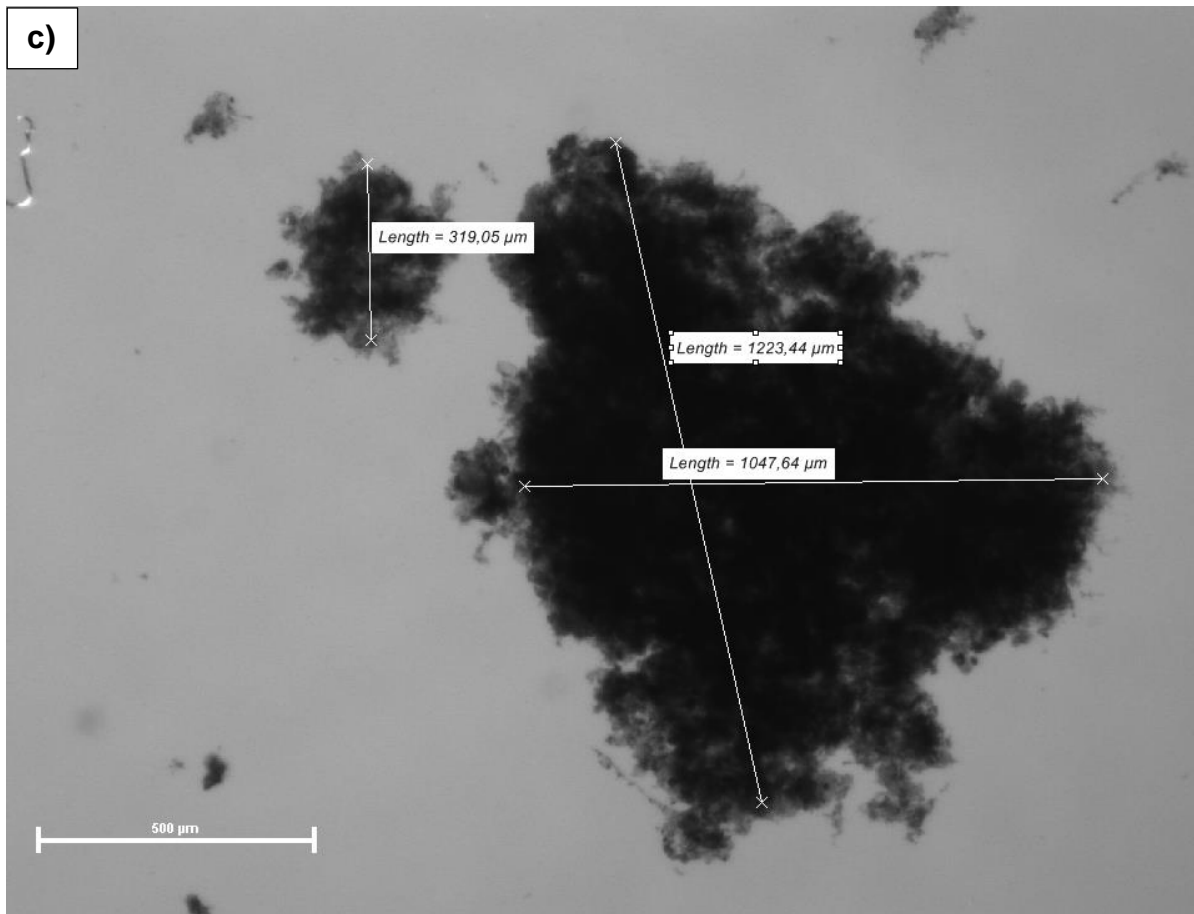
Figure 0-1: Optical microscope image of: **a)** anaerobic sludge, and anaerobic sludge amended with 500 mg/L of GO at **b)** day 1, and **c)** day 15 of the experiment.
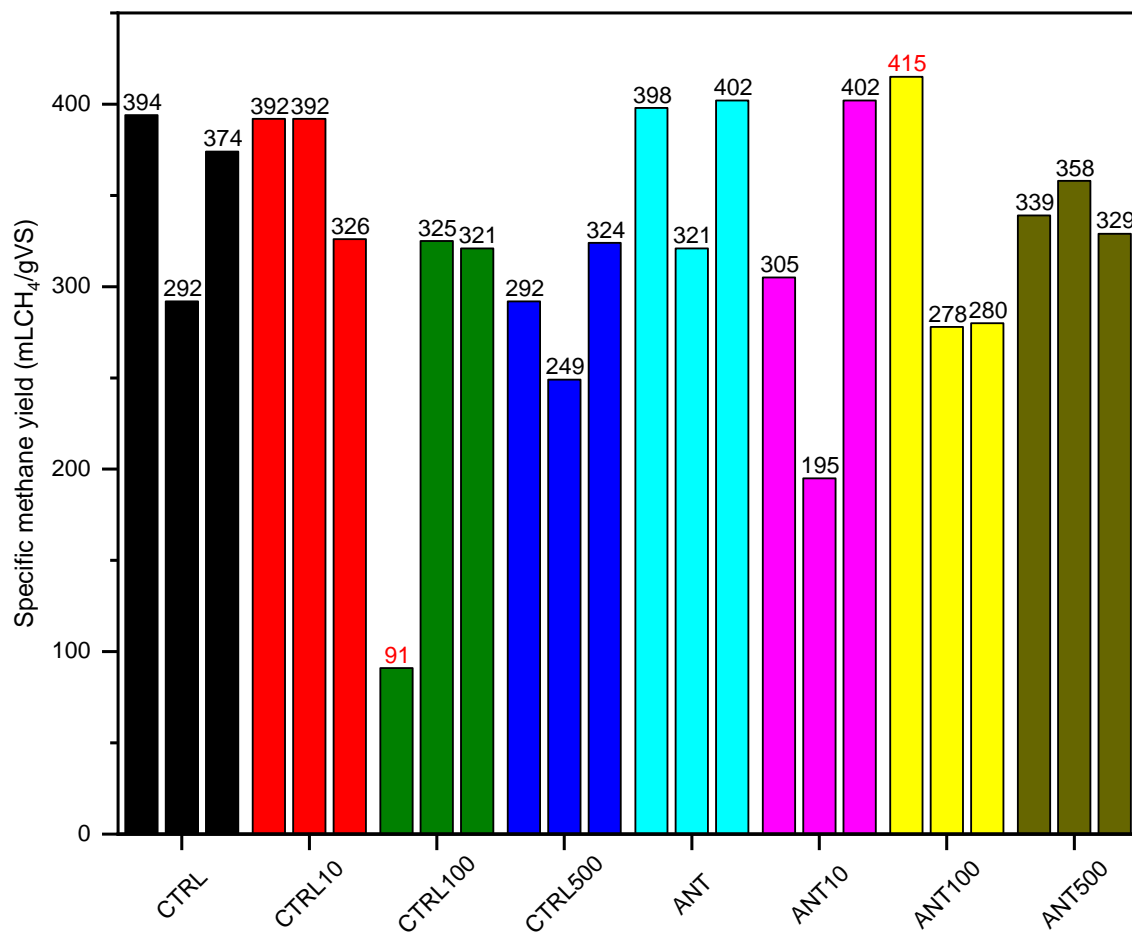
Figure 0-2: Comparison of the specific methane yield for each of three replicates among the different GO dosages and contaminants presence. First replicate in CTRL100 condition, and the first replicate in the ANT100 are identified as outliers (p=0.029, and 0.025, respectively) and were not considered further.
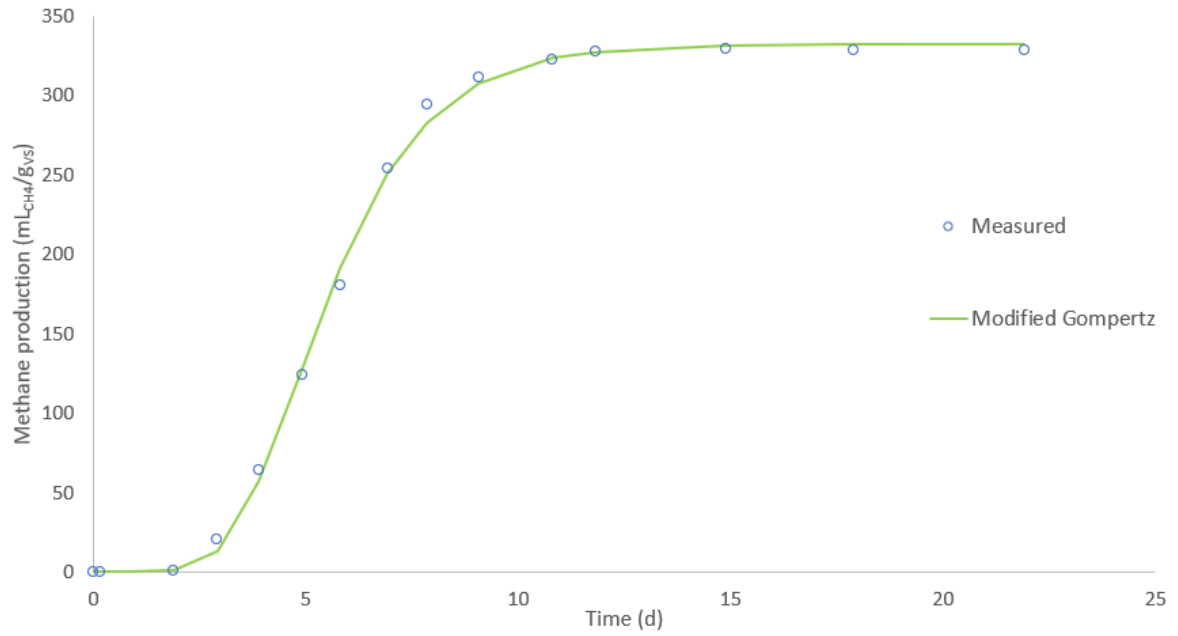
Figure 0-3: Mean experimental values (symbols) and model data (line) of methane production for positive control of cellulose (CTRL).
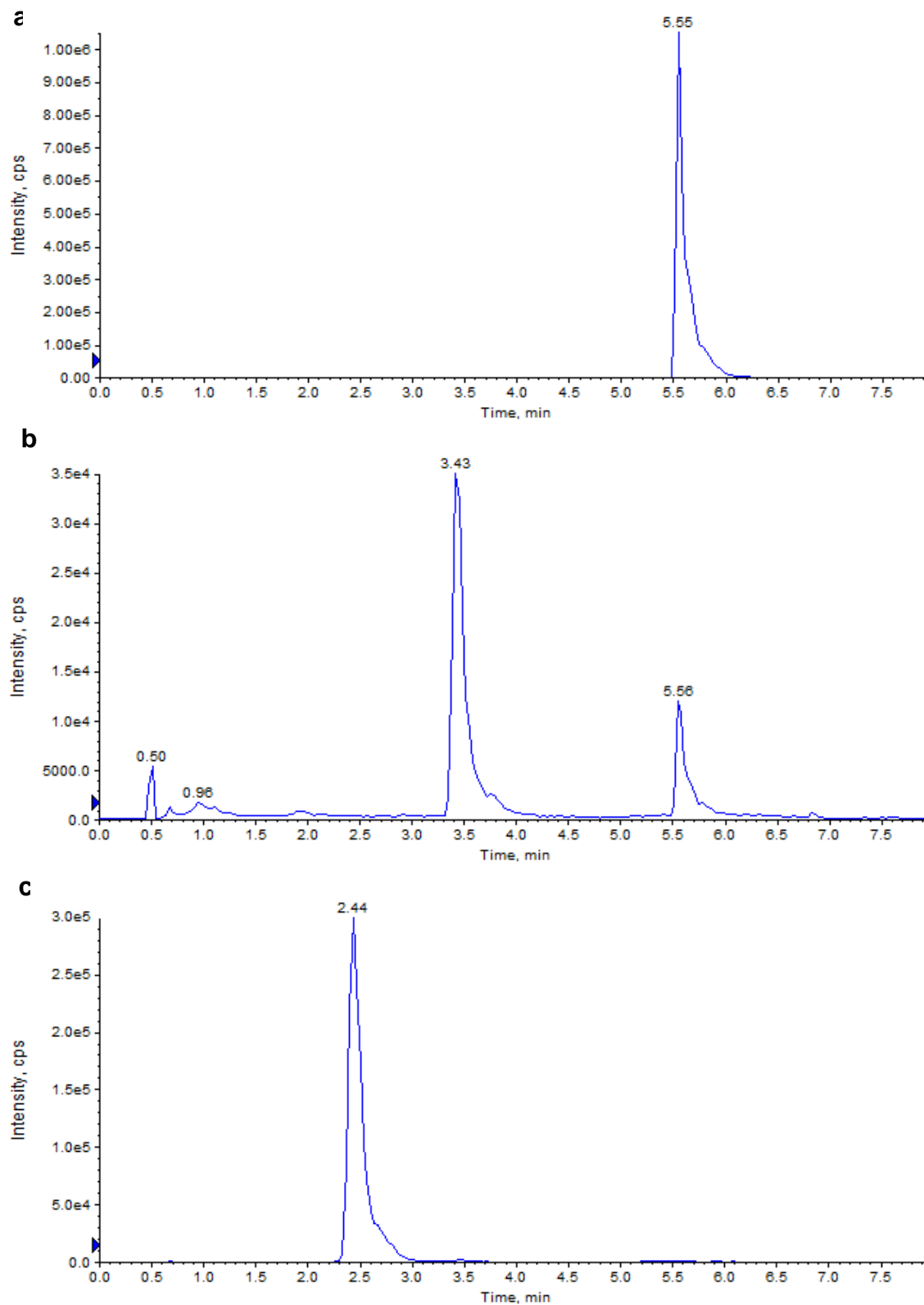
Figure 0-4: Extracted ion chromatogram (XIC) of m/z 254 for anaerobic sludge (AS) amended with SMX: **a)** at day 0, and (**b**) day 3. In figure **b**, the formation of TP253 at 3.43 min can be noticed; **c)** XIC of multiple reaction monitoring (MRM) of TP257 (m/z 258.100), product ion (m/z 156.000) day 15.
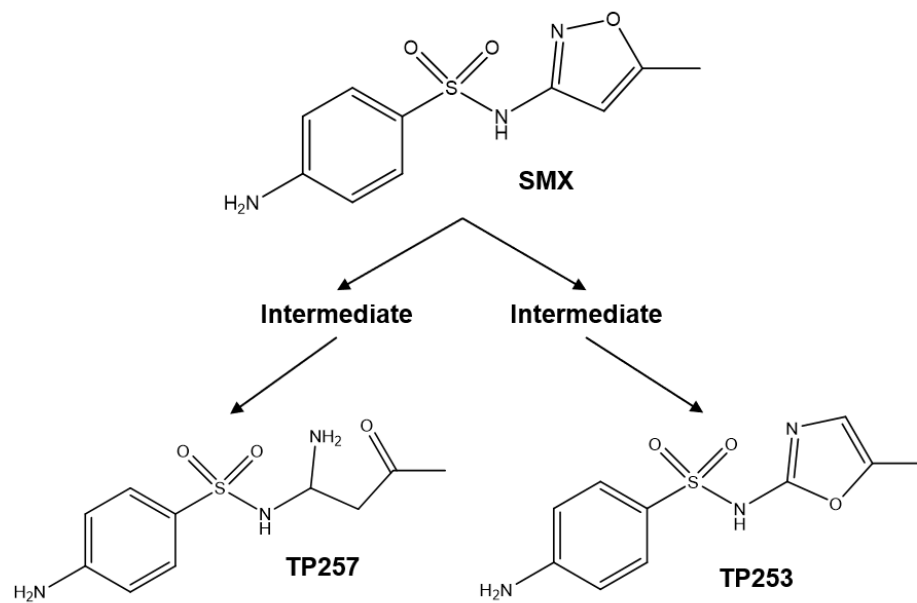
Figure 0-5: Proposed biotransformation pathway for SMX.

Table 0-1: Summary of the characteristics of microcrystalline cellulose (MCC), inoculum, blank (i.e., inoculum only), and control assays without antibiotics (CTRL) and with antibiotics (ANT) at the end of the biochemical methane potential (BMP) tests.

Sample	pH	Conductivity (mS/cm)	TCOD (g/L)	SCOD (mg/L)	N-NH$_4$ (mgN/L)	TS (%)	VS (%)	VS/TS (%)	AlkTot (mgCaCO$_3$/L)
Substrate	-	-	-	-	-	96.76 ± 0.12	96.63 ± 0.19	99.9 ± 0.1	
Inoculum	7.08 ± 0.04		19.35 ± 0.05	202 ± 4	1471 ± 173	1.95 ± 0.00	1.23 ± 0.04	63.4 ± 2.2	2,616 ± 44
Blank	7.38 ± 0.02	4.30 ± 0.28				0.74 ± 0.18	0.42 ± 0.11	57.0 ± 0.8	
CTRL	7.24 ± 0.02	4.22 ± 0.20				1.23 ± 0.13	0.74 ± 0.08	60.4 ± 0.2	
CTRL10	7.23 ± 0.02	4.21 ± 0.25				1.26 ± 0.08	0.75 ± 0.06	60.1 ± 0.9	
CTRL100	7.16 ± 0.07	4.08 ± 0.22				1.32 ± 0.01	0.80 ± 0.01	60.7 ± 0.1	
CTRL500	7.12 ± 0.06	4.15 ± 0.11				1.42 ± 0.08	0.89 ± 0.05	63.0 ± 0.2	
ANT	7.22 ± 0.05	4.41 ± 0.08				1.35 ± 0.05	0.82 ± 0.03	60.6 ± 0.1	
ANT10	7.20 ± 0.06	4.21 ± 0.25				1.42 ± 0.02	0.86 ± 0.01	61.0 ± 0.1	
ANT100	7.19 ± 0.01	4.15 ± 0.25				1.33 ± 0.20	0.88 ± 0.01	67.4 ± 11.3	
ANT500	7.16 ± 0.02	4.07 ± 0.41				1.52 ± 0.03	0.95 ± 0.02	62.5 ± 0.3	

Table 0-2: Experimental and kinetic parameters obtained from the modified Gompertz model. The coefficient of determination (R^2) and the relative root mean square error (rRMSE) are also indicated to evaluate the goodness of fit. Standard errors of three replicates are reported (n=3, *: n=2).

	Experimental	Model data				
	SMP	Modified Gompertz			Model fit	
		B_∞	R_{MAX}	λ	R^2	rRMSE
Sample	$mLCH_4/gVS$	$mLCH_4/gVS$	$mLCH_4/(gVS\cdot d)$	d	-	%
CTRL	354 ± 31	356 ± 54	69 ± 9	2.4 ± 0.0	1.0 ± 0.0	0.0 ± 0.0
CTRL10	370 ± 22	373 ± 38	75 ± 6	2.5 ± 0.0	1.0 ± 0.0	0.0 ± 0.0
CTRL100*	323 ± 2	324 ± 1	62 ± 1	2.5 ± 0.0	1.0 ± 0.0	0.0 ± 0.0
CTRL500	289 ± 22	291 ± 39	65 ± 10	2.9 ± 0.3	1.0 ± 0.0	0.0 ± 0.0
ANT	373 ± 26	377 ± 44	68 ± 9	2.5 ± 0.1	1.0 ± 0.0	0.0 ± 0.0
ANT10	301 ± 60	301 ± 101	56 ± 16	2.3 ± 0.2	1.0 ± 0.0	0.0 ± 0.0
ANT100*	279 ± 1	284 ± 1	54 ± 4	2.7 ± 0.2	1.0 ± 0.0	0.0 ± 0.0
ANT500	342 ± 9	345 ± 16	72 ± 3	2.9 ± 0.3	1.0 ± 0.0	0.0 ± 0.0

Supplementary material Paper III

Table 0-3: Experimental and first-order model methane production and kinetic constants. The relative root mean square error (rRSME) and the coefficient of determination (R^2) are also reported. Five replicates (n = 5) were used to determine the standard deviations, if not indicated differently ([†]: $n = 4$, [‡]: n = 3, ": n = 2, *: n = 1).

	Feed	Experimental	Model			
		BMP (mL$_{CH4}$/g$_{VS}$)	B$_\infty$ (mL$_{CH4}$/g$_{VS}$)	k (d^{-1})	rRSME (%)	R^2
	I	357 ± 8	372 ± 0.0	0.59 ± 0.02	6.8 ± 0.5	0.97 ± 0.00
	II[†]	310 ± 7	311 ± 7	1.39 ± 0.05	3.1 ± 0.4	0.99 ± 0.00
0–2	III[‡]	328 ± 12	327 ± 12	1.50 ± 0.09	2.2 ± 0.1	0.99 ± 0.00
	IV[†]	309 ± 5	309 ± 3	1.30 ± 0.06	3.1 ± 0.4	0.99 ± 0.00
	V*	341	342	1.25	2.8	0.99
	I	343 ± 20	365 ± 12	0.61 ± 0.07	6.9 ± 0.8	0.97 ± 0.01
	II	312 ± 37	313 ± 34	1.54 ± 0.15	3.5 ± 0.5	0.98 ± 0.00
10–2	III	314 ± 10	311 ± 9	1.54 ± 0.07	2.3 ± 0.1	0.99 ± 0.00
	IV[†]	309 ± 4	309 ± 3	1.55 ± 0.04	2.7 ± 0.2	0.99 ± 0.00
	V*	332	322	1.09	4.6	0.96
	I	326 ± 15	355 ± 13	0.57 ± 0.03	6.4 ± 0.2	0.98 ± 0.00
	II	296 ± 13	298 ± 13	1.42 ± 0.09	3.4 ± 0.2	0.98 ± 0.00
20–2	III[‡]	309 ± 6	304 ± 6	1.44 ± 0.06	2.4 ± 0.3	0.99 ± 0.00
	IV[†]	322 ± 7	322 ± 7	1.43 ± 0.08	2.7 ± 0.2	0.99 ± 0.00
	V*	305	302	1.39	1.9	0.99
	I[†]	358 ± 6	372 ± 0	0.61 ± 0.01	7.0 ± 0.4	0.97 ± 0.00
	II	310 ± 7	311 ± 7	1.45 ± 0.06	3.3 ± 0.1	0.98 ± 0.00
0–1	III	313 ± 11	315 ± 9	1.43 ± 0.13	3.4 ± 0.4	0.98 ± 0.00
	IV[‡]	312 ± 9	348 ± 18	0.51 ± 0.05	7.0 ± 0.5	0.97 ± 0.01
	V[‡]	343 ± 14	336 ± 15	1.56 ± 0.04	2.7 ± 0.4	0.98 ± 0.01
	I[†]	335 ± 4	365 ± 6	0.57 ± 0.02	6.5 ± 0.2	0.97 ± 0.00
	II	298 ± 7	301 ± 6	1.44 ± 0.06	3.7 ± 0.1	0.98 ± 0.00
10–1	III	301 ± 6	301 ± 6	1.67 ± 0.09	2.5 ± 0.2	0.99 ± 0.00
	IV[†]	316 ± 7	336 ± 8	0.64 ± 0.04	6.2 ± 0.2	0.97 ± 0.00
	V"	332 ± 0	331 ± 1	1.78 ± 0.07	1.7 ± 0.0	0.99 ± 0.00
	I	326 ± 12	358 ± 9	0.55 ± 0.03	6.5 ± 0.1	0.97 ± 0.00
	II[†]	307 ± 3	308 ± 4	1.41 ± 0.05	3.7 ± 0.0	0.98 ± 0.00

20–1	III[†]	310 ± 10	308 ± 9	1.60 ± 0.04	2.3 ± 0.1	0.99 ± 0.00
	IV[†]	307 ± 8	331 ± 9	0.61 ± 0.01	6.8 ± 0.1	0.96 ± 0.00
	V[†]	335 ± 9	332 ± 8	1.76 ± 0.08	1.8 ± 0.2	0.99 ± 0.00
	I	350 ± 8	372 ± 0	0.56 ± 0.04	6.5 ± 0.5	0.98 ± 0.00
	II[†]	300 ± 9	302 ± 7	1.42 ± 0.02	3.4 ± 0.2	0.98 ± 0.00
0–0.75	III	307 ± 15	307 ± 13	1.44 ± 0.09	3.2 ± 0.3	0.98 ± 0.00
	IV[‡]	337 ± 13	358 ± 24	0.38 ± 0.07	11.6 ± 2.4	0.91 ± 0.06
	V"	339 ± 5	323 ± 9	1.68 ± 0.04	3.5 ± 0.4	0.97 ± 0.01
	I[†]	332 ± 4	364 ± 5	0.56 ± 0.02	6.4 ± 0.2	0.98 ± 0.00
	II	303 ± 6	305 ± 6	1.47 ± 0.04	3.5 ± 0.1	0.98 ± 0.00
10–0.75	III[‡]	305 ± 5	305 ± 4	1.66 ± 0.08	2.5 ± 0.2	0.99 ± 0.00
	IV[‡]	325 ± 19	372 ± 0	0.34 ± 0.02	10.7 ± 2.5	0.93 ± 0.04
	V"	338 ± 43	329 ± 37	1.43 ± 0.10	4.1 ± 0.5	0.97 ± 0.01
	I	318 ± 11	346 ± 12	0.59 ± 0.03	6.5 ± 0.1	0.97 ± 0.00
	II	297 ± 7	299 ± 6	1.48 ± 0.05	3.9 ± 0.3	0.98 ± 0.00
20–0.75	III[†]	296 ± 5	297 ± 6	1.64 ± 0.07	2.5 ± 0.2	0.99 ± 0.00
	IV[†]	322 ± 13	363 ± 11	0.20 ± 0.02	8.2 ± 1.2	0.96 ± 0.01
	V[‡]	304 ± 14	309 ± 15	1.31 ± 0.14	3.8 ± 0.4	0.98 ± 0.00

Table 0-4: Overall three-way ANOVA for the ultimate methane yield B_∞ from Origin 2021.

	Degree of Freedom	Sum of Squares	Mean Square	F-Value	*P*-Value
GO	2	3322.94952	1661.47476	13.52386	4.50341E-6
ISR	2	1064.13914	532.06957	4.33087	0.01506
Feed	4	91174.36975	22793.59244	185.53243	0
GO × ISR	4	1178.02982	294.50745	2.39719	0.05341
GO × ISR	8	1716.566	214.57075	1.74654	0.09335
ISR × Feed	8	16079.85973	2009.98247	16.3606	1.11022E-16
GO × ISR × Feed	16	2459.69914	153.7312	1.25132	0.23831
Model	44	117776.90507	2676.74784	21.78786	0
Error	133	16339.71885	122.85503	0	0
Corrected Total	177	134116.62393	0	0	0

Table 0-5: Interactions among the different means of the ultimate methane yield B_∞ for each tested condition using the Bonferroni Test in Origin 2021.

GO	ISR	Feed	Mean	Groups [1]												
0	2	I	372	A												
10	0.75	IV	372	A	B											
0	1	I	372	A	B											
0	0.75	I	372	A												
10	2	I	365.49403	A	B	C										
10	1	I	365.2831	A	B	C	D									
10	0.75	I	364.38624	A	B	C	D									
20	0.75	IV	362.80431	A	B	C	D	E								
0	0.75	IV	357.98037	A	B	C	D	E	F	G						
20	1	I	357.80345	A	B	C	D	E	F							
20	2	I	354.78967	A	B	C	D	E	F	G						
0	1	IV	348.03364	A	B	C	D	E	F	G	H	I				
20	0.75	I	346.30224		B	C	D	E	F	G	H					
0	2	V	341.52374	A	B	C	D	E	F	G	H	I	J	K	L	M
10	1	IV	336.44378					E	F	G	H	I	J			
0	1	V	336.35243			C	D	E	F	G	H	I	J	K		
20	1	V	332.35585						F	G	H	I	J	K	L	
10	1	V	331.35573				D	E	F	G	H	I	J	K	L	M
20	1	IV	330.59132							G	H	I	J	K	L	M
10	0.75	V	329.48386					E	F	G	H	I	J	K	L	M
0	2	III	327.01213							G	H	I	J	K	L	M
0	0.75	V	322.86852							G	H	I	J	K	L	M
20	2	IV	321.60454								H	I	J	K	L	M
10	2	V	321.51135				D	E	F	G	H	I	J	K	L	M
0	1	III	314.63418										J	K	L	M
10	2	II	312.60576										J	K	L	M
10	2	III	311.38966										J	K	L	M
0	2	II	311.22019										J	K	L	M
0	1	II	310.8593											K	L	M
0	2	IV	309.38486											K	L	M
10	2	IV	309.24517											K	L	M
20	0.75	V	308.61859										J	K	L	M

116

GO	ISR	Feed	Mean	I	J	K	L	M	N
20	1	II	308.43098			K	L	M	
20	1	III	307.59806			K	L	M	N
0	0.75	III	307.12533			K	L	M	N
10	0.75	III	305.35254				L	M	N
10	0.75	II	305.2529					M	N
20	2	III	304.43436			K	L	M	N
0	0.75	II	302.11482						N
20	2	V	302.09481	I	J	K	L	M	N
10	1	III	301.37282						N
10	1	II	300.9247						N
20	0.75	II	299.23791						N
20	2	II	297.96662						N
20	0.75	III	296.77677						N

[1] Means that do not share a letter are significantly different (p < 0.05).

Table 0-6: Overall three-way ANOVA for first-order rate constant k from Origin 2021.

	Degree of Freedom	Sum of Squares	Mean Square	F-Value	*P*-Value
GO	2	0.0731	0.03655	8.26117	4.15125E-4
ISR	2	0.6221	0.31105	70.30133	0
Feed	4	29.3895	7.34737	1660.59201	0
GO × ISR	4	0.0922	0.02305	5.20979	6.25952E-4
GO × ISR	8	0.17166	0.02146	4.84958	2.92017E-5
ISR × Feed	8	7.62922	0.95365	215.53665	0
GO × ISR × Feed	16	0.52437	0.03277	7.40709	3.95861E-12
Model	44	40.45992	0.91954	207.82758	0
Error	133	0.58847	0.00442	0	0
Corrected Total	177	41.04839	0	0	0

Table 0-7: Interactions among the different means of the first-order rate constant k for each tested condition using the Bonferroni Test in Origin 2021.

GO	ISR	Feed	Mean	Groups [1]
10	1	V	1.78214	A
20	1	V	1.75578	A

				A	B	C	D	E	F	G	H	I	J
0	0.75	V	1.67514	A	B	C	D						
10	1	III	1.66651	A	B								
10	0.75	III	1.66212	A	B	C							
20	0.75	III	1.64238	A	B	C							
20	1	III	1.59969	A	B	C	D	E					
0	1	V	1.55734		B	C	D	E	F				
10	2	IV	1.55423		B	C	D	E	F				
10	2	II	1.53805		B	C	D	E	F				
10	2	III	1.53783		B	C	D	E	F				
0	2	III	1.5013		B	C	D	E	F	G			
20	0.75	II	1.48066				D	E	F	G			
10	0.75	II	1.4734					E	F	G			
0	1	II	1.4519					E	F	G			
20	2	III	1.44388					E	F	G	H		
0	0.75	III	1.44227					E	F	G	H		
10	1	II	1.43713						F	G	H		
20	2	IV	1.42697						F	G	H		
0	1	III	1.42685						F	G	H		
10	0.75	V	1.42535					E	F	G	H		
20	2	II	1.42017						F	G	H		
0	0.75	II	1.41745						F	G	H		
20	1	II	1.41093						F	G	H		
20	2	V	1.39474			C	D	E	F	G	H	I	
0	2	II	1.39305						F	G	H		
20	0.75	V	1.3145							G	H	I	
0	2	IV	1.29726								H	I	
0	2	V	1.2461							G	H	I	
10	2	V	1.08528									I	
10	1	IV	0.6439										J
20	1	IV	0.61478										J
0	1	I	0.61027										J
10	2	I	0.60686										J
20	0.75	I	0.58751										J
0	2	I	0.58549										J
10	1	I	0.57035										J

GO	ISR	Feed	Mean	Groups			
20	2	I	0.56792	J			
10	0.75	I	0.56385	J	K		
0	0.75	I	0.56294	J			
20	1	I	0.55091	J	K		
0	1	IV	0.51446	J	K	L	
0	0.75	IV	0.38066		K	L	M
10	0.75	IV	0.33926			L	M
20	0.75	IV	0.19877				M

[1] Means that do not share a letter are significantly different (p < 0.05).

Table 0-8: Overall three-way ANOVA for pH values for the two measures carried out at feed IV (day 2) and feed V (end of experiment) from Origin 2021.

	Degree of Freedom	Sum of Squares	Mean Square	F-Value	*P*-Value
GO	2	0.40782	0.20391	19.18411	2.37029E-6
ISR	2	1.87881	0.9394	88.37931	2.08722E-14
Feed	1	4.40231	4.40231	414.17052	0
GO × ISR	4	0.15565	0.03891	3.66091	0.01359
GO × ISR	2	0.07318	0.03659	3.44241	0.04317
ISR × Feed	2	1.54419	0.7721	72.63908	3.48499E-13
GO × ISR × Feed	4	0.05673	0.01418	1.33425	0.27664
Model	17	8.51014	0.5006	47.09625	0
Error	35	0.37202	0.01063	0	0
Corrected Total	52	8.88216	0	0	0

Table 0-9: Interactions among the different means of pH for each tested condition at day 2 of feed IV and end of feed V using the Bonferroni Test in Origin 2021.

GO	ISR	Feed	Mean	Groups [1]	
0	1	V	7.56667	A	
0	2	V	7.53333	A	
10	0.75	V	7.53333	A	
0	2	IV	7.477	A	B
20	1	V	7.46667	A	B
0	0.75	V	7.46667	A	B

GO	ISR	Feed	Mean	A	B	C	D	E	F	G	H
20	2	V	7.43333	A	B						
10	2	V	7.4	A	B						
10	2	IV	7.366	A	B	C					
10	1	V	7.33333	A	B	C					
20	0.75	V	7.23333		B	C					
20	2	IV	7.09667			C	D				
0	1	IV	6.9				D	E			
10	1	IV	6.83333				D	E	F		
20	1	IV	6.75					E	F	G	
0	0.75	IV	6.56667						F	G	
10	0.75	IV	6.53333							G	
20	0.75	IV	6.23333								H

[1] Means that do not share a letter are significantly different (p < 0.05).

Table 0-10: Overall three-way ANOVA for FOS/TAC values for the two measures carried out at feed IV (day 2) and feed V (end of experiment) from Origin 2021.

	Degree of Freedom	Sum of Squares	Mean Square	F-Value	*P*-Value
GO	2	0.06733	0.03367	1.2821	0.30296
ISR	2	4.36054	2.18027	83.03204	1.68535E-9
Feed	1	7.04736	7.04736	268.38742	7.58316E-12
GO × ISR	4	0.04201	0.0105	0.39999	0.80594
GO × ISR	2	0.06296	0.03148	1.19881	0.3258
ISR × Feed	2	2.88591	1.44296	54.95272	3.79519E-8
GO × ISR × Feed	4	0.02813	0.00703	0.26778	0.89462
Model	17	21.83052	1.28415	48.90475	4.0153E-11
Error	17	0.44639	0.02626	0	0
Corrected Total	34	22.27691	0	0	0

Table 0-11: Interactions among the different means of FOS/TAC for each tested condition at day 2 of feed IV and end of feed V using the Bonferroni Test in Origin 2021.

GO	ISR	Feed	Mean	Groups [1]
20	0.75	IV	2.51326	A
0	0.75	IV	2.23356	A

10	0.75	IV	2.11869	A		
20	1	IV	1.39861		B	
0	1	IV	1.1696		B	
10	1	IV	1.13837		B	
0	2	IV	0.58873			C
20	2	IV	0.51284			C
20	0.75	V	0.45336			C
10	2	IV	0.44283			C
10	0.75	V	0.42239			C
0	0.75	V	0.41849			C
0	2	V	0.28229			C
10	1	V	0.27758			C
0	1	V	0.26984			C
20	2	V	0.25132			C
20	1	V	0.24618			C
10	2	V	0.23531			C

[1] Means that do not share a letter are significantly different ($p < 0.05$).

9. References

[1] United Nations, The United Nations World Water Development Report 2020: Water and Climate Change, (2020) 12. https://unesdoc.unesco.org/ark:/48223/pf0000372985.locale=en.

[2] European Commission, 2022/C 298/01, (2022). https://eur-lex.europa.eu/legal-content/EN/TXT/?uri=uriserv%3AOJ.C_.2022.298.01.0001.01.ENG&toc=OJ%3AC%3A 2022%3A298%3ATOC.

[3] The European Parliament and the Council, Regulation (EU) 2020/741, Minimum requirements for water reuse, Off. J. Eur. Union. 177/33 (2020) 32–55.

[4] European Commission, Circular Economy Action Plan, #EUGreenDeal. (2020) 4. https://doi.org/10.2775/855540.

[5] W.W. Li, H.Q. Yu, Advances in Energy-Producing Anaerobic Biotechnologies for Municipal Wastewater Treatment, Engineering. 2 (2016) 438–446. https://doi.org/10.1016/J.ENG.2016.04.017.

[6] H.H. Ngo, H.N.P. Vo, W. Guo, Z. Chen, Y. Liu, S. Varjani, Chapter 1 - Sustainable management and treatment technologies for micro-pollutants in wastewater, Elsevier B.V., 2020. https://doi.org/10.1016/b978-0-12-819594-9.00001-2.

[7] European Commission, 2022/1307 - Watch list of substances, (2022).

[8] EU Regulation 2020/741, Proposal for a DIRECTIVE OF THE EUROPEAN PARLIAMENT AND OF THE COUNCIL concerning urban wastewater treatment (recast), Off. J. Eur. Union. 0345 (2022) 1–68.

[9] A.K. Ghattas, F. Fischer, A. Wick, T.A. Ternes, Anaerobic biodegradation of (emerging) organic contaminants in the aquatic environment, Water Res. 116 (2017) 268–295. https://doi.org/10.1016/j.watres.2017.02.001.

[10] L. Leng, P. Yang, S. Singh, H. Zhuang, L. Xu, W.H. Chen, J. Dolfing, D. Li, Y. Zhang, H.

Zeng, W. Chu, P.H. Lee, A review on the bioenergetics of anaerobic microbial metabolism close to the thermodynamic limits and its implications for digestion applications, Bioresour. Technol. 247 (2018) 1095–1106. https://doi.org/10.1016/j.biortech.2017.09.103.

[11] A. Castellano-Hinojosa, C. Armato, C. Pozo, A. González-Martínez, J. González-López, New concepts in anaerobic digestion processes: recent advances and biological aspects, Appl. Microbiol. Biotechnol. 102 (2018) 5065–5076. https://doi.org/10.1007/s00253-018-9039-9.

[12] D.R. Lovley, Syntrophy Goes Electric: Direct Interspecies Electron Transfer, Annu. Rev. Microbiol. 71 (2017) 643–664. https://doi.org/10.1146/annurev-micro-030117-020420.

[13] G. Baek, J. Kim, J. Kim, C. Lee, Role and potential of direct interspecies electron transfer in anaerobic digestion, Energies. 11 (2018) 107. https://doi.org/10.3390/en11010107.

[14] Q. Cheng, D.F. Call, Hardwiring microbes: Via direct interspecies electron transfer: Mechanisms and applications, Environ. Sci. Process. Impacts. 18 (2016) 968–980. https://doi.org/10.1039/c6em00219f.

[15] J. Park, H. Kang, K. Park, H. Park, Direct interspecies electron transfer via conductive materials : A perspective for anaerobic digestion applications, Bioresour. Technol. 254 (2018) 300–311. https://doi.org/10.1016/j.biortech.2018.01.095.

[16] Y. Dang, D.E. Holmes, Z. Zhao, T.L. Woodard, Y. Zhang, D. Sun, L.Y. Wang, K.P. Nevin, D.R. Lovley, Enhancing anaerobic digestion of complex organic waste with carbon-based conductive materials, Bioresour. Technol. 220 (2016) 516–522. https://doi.org/10.1016/j.biortech.2016.08.114.

[17] S. Barua, B.R. Dhar, Advances towards understanding and engineering direct interspecies electron transfer in anaerobic digestion, Bioresour. Technol. 244 (2017) 698–707. https://doi.org/10.1016/j.biortech.2017.08.023.

[18] Z. Zhao, Y. Li, X. Quan, Y. Zhang, Towards engineering application: Potential mechanism for enhancing anaerobic digestion of complex organic waste with different types of conductive materials, Water Res. 115 (2017) 266–277. https://doi.org/10.1016/j.watres.2017.02.067.

[19]   J. Zhang, W. Zhao, H. Zhang, Z. Wang, C. Fan, L. Zang, Recent achievements in enhancing anaerobic digestion with carbon- based functional materials, Bioresour. Technol. 266 (2018) 555–567. https://doi.org/10.1016/j.biortech.2018.07.076.

[20]   E.C. Salas, Z. Sun, A. Lüttge, J.M. Tour, Reduction of graphene oxide via bacterial respiration, ACS Nano. 4 (2010) 4852–4856. https://doi.org/10.1021/nn101081t.

[21]   S. Gurunathan, J.W. Han, V. Eppakayala, J.H. Kim, Microbial reduction of graphene oxide by Escherichia coli: A green chemistry approach, Colloids Surfaces B Biointerfaces. 102 (2013) 772–777. https://doi.org/10.1016/j.colsurfb.2012.09.011.

[22]   B. Virdis, P.G. Dennis, The nanostructure of microbially-reduced graphene oxide fosters thick and highly-performing electrochemically-active biofilms, J. Power Sources. 356 (2017) 556–565. https://doi.org/10.1016/j.jpowsour.2017.02.086.

[23]   Y. Lu, L. Zhong, L. Tang, H. Wang, Z. Yang, Q. Xie, H. Feng, M. Jia, C. Fan, Extracellular electron transfer leading to the biological mediated production of reduced graphene oxide, Chemosphere. 256 (2020) 127141. https://doi.org/10.1016/j.chemosphere.2020.127141.

[24]   O. Akhavan, E. Ghaderi, Escherichia coli bacteria reduce graphene oxide to bactericidal graphene in a self-limiting manner, Carbon N. Y. 50 (2012) 1853–1860. https://doi.org/10.1016/j.carbon.2011.12.035.

[25]   D.R. Shaw, M. Ali, K.P. Katuri, J.A. Gralnick, L. Van Niftrik, M.S.M. Jetten, P.E. Saikaly, J. Reimann, R. Mesman, Extracellular electron transfer-dependent anaerobic oxidation of ammonium by anammox bacteria, Nat. Commun. 11 (2020) 2058. https://doi.org/10.1038/s41467-020-16016-y.

[26]   L. Shen, Z. Jin, D. Wang, Y. Wang, Y. Lu, Enhance wastewater biological treatment through the bacteria induced graphene oxide hydrogel, Chemosphere. 190 (2018) 201–210. https://doi.org/10.1016/j.chemosphere.2017.09.105.

[27]   B.A.E. Lehner, V.A.E.C. Janssen, E.M. Spiesz, D. Benz, S.J.J. Brouns, A.S. Meyer, H.S.J. van der Zant, Creation of Conductive Graphene Materials by Bacterial Reduction Using Shewanella Oneidensis, ChemistryOpen. 8 (2019) 888–895. https://doi.org/10.1002/open.201900186.

[28] T. Pan, B. Chen, Facile fabrication of Shewanella@graphene core-shell material and its enhanced performance in nitrobenzene reduction, Sci. Total Environ. 658 (2019) 324–332. https://doi.org/10.1016/j.scitotenv.2018.12.028.

[29] C. Guo, Y. Wang, Y. Luo, X. Chen, Y. Lin, X. Liu, Effect of graphene oxide on the bioactivities of nitrifying and denitrifying bacteria in aerobic granular sludge, Ecotoxicol. Environ. Saf. 156 (2018) 287–293. https://doi.org/10.1016/j.ecoenv.2018.03.036.

[30] J. Zhao, F. Ning, X. Cao, H. Yao, Z. Wang, B. Xing, Photo-transformation of graphene oxide in the presence of co-existing metal ions regulated its toxicity to freshwater algae, Water Res. 176 (2020) 115735. https://doi.org/10.1016/j.watres.2020.115735.

[31] D. Wang, G. Wang, G. Zhang, X. Xu, F. Yang, Using graphene oxide to enhance the activity of anammox bacteria for nitrogen removal, Bioresour. Technol. 131 (2013) 527–530. https://doi.org/10.1016/j.biortech.2013.01.099.

[32] S. Ahmad, A. Ahmad, S. Khan, S. Ahmad, I. Khan, S. Zada, P. Fu, Algal extracts based biogenic synthesis of reduced graphene oxides (rGO) with enhanced heavy metals adsorption capability, J. Ind. Eng. Chem. 72 (2019) 117–124. https://doi.org/10.1016/j.jiec.2018.12.009.

[33] G. Liu, X. Zhang, J. Zhou, A. Wang, J. Wang, R. Jin, H. Lv, Quinone-mediated microbial synthesis of reduced graphene oxide with peroxidase-like activity, Bioresour. Technol. 149 (2013) 503–508. https://doi.org/10.1016/j.biortech.2013.09.115.

[34] J.I. Bueno-López, J.R. Rangel-Mendez, F. Alatriste-Mondragón, F. Pérez-Rodríguez, V. Hernández-Montoya, F.J. Cervantes, Graphene oxide triggers mass transfer limitations on the methanogenic activity of an anaerobic consortium with a particulate substrate, Chemosphere. 211 (2018) 709–716. https://doi.org/10.1016/j.chemosphere.2018.08.001.

[35] J.I. Bueno-López, C.H. Nguyen, J.R. Rangel-Mendez, R. Sierra-Alvarez, J.A. Field, F.J. Cervantes, Effects of graphene oxide and reduced graphene oxide on acetoclastic, hydrogenotrophic and methylotrophic methanogenesis, Biodegradation. 31 (2020) 35–45. https://doi.org/10.1007/s10532-020-09892-0.

[36] H. Zhao, C. Zhang, Y. Wang, W. Chen, P.J.J. Alvarez, Self-Damaging Aerobic Reduction

of Graphene Oxide by Escherichia coli : Role of GO-Mediated Extracellular Superoxide Formation, Environ. Sci. Technol. 52 (2018) 12783–12791. https://doi.org/10.1021/acs.est.8b03753.

[37] S. Lian, Y. Qu, S. Li, Z. Zhang, H. Zhang, C. Dai, Y. Deng, Interaction of graphene-family nanomaterials with microbial communities in sequential batch reactors revealed by high-throughput sequencing, Environ. Res. 184 (2020) 109392. https://doi.org/10.1016/j.envres.2020.109392.

[38] H.N. Nguyen, D.F. Rodrigues, Chronic toxicity of graphene and graphene oxide in sequencing batch bioreactors: A comparative investigation, J. Hazard. Mater. 343 (2018) 200–207. https://doi.org/10.1016/j.jhazmat.2017.09.032.

[39] M. Tomaszewski, G. Cema, S. Ciesielski, D. Łukowiec, A. Ziembińska-Buczyńska, Cold anammox process and reduced graphene oxide - Varieties of effects during long-term interaction, Water Res. 156 (2019) 71–81. https://doi.org/10.1016/j.watres.2019.03.006.

[40] X. Yin, S. Qiao, J. Zhou, X. Tang, Fast start-up of the anammox process with addition of reduced graphene oxides, Chem. Eng. J. 283 (2016) 160–166. https://doi.org/10.1016/j.cej.2015.07.059.

[41] Y. Chen, Y. Niu, T. Tian, J. Zhang, Y. Wang, Y. Li, L.C. Qin, Microbial reduction of graphene oxide by Azotobacter chroococcum, Chem. Phys. Lett. 677 (2017) 143–147. https://doi.org/10.1016/j.cplett.2017.04.002.

[42] G.P. Kotchey, B.L. Allen, H. Vedala, N. Yanamala, A.A. Kapralov, Y.Y. Tyurina, J. Klein-Seetharaman, V.E. Kagan, A. Star, The enzymatic oxidation of graphene oxide, ACS Nano. 5 (2011) 2098–2108. https://doi.org/10.1021/nn103265h.

[43] G. Lalwani, W. Xing, B. Sitharaman, Enzymatic degradation of oxidized and reduced graphene nanoribbons by lignin peroxidase, J. Mater. Chem. B. 2 (2014) 6354–6362. https://doi.org/10.1039/c4tb00976b.

[44] Y. Jiao, F. Qian, Y. Li, G. Wang, C.W. Saltikov, J.A. Gralnick, Deciphering the electron transport pathway for graphene oxide reduction by Shewanella oneidensis MR-1, J. Bacteriol. 193 (2011) 3662–3665. https://doi.org/10.1128/JB.00201-11.

[45] N. Yoshida, Y. Miyata, K. Doi, Y. Goto, Y. Nagao, R. Tero, A. Hiraishi, Graphene oxide-dependent growth and self-aggregation into a hydrogel complex of exoelectrogenic bacteria, Sci. Rep. 6 (2016) 21867. https://doi.org/10.1038/srep21867.

[46] D.R. Lovley, Electromicrobiology, Annu. Rev. Microbiol. 66 (2012) 391–409. https://doi.org/10.1146/annurev-micro-092611-150104.

[47] N. Yoshida, Y. Miyata, A. Mugita, K. Iida, Electricity recovery from municipal sewage wastewater using a hydrogel complex composed of microbially reduced graphene oxide and sludge, Materials (Basel). 9 (2016) 1–13. https://doi.org/10.3390/ma9090742.

[48] E. Toral-Sánchez, J.R. Rangel-Mendez, J.A. Ascacio Valdés, C.N. Aguilar, F.J. Cervantes, Tailoring partially reduced graphene oxide as redox mediator for enhanced biotransformation of iopromide under methanogenic and sulfate-reducing conditions, Bioresour. Technol. 223 (2017) 269–276. https://doi.org/10.1016/j.biortech.2016.10.062.

[49] J. Wang, D. Wang, G. Liu, R. Jin, H. Lu, Enhanced nitrobenzene biotransformation by graphene-anaerobic sludge composite, J. Chem. Technol. Biotechnol. 89 (2014) 750–755. https://doi.org/10.1002/jctb.4182.

[50] A. Colunga, J.R. Rangel-Mendez, L.B. Celis, F.J. Cervantes, Graphene oxide as electron shuttle for increased redox conversion of contaminants under methanogenic and sulfate-reducing conditions, Bioresour. Technol. 175 (2015) 309–314. https://doi.org/10.1016/j.biortech.2014.10.101.

[51] H. Fu, D. Zhu, Graphene oxide-facilitated reduction of nitrobenzene in sulfide-containing aqueous solutions, Environ. Sci. Technol. 47 (2013) 4204–4210. https://doi.org/10.1021/es304872k.

[52] E. Toral-Sánchez, R.H. Hurt, J.A. Ascacio Valdés, C.N. Aguilar, F.J. Cervantes, R. Rangel-Mendez, Improved reductive transformation of iopromide by magnetite containing reduced graphene oxide nanosacks as electron shuttles, Colloids Surfaces A Physicochem. Eng. Asp. 566 (2019) 188–195. https://doi.org/10.1016/j.colsurfa.2019.01.026.

[53] E. Toral-Sánchez, J.A. Ascacio Valdés, C.N. Aguilar, F.J. Cervantes, J.R. Rangel-Mendez, Role of the intrinsic properties of partially reduced graphene oxides on the chemical

transformation of iopromide, Carbon N. Y. 99 (2016) 456–465. https://doi.org/10.1016/j.carbon.2015.12.067.

[54] L. Li, Q. Liu, Y. Wang, H. Zhao, C. He, H. Yang, L. Gong, Facilitated biological reduction of nitroaromatic compounds by reduced graphene oxide and the role of its surface characteristics, Nat. Publ. Gr. (2016) 1–10. https://doi.org/10.1038/srep30082.

[55] F.P. Van Der Zee, F.J. Cervantes, Impact and application of electron shuttles on the redox (bio) transformation of contaminants : A review, Biotechnol. Adv. 27 (2009) 256–277. https://doi.org/10.1016/j.biotechadv.2009.01.004.

[56] J. Wang, H. Zhang, D. Wang, H. Lu, J. Zhou, Effect of bioreduced graphene oxide on anaerobic biotransformation of nitrobenzene in an anaerobic reactor, Environ. Technol. (United Kingdom). 37 (2016) 39–45. https://doi.org/10.1080/09593330.2015.1059492.

[57] H. Lu, T. Zhang, Y. Zhou, J. Zhou, J. Wang, X. Wang, Enhanced dechlorination and biodegradation of 2-chloroaniline by a 2-aminoanthraquinone-graphene oxide composite under anaerobic conditions, Sci. Rep. 9 (2019) 1–11. https://doi.org/10.1038/s41598-019-48904-9.

[58] Y. Gao, D. Ma, C. Wang, J. Guan, X. Bao, Reduced graphene oxide as a catalyst for hydrogenation of nitrobenzene at room temperature, Chem. Commun. 47 (2011) 2432–2434. https://doi.org/10.1039/c0cc04420b.

[59] H. Fu, Y. Guo, W. Chen, C. Gu, D. Zhu, Reductive dechlorination of hexachloroethane by sulfide in aqueous solutions mediated by graphene oxide and carbon nanotubes, Carbon N. Y. 72 (2014) 74–81. https://doi.org/10.1016/j.carbon.2014.01.053.

[60] L. Gonzalez-Gil, D. Krah, A.K. Ghattas, M. Carballa, A. Wick, L. Helmholz, J.M. Lema, T.A. Ternes, Biotransformation of organic micropollutants by anaerobic sludge enzymes, Water Res. 152 (2019) 202–214. https://doi.org/10.1016/j.watres.2018.12.064.

[61] L. Li, Q. Liu, Y.X. Wang, H.Q. Zhao, C.S. He, H.Y. Yang, L. Gong, Y. Mu, H.Q. Yu, Facilitated biological reduction of nitroaromatic compounds by reduced graphene oxide and the role of its surface characteristics, Sci. Rep. 6 (2016) 30082. https://doi.org/10.1038/srep30082.

[62]   A. Tawfik, K. Hasanan, M. Abdullah, O.A. Badr, H.M. Awad, M. Elsamadony, A. El-Dissouky, M.A. Qyyum, A.S. Nizami, Graphene enhanced detoxification of wastewater rich 4-nitrophenol in multistage anaerobic reactor followed by baffled high-rate algal pond, J. Hazard. Mater. 424 (2022) 127395. https://doi.org/10.1016/j.jhazmat.2021.127395.

[63]   Z. Liang, N. Shen, H. Huang, Y. Chen, Evaluating decolorization capacity about alginate encapsulation system of Shewanella oneidensis MR-1 mingled with conductive materials, Environ. Technol. Innov. 21 (2021) 101344. https://doi.org/10.1016/j.eti.2020.101344.

[64]   L. Shen, Z. Jin, W. Xu, X. Jiang, Y.X. Shen, Y. Wang, Y. Lu, Enhanced Treatment of Anionic and Cationic Dyes in Wastewater through Live Bacteria Encapsulation Using Graphene Hydrogel, Ind. Eng. Chem. Res. 58 (2019) 7817–7824. https://doi.org/10.1021/acs.iecr.9b01950.

[65]   R. Lin, J. Cheng, J. Zhang, J. Zhou, K. Cen, J.D. Murphy, Boosting biomethane yield and production rate with graphene: The potential of direct interspecies electron transfer in anaerobic digestion, Bioresour. Technol. 239 (2017) 345–352. https://doi.org/10.1016/j.biortech.2017.05.017.

[66]   J. Zhang, Z. Wang, Y. Wang, H. Zhong, Q. Sui, C. Zhang, Y. Wei, Effects of graphene oxide on the performance, microbial community dynamics and antibiotic resistance genes reduction during anaerobic digestion of swine manure, Bioresour. Technol. 245 (2017) 850–859. https://doi.org/10.1016/j.biortech.2017.08.217.

[67]   J.I. Bueno-López, A. Díaz-Hinojosa, J.R. Rangel-Mendez, F. Alatriste-Mondragón, F. Pérez-Rodríguez, V. Hernández-Montoya, F.J. Cervantes, Methane production enhanced by reduced graphene oxide in an anaerobic consortium supplied with particulate and soluble substrates, J. Chem. Technol. Biotechnol. 95 (2020) 2983–2990. https://doi.org/10.1002/jctb.6459.

[68]   J. Zhang, Z. Wang, Y. Wang, H. Zhong, Q. Sui, C. Zhang, Y. Wei, Effects of graphene oxide on the performance, microbial community dynamics and antibiotic resistance genes reduction during anaerobic digestion of swine manure, Bioresour. Technol. 245 (2017) 850–859. https://doi.org/10.1016/j.biortech.2017.08.217.

[69] T. Tian, S. Qiao, X. Li, M. Zhang, J. Zhou, Nano-graphene induced positive effects on methanogenesis in anaerobic digestion, Bioresour. Technol. 224 (2017) 41–47. https://doi.org/10.1016/j.biortech.2016.10.058.

[70] P. Wang, Y. Zheng, P. Lin, J. Li, H. Dong, H. Yu, L. Qi, L. Ren, Effects of graphite, graphene, and graphene oxide on the anaerobic co-digestion of sewage sludge and food waste: Attention to methane production and the fate of antibiotic resistance genes, Bioresour. Technol. 339 (2021) 125585. https://doi.org/10.1016/j.biortech.2021.125585.

[71] B. Dong, Z. Xia, J. Sun, X. Dai, X. Chen, B.J. Ni, The inhibitory impacts of nano-graphene oxide on methane production from waste activated sludge in anaerobic digestion, Sci. Total Environ. 646 (2019) 1376–1384. https://doi.org/10.1016/j.scitotenv.2018.07.424.

[72] H. Muratçobanoğlu, Ö.B. Gökçek, R.A. Mert, R. Zan, S. Demirel, The impact of reduced graphene oxide (rGO) supplementation on cattle manure anaerobic digestion: Focusing on process performance and microbial syntrophy, Biochem. Eng. J. 173 (2021). https://doi.org/10.1016/j.bej.2021.108080.

[73] Ö.B. Gökçek, F. Muratçobanoğlu, H. Muratçobanoğlu, D. Uçar, R.A. Mert, B. Yıldırım, R. Zan, S. Demirel, The effect of reduced graphene oxide addition on methane production from municipal organic solid waste, J. Chem. Technol. Biotechnol. 96 (2021) 2845–2851. https://doi.org/10.1002/jctb.6835.

[74] T. Zhang, P.L. Tremblay, Graphene: An Antibacterial Agent or a Promoter of Bacterial Proliferation?, IScience. 23 (2020) 101787. https://doi.org/10.1016/j.isci.2020.101787.

[75] S. Liu, T.H. Zeng, M. Hofmann, E. Burcombe, J. Wei, R. Jiang, J. Kong, Y. Chen, Antibacterial activity of graphite, graphite oxide, graphene oxide, and reduced graphene oxide: Membrane and oxidative stress, ACS Nano. 5 (2011) 6971–6980. https://doi.org/10.1021/nn202451x.

[76] O. Akhavan, E. Ghaderi, A. Esfandiar, Wrapping Bacteria by Graphene Nanosheets for Isolation from Environment, Reactivation by Sonication, and Inactivation by Near-Infrared Irradiation, J. Phys. Chem. B. 115 (2011) 6279–6288. https://doi.org/10.1021/jp200686k.

[77] Z. Guo, C. Xie, P. Zhang, J. Zhang, G. Wang, X. He, Y. Ma, B. Zhao, Z. Zhang, Toxicity

and transformation of graphene oxide and reduced graphene oxide in bacteria biofilm, Sci. Total Environ. 580 (2017) 1300–1308. https://doi.org/10.1016/j.scitotenv.2016.12.093.

[78]   W. Xu, Z. Jin, X. Pang, Y. Zeng, X. Jiang, Y. Lu, L. Shen, Interaction between Biocompatible Graphene Oxide and Live Shewanella in the Self-Assembled Hydrogel: The Role of Physicochemical Properties, ACS Appl. Bio Mater. 3 (2020) 4263–4272. https://doi.org/10.1021/acsabm.0c00327.

[79]   R.A. Pereira, M.F.R. Pereira, M.M. Alves, L. Pereira, Carbon based materials as novel redox mediators for dye wastewater biodegradation, Appl. Catal. B Environ. 144 (2014) 713–720. https://doi.org/10.1016/j.apcatb.2013.07.009.

[80]   W. Yu, S. Zhan, Z. Shen, Q. Zhou, D. Yang, Efficient removal mechanism for antibiotic resistance genes from aquatic environments by graphene oxide nanosheet, Chem. Eng. J. 313 (2017) 836–846. https://doi.org/10.1016/j.cej.2016.10.107.

[81]   I. Angelidaki, M. Alves, D. Bolzonella, L. Borzacconi, J.L. Campos, A.J. Guwy, S. Kalyuzhnyi, P. Jenicek, J.B. Van Lier, Defining the biomethane potential (BMP) of solid organic wastes and energy crops: A proposed protocol for batch assays, Water Sci. Technol. 59 (2009) 927–934. https://doi.org/10.2166/wst.2009.040.

[82]   S. Pei, H.M. Cheng, The reduction of graphene oxide, Carbon N. Y. 50 (2012) 3210–3228. https://doi.org/10.1016/j.carbon.2011.11.010.

[83]   Z. Yang, H. Yan, H. Yang, H. Li, A. Li, R. Cheng, Flocculation performance and mechanism of graphene oxide for removal of various contaminants from water, Water Res. 47 (2013) 3037–3046. https://doi.org/10.1016/j.watres.2013.03.027.

[84]   B. Song, J. Tang, M. Zhen, X. Liu, Influence of graphene oxide and biochar on anaerobic degradation of petroleum hydrocarbons, J. Biosci. Bioeng. 128 (2019) 72–79. https://doi.org/10.1016/j.jbiosc.2019.01.006.

[85]   T.-H. Tsui, L. Zhang, E.Y. Lim, J.T.E. Lee, Y.W. Tong, Timing of biochar dosage for anaerobic digestion treating municipal leachate: Altered conversion pathways of volatile fatty acids, Bioresour. Technol. 335 (2021) 125283. https://doi.org/10.1016/j.biortech.2021.125283.

[86]   G. Wang, Q. Li, C. Yuwen, K. Gong, L. Sheng, Y. Li, Y. Xing, R. Chen, Biochar triggers methanogenesis recovery of a severely acidified anaerobic digestion system via hydrogen-based syntrophic pathway inhibition, Int. J. Hydrogen Energy. 46 (2021) 9666–9677. https://doi.org/10.1016/j.ijhydene.2020.03.115.

[87]   N. Aramrueang, R. Zhang, X. Liu, Application of biochar and alkalis for recovery of sour anaerobic digesters, J. Environ. Manage. 307 (2022) 114538. https://doi.org/10.1016/j.jenvman.2022.114538.

[88]   D. Sedlak, Water 4.0: The past, present, and future of the world's most vital resource, 2014. https://doi.org/10.5860/choice.52-0292.

[89]   W.W. Li, H.Q. Yu, B.E. Rittmann, Chemistry: Reuse water pollutants, Nature. 528 (2015) 29–31. https://doi.org/10.1038/528029a.

[90]   P.L. McCarty, J. Bae, J. Kim, Domestic wastewater treatment as a net energy producer-can this be achieved?, Environ. Sci. Technol. 45 (2011) 7100–7106. https://doi.org/10.1021/es2014264.

[91]   C. Grandclément, I. Seyssiecq, A. Piram, P. Wong-Wah-Chung, G. Vanot, N. Tiliacos, N. Roche, P. Doumenq, From the conventional biological wastewater treatment to hybrid processes, the evaluation of organic micropollutant removal: A review, Water Res. 111 (2017) 297–317. https://doi.org/10.1016/j.watres.2017.01.005.

[92]   J. Zhang, W. Zhao, H. Zhang, Z. Wang, C. Fan, L. Zang, Recent achievements in enhancing anaerobic digestion with carbon- based functional materials, Bioresour. Technol. 266 (2018) 555–567. https://doi.org/10.1016/j.biortech.2018.07.076.

[93]   Z. Chen, H. Li, W. Ma, D. Fu, K. Han, H. Wang, N. He, Q. Li, Y. Wang, Addition of graphene sheets enhances reductive dissolution of arsenic and iron from arsenic contaminated soil, L. Degrad. Dev. 29 (2018) 572–584. https://doi.org/10.1002/ldr.2892.

[94]   G. Wang, F. Qian, C.W. Saltikov, Y. Jiao, Y. Li, Microbial reduction of graphene oxide by Shewanella, Nano Res. 4 (2011) 563–570. https://doi.org/10.1007/s12274-011-0112-2.

[95]   T. Tian, S. Qiao, X. Li, M. Zhang, J. Zhou, Nano-graphene induced positive effects on methanogenesis in anaerobic digestion, Bioresour. Technol. 224 (2017) 41–47.

https://doi.org/10.1016/j.biortech.2016.10.058.

[96] F. Perreault, A.F. De Faria, S. Nejati, M. Elimelech, Antimicrobial Properties of Graphene Oxide Nanosheets: Why Size Matters, ACS Nano. 9 (2015) 7226–7236. https://doi.org/10.1021/acsnano.5b02067.

[97] Team JRC, JRC Technical Report: Selection of substances for the 3rd Watch List under WFD, 2020. https://doi.org/10.2760/194067.

[98] S. Aydin, B. Ince, Z. Cetecioglu, O. Arikan, E.G. Ozbayram, A. Shahi, O. Ince, Combined effect of erythromycin, tetracycline and sulfamethoxazole on performance of anaerobic sequencing batch reactors, Bioresour. Technol. 186 (2015) 207–214. https://doi.org/10.1016/j.biortech.2015.03.043.

[99] V. Mazzurco Miritana, G. Massini, A. Visca, P. Grenni, L. Patrolecco, F. Spataro, J. Rauseo, G.L. Garbini, A. Signorini, S. Rosa, A. Barra Caracciolo, Effects of Sulfamethoxazole on the Microbial Community Dynamics During the Anaerobic Digestion Process, Front. Microbiol. 11 (2020) 1–12. https://doi.org/10.3389/fmicb.2020.537783.

[100] T. Tang, M. Liu, Y. Chen, Y. Du, J. Feng, H. Feng, Influence of sulfamethoxazole on anaerobic digestion: Methanogenesis, degradation mechanism and toxicity evolution, J. Hazard. Mater. 431 (2022). https://doi.org/10.1016/j.jhazmat.2022.128540.

[101] M. Gros, S. Rodríguez-Mozaz, D. Barceló, Rapid analysis of multiclass antibiotic residues and some of their metabolites in hospital, urban wastewater and river water by ultra-high-performance liquid chromatography coupled to quadrupole-linear ion trap tandem mass spectrometry, J. Chromatogr. A. 1292 (2013) 173–188. https://doi.org/10.1016/j.chroma.2012.12.072.

[102] A. Göbel, A. Thomsen, C.S. McArdell, A.C. Alder, W. Giger, N. Theiß, D. Löffler, T.A. Ternes, Extraction and determination of sulfonamides, macrolides, and trimethoprim in sewage sludge, J. Chromatogr. A. 1085 (2005) 179–189. https://doi.org/10.1016/j.chroma.2005.05.051.

[103] C. Holliger, M. Alves, D. Andrade, I. Angelidaki, S. Astals, U. Baier, C. Bougrier, P. Buffière, M. Carballa, V. De Wilde, F. Ebertseder, B. Fernández, E. Ficara, I. Fotidis, J.C.

Frigon, H.F. De Laclos, D.S.M. Ghasimi, G. Hack, M. Hartel, J. Heerenklage, I.S. Horvath, P. Jenicek, K. Koch, J. Krautwald, J. Lizasoain, J. Liu, L. Mosberger, M. Nistor, H. Oechsner, J.V. Oliveira, M. Paterson, A. Pauss, S. Pommier, I. Porqueddu, F. Raposo, T. Ribeiro, F.R. Pfund, S. Strömberg, M. Torrijos, M. Van Eekert, J. Van Lier, H. Wedwitschka, I. Wierinck, Towards a standardization of biomethane potential tests, Water Sci. Technol. 74 (2016) 2515–2522. https://doi.org/10.2166/wst.2016.336.

[104] S.D. Hafner, S. Astals, P. Buffiere, N. Løjborg, C. Holliger, K. Koch, S. Weinrich, Calculation of Methane Production From From Manometric Measurements, Stand. BMP Methods Doc. 201, Version 2.6. (2020) Available online: https://www.dbfz.de/en/BMP. https://www.dbfz.de/en/BMP.

[105] S.D. Hafner, S. Astals, C. Holliger, K. Koch, S. Weinrich, Calculation of Biochemical Methane Potential (BMP), Stand. BMP Methods Doc. 200, Version 1.6. (2020) Available online https://www.dbfz.de/en/BMP. https://www.dbfz.de/en/BMP.

[106] R.B. Baird, A.D. Eaton, E.W. Rice, Standard Methods for the Examination of Water and Wastewater, 23rd ed., Washington, D.C., 2017.

[107] M.H. Zwietering, I. Jongenburger, F.M. Rombouts, K. Van't Riet, Modeling of the bacterial growth curve, Appl. Environ. Microbiol. 56 (1990) 1875–1881. https://doi.org/10.1128/aem.56.6.1875-1881.1990.

[108] S. Weinrich, M. Nelles, Basics of Anaerobic Digestion - Biochemical Conversion and Process Modelling, 2021. www.dnb.de.

[109] S.D. Hafner, K. Koch, H. Carrere, S. Astals, S. Weinrich, C. Rennuit, Software for biogas research: Tools for measurement and prediction of methane production, SoftwareX. 7 (2018) 205–210. https://doi.org/10.1016/j.softx.2018.06.005.

[110] K. Saravanan, G. Jayalakshmi, K. Suresh, B. Sundaravel, B.K. Panigrahi, D.M. Phase, Structural evaluation of reduced graphene oxide in graphene oxide during ion irradiation: X-ray absorption spectroscopy and in-situ sheet resistance studies, Appl. Phys. Lett. 112 (2018). https://doi.org/10.1063/1.5025097.

[111] D. López-Díaz, M. López Holgado, J.L. García-Fierro, M.M. Velázquez, Evolution of the

Raman Spectrum with the Chemical Composition of Graphene Oxide, J. Phys. Chem. C. 121 (2017) 20489–20497. https://doi.org/10.1021/acs.jpcc.7b06236.

[112] Z. Lu, P. Girguis, P. Liang, H. Shi, G. Huang, L. Cai, L. Zhang, Biological capacitance studies of anodes in microbial fuel cells using electrochemical impedance spectroscopy, Bioprocess Biosyst. Eng. 38 (2015) 1325–1333. https://doi.org/10.1007/s00449-015-1373-z.

[113] K. Koch, S.D. Hafner, S. Astals, S. Weinrich, Evaluation of common supermarket products as positive controls in biochemical methane potential (BMP) tests, Water (Switzerland). 12 (2020). https://doi.org/10.3390/W12051223.

[114] C. Holliger, H. Fruteau de Laclos, S.D. Hafner, K. Koch, S. Weinrich, S. Astals, M. Alves, D. Andrade, I. Angelidaki, L. Appels, S. Astals, S. Azman, E. Al., Requirements for measurement and validation of biochemical methane potential (BMP), Stand. BMP Methods Doc. 100, Version 1.3. (2020) Available online: https://www.dbfz.de/en/BMP. https://www.dbfz.de/en/BMP.

[115] J.T. Trevors, Sterilization and inhibition of microbial activity in soil, J. Microbiol. Methods. 26 (1996) 53–59. https://doi.org/10.1016/0167-7012(96)00843-3.

[116] F. Wang, S. Ma, Y. Si, L. Dong, X. Wang, J. Yao, H. Chen, Z. Yi, W. Yao, B. Xing, Interaction mechanisms of antibiotic sulfamethoxazole with various graphene-based materials and multiwall carbon nanotubes and the effect of humic acid in water, Carbon N. Y. 114 (2017) 671–678. https://doi.org/10.1016/j.carbon.2016.12.080.

[117] S. Bai, X. Shen, G. Zhu, A. Yuan, J. Zhang, Z. Ji, D. Qiu, The influence of wrinkling in reduced graphene oxide on their adsorption and catalytic properties, Carbon N. Y. 60 (2013) 157–168. https://doi.org/10.1016/j.carbon.2013.04.009.

[118] D.H. Carrales-Alvarado, I. Rodríguez-Ramos, R. Leyva-Ramos, E. Mendoza-Mendoza, D.E. Villela-Martínez, Effect of surface area and physical–chemical properties of graphite and graphene-based materials on their adsorption capacity towards metronidazole and trimethoprim antibiotics in aqueous solution, Chem. Eng. J. 402 (2020) 126155. https://doi.org/10.1016/j.cej.2020.126155.

[119] J. Aagaard, P.O. Madsen, P. Rhodes, T. Gasser, MICs of ciprofloxacin and trimethoprim for Escherichia coli: Influence of pH, inoculum size and various body fluids, Infection. 19 (1991) 167–169. https://doi.org/10.1007/BF01643691.

[120] A.L. Boreen, W.A. Arnold, K. McNeill, Photochemical fate of sulfa drugs in then aquatic environment: Sulfa drugs containing five-membered heterocyclic groups, Environ. Sci. Technol. 38 (2004) 3933–3940. https://doi.org/10.1021/es0353053.

[121] S.W. Nam, C. Jung, H. Li, M. Yu, J.R.V. Flora, L.K. Boateng, N. Her, K.D. Zoh, Y. Yoon, Adsorption characteristics of diclofenac and sulfamethoxazole to graphene oxide in aqueous solution, Chemosphere. 136 (2015) 20–26. https://doi.org/10.1016/j.chemosphere.2015.03.061.

[122] H. Chen, B. Gao, H. Li, Removal of sulfamethoxazole and ciprofloxacin from aqueous solutions by graphene oxide, J. Hazard. Mater. 282 (2015) 201–207. https://doi.org/10.1016/j.jhazmat.2014.03.063.

[123] R.B. Carneiro, L. Gonzalez-Gil, Y.A. Londoño, M. Zaiat, M. Carballa, J.M. Lema, Acidogenesis is a key step in the anaerobic biotransformation of organic micropollutants, J. Hazard. Mater. 389 (2020) 121888. https://doi.org/10.1016/j.jhazmat.2019.121888.

[124] S. Wang, R. Yuan, H. Chen, F. Wang, B. Zhou, Anaerobic biodegradation of four sulfanilamide antibiotics: Kinetics, pathways and microbiological studies, J. Hazard. Mater. 416 (2021) 125840. https://doi.org/10.1016/j.jhazmat.2021.125840.

[125] B. Liang, D. Kong, M. Qi, H. Yun, Z. Li, K. Shi, E. Chen, A.S. Vangnai, A. Wang, Anaerobic biodegradation of trimethoprim with sulfate as an electron acceptor, Front. Environ. Sci. Eng. 13 (2019). https://doi.org/10.1007/s11783-019-1168-6.

[126] W.Y. Ouyang, J. Birkigt, H.H. Richnow, L. Adrian, Anaerobic Transformation and Detoxification of Sulfamethoxazole by Sulfate-Reducing Enrichments and Desulfovibrio vulgaris, Environ. Sci. Technol. 55 (2021) 271–282. https://doi.org/10.1021/acs.est.0c03407.

[127] Y. Jia, S.K. Khanal, H. Zhang, G.H. Chen, H. Lu, Sulfamethoxazole degradation in anaerobic sulfate-reducing bacteria sludge system, Water Res. 119 (2017) 12–20.

https://doi.org/10.1016/j.watres.2017.04.040.

[128] T. Alvarino, P. Nastold, S. Suarez, F. Omil, P.F.X. Corvini, H. Bouju, Role of biotransformation, sorption and mineralization of 14C-labelled sulfamethoxazole under different redox conditions, Sci. Total Environ. 542 (2016) 706–715. https://doi.org/10.1016/j.scitotenv.2015.10.140.

[129] M.T. Zumstein, D.E. Helbling, Biotransformation of antibiotics: Exploring the activity of extracellular and intracellular enzymes derived from wastewater microbial communities, Water Res. 155 (2019) 115–123. https://doi.org/10.1016/j.watres.2019.02.024.

[130] Y. Jia, S.K. Khanal, H. Shu, H. Zhang, G.H. Chen, H. Lu, Ciprofloxacin degradation in anaerobic sulfate-reducing bacteria (SRB) sludge system: Mechanism and pathways, Water Res. 136 (2018) 64–74. https://doi.org/10.1016/j.watres.2018.02.057.

[131] S.A. Maves, Understanding thermostability in cytochrome P450 by combinatorial mutagenesis, Protein Sci. 10 (2001) 161–168. https://doi.org/10.1110/ps.17601.

[132] European Commission, REPowerEU : Joint European action for more affordable , secure and sustainable energy, (2022) 1–3. https://ec.europa.eu/commission/presscorner/detail/en/ip_22_1511 (accessed March 16, 2022).

[133] Q. Yin, M. Gu, G. Wu, Inhibition mitigation of methanogenesis processes by conductive materials: A critical review, Bioresour. Technol. 317 (2020) 123977. https://doi.org/10.1016/j.biortech.2020.123977.

[134] Z. Zhao, Y. Li, Y. Zhang, D.R. Lovley, Sparking Anaerobic Digestion: Promoting Direct Interspecies Electron Transfer to Enhance Methane Production, IScience. 23 (2020) 101794. https://doi.org/10.1016/j.isci.2020.101794.

[135] G. Wang, Q. Li, X. Gao, X.C. Wang, Synergetic promotion of syntrophic methane production from anaerobic digestion of complex organic wastes by biochar: Performance and associated mechanisms, Bioresour. Technol. 250 (2018) 812–820. https://doi.org/10.1016/j.biortech.2017.12.004.

[136] Y. Yang, Y. Zhang, Z. Li, Z. Zhao, X. Quan, Z. Zhao, Adding granular activated carbon

into anaerobic sludge digestion to promote methane production and sludge decomposition, J. Clean. Prod. 149 (2017) 1101–1108. https://doi.org/10.1016/j.jclepro.2017.02.156.

[137] D. Kundu, S. Banerjee, S. Karmakar, R. Banerjee, A new insight on improved biomethanation using graphene oxide from fermented Assam lemon waste, Fuel. 309 (2022) 122195. https://doi.org/10.1016/j.fuel.2021.122195.

[138] M. Ponzelli, S. Zahedi, K. Koch, J.E. Drewes, J. Radjenovic, Rapid biological reduction of graphene oxide: Impact on methane production and micropollutant transformation, J. Environ. Chem. Eng. 10 (2022) 108373. https://doi.org/10.1016/j.jece.2022.108373.

[139] R. Font, J.M. López Cabanes, Fermentation in fed-batch reactors-Application to the sewage sludge anaerobic digestion, Chem. Eng. Sci. 50 (1995) 2117–2126. https://doi.org/10.1016/0009-2509(95)00058-D.

[140] C. Holliger, S. Astals, H.F. de Laclos, S.D. Hafner, K. Koch, S. Weinrich, Towards a standardization of biomethane potential tests: A commentary, Water Sci. Technol. 83 (2021) 247–250. https://doi.org/10.2166/wst.2020.569.

[141] A. Veeken, B. Hamelers, Effect of temperature on hydrolysis rates of selected biowaste components, Bioresour. Technol. 69 (1999) 249–254. https://doi.org/10.1016/S0960-8524(98)00188-6.

[142] B. Linke, Kinetic study of thermophilic anaerobic digestion of solid wastes from potato processing, Biomass and Bioenergy. 30 (2006) 892–896. https://doi.org/10.1016/j.biombioe.2006.02.001.

[143] M. Brulé, H. Oechsner, T. Jungbluth, Exponential model describing methane production kinetics in batch anaerobic digestion: A tool for evaluation of biochemical methane potential assays, Bioprocess Biosyst. Eng. 37 (2014) 1759–1770. https://doi.org/10.1007/s00449-014-1150-4.

[144] A. Ware, N. Power, Modelling methane production kinetics of complex poultry slaughterhouse wastes using sigmoidal growth functions, Renew. Energy. 104 (2017) 50–59. https://doi.org/10.1016/j.renene.2016.11.045.

[145] K. Koch, T. Lippert, J.E. Drewes, The role of inoculum's origin on the methane yield of

different substrates in biochemical methane potential (BMP) tests, Bioresour. Technol. 243 (2017) 457–463. https://doi.org/10.1016/j.biortech.2017.06.142.

[146] M. Fujii, M. Shimizu, Synergism of endoenzyme and exoenzyme on hydrolysis of soluble cellulose derivatives, Biotechnol. Bioeng. 28 (1986) 878–882. https://doi.org/10.1002/bit.260280615.

[147] X. Wang, X. Lu, F. Li, G. Yang, Effects of temperature and Carbon-Nitrogen (C/N) ratio on the performance of anaerobic co-digestion of dairy manure, chicken manure and rice straw: Focusing on ammonia inhibition, PLoS One. 9 (2014) e97265. https://doi.org/10.1371/journal.pone.0097265.

[148] R. Lin, C. Deng, J. Cheng, A. Xia, P.N.L. Lens, S.A. Jackson, A.D.W. Dobson, J.D. Murphy, Graphene Facilitates Biomethane Production from Protein-Derived Glycine in Anaerobic Digestion, IScience. 10 (2018) 158–170. https://doi.org/10.1016/j.isci.2018.11.030.

[149] J. Quintana-Najera, A.J. Blacker, L.A. Fletcher, A.B. Ross, Influence of augmentation of biochar during anaerobic co-digestion of Chlorella vulgaris and cellulose, Bioresour. Technol. 343 (2022) 126086. https://doi.org/10.1016/j.biortech.2021.126086.

[150] J. Liebetrau, N. Rensberg, D. Maguire, D. Archer, D. Wall, Renewable Gas–discussion on the state of the industry and its future in a decarbonised world,Murphy, J.D. (Ed.) IEA Bioenergy Task 37, 2021.

[151] L. Appels, J. Baeyens, J. Degrève, R. Dewil, Principles and potential of the anaerobic digestion of waste-activated sludge, Prog. Energy Combust. Sci. 34 (2008) 755–781. https://doi.org/10.1016/j.pecs.2008.06.002.

[152] C. Mao, Y. Feng, X. Wang, G. Ren, Review on research achievements of biogas from anaerobic digestion, Renew. Sustain. Energy Rev. 45 (2015) 540–555. https://doi.org/10.1016/j.rser.2015.02.032.

[153] H. Wang, X. Yuan, Y. Wu, H. Huang, X. Peng, G. Zeng, H. Zhong, J. Liang, M.M. Ren, Graphene-based materials: Fabrication, characterization and application for the decontamination of wastewater and wastegas and hydrogen storage/generation, Adv.

Colloid Interface Sci. 195–196 (2013) 19–40. https://doi.org/10.1016/j.cis.2013.03.009.

[154] B. Song, J. Tang, M. Zhen, X. Liu, Influence of graphene oxide and biochar on anaerobic degradation of petroleum hydrocarbons, J. Biosci. Bioeng. 128 (2019) 72–79. https://doi.org/10.1016/j.jbiosc.2019.01.006.

[155] B. Basak, S.M. Patil, S. Saha, M.B. Kurade, G.-S. Ha, S.P. Govindwar, S.S. Lee, S.W. Chang, W.J. Chung, B.-H. Jeon, Rapid recovery of methane yield in organic overloaded-failed anaerobic digesters through bioaugmentation with acclimatized microbial consortium, Sci. Total Environ. 764 (2021) 144219. https://doi.org/10.1016/j.scitotenv.2020.144219.

[156] M. Ponzelli, J. Radjenovic, J.E. Drewes, K. Koch, Enhanced methane production kinetics by graphene oxide in fed-batch tests, Bioresour. Technol. 360 (2022). https://doi.org/10.1016/j.biortech.2022.127642.

[157] K. Koch, S. Hafner, S. Astals, S. Weinrich, Evaluation of Common Supermarket Products as Positive Controls in Biochemical Methane Potential (BMP) Tests, Water. 12 (2020) 1223. https://doi.org/10.3390/w12051223.

[158] L.M. Rodriguez-Chiang, O.P. Dahl, Effect of inoculum to substrate ratio on the methane potential of microcrystalline cellulose production wastewater, BioResources. 10 (2015) 898–911. https://doi.org/10.15376/biores.10.1.898-911.

[159] A. Khadka, A. Parajuli, S. Dangol, B. Thapa, L. Sapkota, A.A. Carmona-Martínez, A. Ghimire, Effect of the Substrate to Inoculum Ratios on the Kinetics of Biogas Production during the Mesophilic Anaerobic Digestion of Food Waste, Energies. 15 (2022). https://doi.org/10.3390/en15030834.

[160] X. Liu, L. André, M. Mercier-Huat, J.M. Grosmaître, A. Pauss, T. Ribeiro, Accurate estimation of bicarbonate and acetic acid concentrations with wider ranges in anaerobic media using classical fos/tac titration method, Appl. Sci. 11 (2021). https://doi.org/10.3390/app112411843.

[161] N. Basset, E. Santos, J. Dosta, J. Mata-Álvarez, Start-up and operation of an AnMBR for winery wastewater treatment, Ecol. Eng. 86 (2016) 279–289.

https://doi.org/10.1016/j.ecoleng.2015.11.003.

[162] B. Drosg, Process monitoring in biogas plants Technical Brochure, 2013. https://www.uibk.ac.at/umwelttechnik/teaching/phd/diss_schoen_2009_numerical-modelling-of-biogas-plants.pdf.

[163] W. Nordmann, Die Überwachung der Schlammfaulung. KA-Informationen für das Betriebspersonal, , (737), 77., Beilage Zur Korrespondenz Abwasser. 3 (1977) 77.

[164] S. Astals, D.J. Batstone, J. Mata-alvarez, P.D. Jensen, Identification of synergistic impacts during anaerobic co-digestion of organic wastes, Bioresour. Technol. 169 (2014) 421–427. https://doi.org/10.1016/j.biortech.2014.07.024.

[165] U. Egwu, E. Oko, M. Chinenye, P. Sallis, Novel low-cost pre-treatment material for enhancing the methane yield during anaerobic digestion of lignocellulosic biomass feedstocks : Experimental and kinetic study, Renew. Energy. 179 (2021) 584–592. https://doi.org/10.1016/j.renene.2021.07.064.

[166] K. Tsigkou, D. Zagklis, M. Parasoglou, C. Zafiri, M. Kornaros, Proposed protocol for rate-limiting step determination during anaerobic digestion of complex substrates, Bioresour. Technol. 361 (2022) 127660. https://doi.org/10.1016/j.biortech.2022.127660.

[167] K.K.H. De Silva, H.H. Huang, R.K. Joshi, M. Yoshimura, Chemical reduction of graphene oxide using green reductants, Carbon N. Y. 119 (2017) 190–199. https://doi.org/10.1016/j.carbon.2017.04.025.

[168] V. Agarwal, P.B. Zetterlund, Strategies for reduction of graphene oxide – A comprehensive review, Chem. Eng. J. 405 (2021) 127018. https://doi.org/10.1016/j.cej.2020.127018.

[169] F.O. Agyeman, Y. Han, W. Tao, Elucidating the kinetics of ammonia inhibition to anaerobic digestion through extended batch experiments and stimulation-inhibition modeling, Bioresour. Technol. 340 (2021) 125744. https://doi.org/10.1016/j.biortech.2021.125744.

[170] X. Peng, S.Y. Zhang, L. Li, X. Zhao, Y. Ma, D. Shi, Long-term high-solids anaerobic digestion of food waste: Effects of ammonia on process performance and microbial community, Bioresour. Technol. 262 (2018) 148–158. https://doi.org/10.1016/j.biortech.2018.04.076.

[171] X. Shi, J. Lin, J. Zuo, P. Li, X. Li, X. Guo, Effects of free ammonia on volatile fatty acid accumulation and process performance in the anaerobic digestion of two typical bio-wastes, J. Environ. Sci. (China). 55 (2017) 49–57. https://doi.org/10.1016/j.jes.2016.07.006.

[172] E.Y. Lim, J.T.E. Lee, L. Zhang, H. Tian, K.C. Ong, Z.K. Tio, J. Zhang, Y.W. Tong, Abrogating the inhibitory effects of volatile fatty acids and ammonia in overloaded food waste anaerobic digesters via the supplementation of nano-zero valent iron modified biochar, Sci. Total Environ. 817 (2022) 152968. https://doi.org/10.1016/j.scitotenv.2022.152968.

[173] R. Kurapati, S.P. Mukherjee, C. Martín, G. Bepete, E. Vázquez, A. Pénicaud, B. Fadeel, A. Bianco, Degradation of Single-Layer and Few-Layer Graphene by Neutrophil Myeloperoxidase, Angew. Chemie - Int. Ed. 57 (2018) 11722–11727. https://doi.org/10.1002/anie.201806906.

[174] Z. Liu, J. Zhao, K. Lu, Z. Wang, L. Yin, H. Zheng, X. Wang, L. Mao, B. Xing, Biodegradation of Graphene Oxide by Insects (Tenebrio molitor Larvae): Role of the Gut Microbiome and Enzymes, Environ. Sci. Technol. (2022). https://doi.org/10.1021/acs.est.2c03342.

[175] Graphene Flagship, Graphene Flagship Annual report 2020, AIMS Math. 6 (2021). https://doi.org/10.3934/math.2021814.

[176] R. Barrena, M. del C. Vargas-García, P. Catacora-Padilla, T. Gea, A. Abo Markeb, J. Moral-Vico, A. Sánchez, X. Font, T.J. Aspray, Magnetite-based nanoparticles and nanocomposites for recovery of overloaded anaerobic digesters, Bioresour. Technol. 372 (2023). https://doi.org/10.1016/j.biortech.2023.128632.

[177] S. Zahedi, P. Icaran, Z. Yuan, M. Pijuan, Assessment of free nitrous acid pre-treatment on a mixture of primary sludge and waste activated sludge: Effect of exposure time and concentration, Bioresour. Technol. 216 (2016) 870–875. https://doi.org/10.1016/j.biortech.2016.06.038.

[178] D.X. Luong, K. V. Bets, W.A. Algozeeb, M.G. Stanford, C. Kittrell, W. Chen, R. V. Salvatierra, M. Ren, E.A. McHugh, P.A. Advincula, Z. Wang, M. Bhatt, H. Guo, V.

Mancevski, R. Shahsavari, B.I. Yakobson, J.M. Tour, Gram-scale bottom-up flash graphene synthesis, Nature. 577 (2020) 647–651. https://doi.org/10.1038/s41586-020-1938-0.

[179] T. Hao, Y. Xiao, S. Varjani, Transiting from the inhibited steady-state to the steady-state through the ammonium bicarbonate mediation in the anaerobic digestion of low-C/N-ratio food wastes, Bioresour. Technol. 351 (2022) 127046. https://doi.org/10.1016/j.biortech.2022.127046.

[180] S. García-Gen, A. Vande Wouwer, A model-based optimisation strategy for the start-up of anaerobic co-digestion processes, Renew. Energy. 170 (2021) 693–702. https://doi.org/10.1016/j.renene.2021.02.007.

[181] J.P. Steyer, O. Bernard, D.J. Batstone, I. Angelidaki, Lessons learnt from 15 years of ICA in anaerobic digesters, Water Sci. Technol. 53 (2006) 25–33. https://doi.org/10.2166/wst.2006.107.

[182] O.M. Rodriguez-Narvaez, J.M. Peralta-Hernandez, A. Goonetilleke, E.R. Bandala, Treatment technologies for emerging contaminants in water: A review, Chem. Eng. J. 323 (2017) 361–380. https://doi.org/10.1016/j.cej.2017.04.106.